2007

Role of Sodium Arsenite in Atherogenesis

Flavia Elias Pereira
The University of Montana

ROLE OF SODIUM ARSENITE IN ATHEROGENESIS

By

Flavia Elias Pereira

Bachelor of Pharmaceutical Sciences
University Department of Chemical Technology, Mumbai, India, 2001

Dissertation

presented in partial fulfillment of the requirements
for the degree of

Doctor of Philosophy
in Pharmacology/Pharmaceutical Sciences

The University of Montana
Missoula, MT

Summer 2007

Approved by:

Dr. David A. Strobel, Dean
Graduate School

Howard D. Beall, Chair
Department of Biomedical and Pharmaceutical Sciences

J. Douglas Coffin
Department of Biomedical and Pharmaceutical Sciences

Jean C. Pfau
Department of Biomedical and Pharmaceutical Sciences

Fernando Cardozo-Pelaez
Department of Biomedical and Pharmaceutical Sciences

Scott Wetzel
Department of Biological Sciences

Stephen Lodmell
Department of Biological Sciences

Pereira, Flavia E., Ph.D., July 2007 Pharmacology/Pharmaceutical Sciences

Role of Sodium Arsenite in Atherogenesis

Chairperson: Howard D. Beall

Epidemiological studies as well as controlled animal studies have associated exposure to arsenic through drinking water with the development of atherosclerosis. In this study, we have shown for the first time that low and environmentally relevant concentrations of arsenic accelerate atherogenesis. The objective of this study was to elucidate the mechanisms of arsenic-induced atherosclerosis by (1) characterizing the time- and concentration-dependent effects of sodium arsenite [As(III)] on the development of atherosclerosis in ApoE-/- /LDLr-/- mice, (2) determining whether As(III)-induced peroxynitrite activates protein kinase C (PKC) isotypes, α and β, in human aortic endothelial cells (HAECs) and (3) determining the effects of activation of PKC isotypes, α and β, on the endothelial barrier. Accordingly, exposure of ApoE-/- /LDLr-/- mice to As(III) in drinking water showed an increasing trend in atherosclerotic plaque formation in as early as 5 weeks within the innominate arteries. Most remarkable was the evidence that environmentally relevant concentrations of As(III) resulted in significant increase in plaque formation. Initiation of atherosclerosis results from activation/dysfunction of the vascular endothelium that maintains a semipermeable barrier between the blood and vessel wall. To elucidate the mechanism of arsenic-induced atherosclerosis, we analyzed the effect of As(III) on the endothelial monolayer integrity. Endothelial barrier is maintained by proteins of the adherens junction (AJ) such as vascular endothelial cadherin (VE-cadherin) and β-catenin, and their association with the actin cytoskeleton. Treatment of HAECs with As(III) resulted in reorganization of actin filaments into stress fibers and non-uniform VE-cadherin and β-catenin staining at cell-cell junctions. Intercellular gaps were observed with a measured increase in endothelial permeability. In addition, an increase in tyrosine phosphorylation (PY) of β-catenin was observed. These effects were mediated through As(III)-induced activation of PKCα without peroxynitrite formation. No change in PKCβ levels was detected with As(III) treatment. Inhibition of PKCα restored VE-cadherin and β-catenin staining at cell-cell junctions and abolished the formation of intercellular gaps and stress fibers. Endothelial permeability and PY of β-catenin were also reduced to basal levels. These results demonstrate that As(III) induced activation of PKCα causes PY of β-catenin and formation of stress fibers. PY of β-catenin causes weakening of the AJ and this in association with the contractile force generated by stress fibers results in gap formation and increased endothelial permeability. This could potentially accelerate the development of atherosclerosis by increasing the accumulation of oxidized low density lipoproteins and monocytes into the neo-intima of the blood vessel. The findings in this study demonstrate that arsenic disrupts the endothelial monolayer by activation of PKC signaling. Damage to the endothelium plausibly accelerates the process of atherosclerosis at an early stage as evidenced by the increase in atherosclerotic plaques in the ApoE-/- /LDLr-/- mouse model.

Acknowledgements

I want to thank the Department of Biomedical and Pharmaceutical Sciences and the Center for Environmental Health Sciences for providing me with the opportunity for an excellent higher education. The cooperative research environment offered the prospects to interact or seek assistance from faculty members and colleagues with different scientific backgrounds.

I especially want to thank my advisor, Dr. Howard D. Beall for his constant support, patience, encouragement and guidance in helping me with the project and molding me as a scientist.

I also acknowledge and appreciate the valuable contributions of my dissertation committee members: Dr. Howard D. Beall, Dr. J. Douglas Coffin, Dr. Jean C. Pfau, Dr. Fernando Cardozo-Pelaez, Dr. Stephen Lodmell and Dr. Scott Wetzel.

I would also like to thank all my colleagues and friends who made me feel always welcomed and at home away from home. Finally, I want to thank my family for the support and encouragement, without which I could not have done this.

Table of Contents

List of Tables

List of Figures

Chapter 1

Chapter 2

Chapter 3

Chapter 4

Chapter 5

Chapter 1

Introduction

1.1 Rationale

Millions of people worldwide are exposed to arsenic through drinking water that has been associated with the development of cardiovascular diseases such as carotid atherosclerosis, ischemic heart disease and hypertension. Atherosclerosis is the fundamental cause of major cardiovascular diseases including ischemic heart disease, myocardial infarction and stroke. The focus of our laboratory has been to elucidate the mechanisms of arsenic-induced cardiovascular disease. The objective of this study was to determine the effects of arsenic on endothelial cell biology and the development of atherosclerosis. The *in vivo* effects of environmentally relevant concentrations of arsenic in atherogenesis were analyzed using the ApoE-/- /LDLr-/- mouse, which is a well-established model of human atherosclerosis. The *in vitro* studies focused on determining the mechanism of arsenic-induced atherosclerosis by using human aortic endothelial cells. The research presented here lends a valuable contribution towards understanding the role of arsenic in cardiovascular toxicity and will aid in developing future treatment and prevention strategies.

Specific Aim 1: Characterize the time- and concentration-dependent effects of As(III) on the initiation and progression of atherosclerosis in ApoE-/- /LDLr-/- atherosclerotic mouse model.

Specific Aim 2: Determine the effects of As(III)-induced peroxynitrite on the activation of calcium-dependent cPKC isotypes, α and β, in human aortic endothelial cells.

Specific Aim 3: Determine whether activation of the cPKC isotypes, α and β, by As(III) is involved in endothelial barrier disruption.

1.2 Cardiovascular Disease

1.2.1 Statistics

Cardiovascular disease (CVD) is the number one killer in the United States as well as developed Western countries. According to current estimates from the American Heart Association (Heart Disease and Stroke Statistics, 2007 update), about 80 million Americans have one or more types of CVD. The percentage breakdown of deaths from CVD is coronary heart disease (52%), stroke (17%), heart failure (7%), high blood pressure (6%), disease of arteries (4%), congenital cardiovascular defects (0.5%), rheumatic heart disease (0.4%) and other (13%). Atherosclerosis is the underlying cause of major clinical cardiovascular events.

1.2.2 Risk Factors

The American Heart Association has identified several risk factors for CVD based on extensive clinical and statistical studies. Some of the risk factors can be controlled through adequate lifestyle changes and/or use of medication, whereas others cannot be controlled. The controllable risk factors include cigarette smoking, high blood pressure, high blood cholesterol, diabetes mellitus, physical inactivity and obesity. The uncontrollable risk factors include increasing age, gender and heredity. Other risk factors have been associated with CVD, but their significance and prevalence are yet to be

confirmed. These factors are known as ‘contributing risk factors’ and include stress and excessive alcohol intake.

1.2.3 Atherosclerosis

Atherosclerosis is a complex, progressive and multifactorial disease characterized by deposition of lipid and fibrous elements in the subendothelial space. It is the underlying cause of serious clinical manifestations such as ischemic heart disease, myocardial infarction and stroke.

The normal large artery consists of three layers; the intima, media and adventitia (Fig. 1). The intima, the innermost layer, consists of extracellular connective tissue matrix, primarily collagen and proteoglycans. The intima is bounded by the endothelial monolayer on luminal side and elastic lamina on the peripheral side. The media, the middle layer, consists of smooth muscle cells. The adventitia is the outermost layer and consists of connective tissue with interspersed fibroblast and smooth muscle cells (Lusis, 2000). An initiating event in the development of an atherosclerotic lesion or fatty streak is the accumulation of oxidized low density lipoproteins (oxLDLs) into the intima of blood vessel. The oxLDLs stimulate the overlying endothelial cells to express cell adhesion molecules such as vascular cell adhesion molecule-1 (VCAM-1) and intercellular cell adhesion molecule-1 (ICAM-1), proinflammatory cytokines such as interleukin-1 (IL-1) and IL-6, and chemokines such as monocyte chemottractant protein-1 (MCP-1) and IL-8 (Tedgui and Mallat, 2006) (Fig. 2). The VCAM-1 expressed by endothelial cells play a major role in transmigration of monocytes from the blood into the intima (Cybulsky et al., 2001, Nakashima et al., 1998) along with MCP-1 (Libby, 2002).

Once inside the intima, the monocytes differentiate into macrophages and internalize oxLDLs resulting in the formation of lipid laden foam cells. The activated macrophages further secrete proinflammatory cytokines such as tumor necrosis factor α (TNFα), IL-1, and IL-6, and chemokines such as IL-8 and MCP-1 that in turn can activate endothelial cells, smooth muscle cells (SMC) and resident macrophages leading to a self-perpetuating inflammatory process (Tedgui and Mallat, 2006).

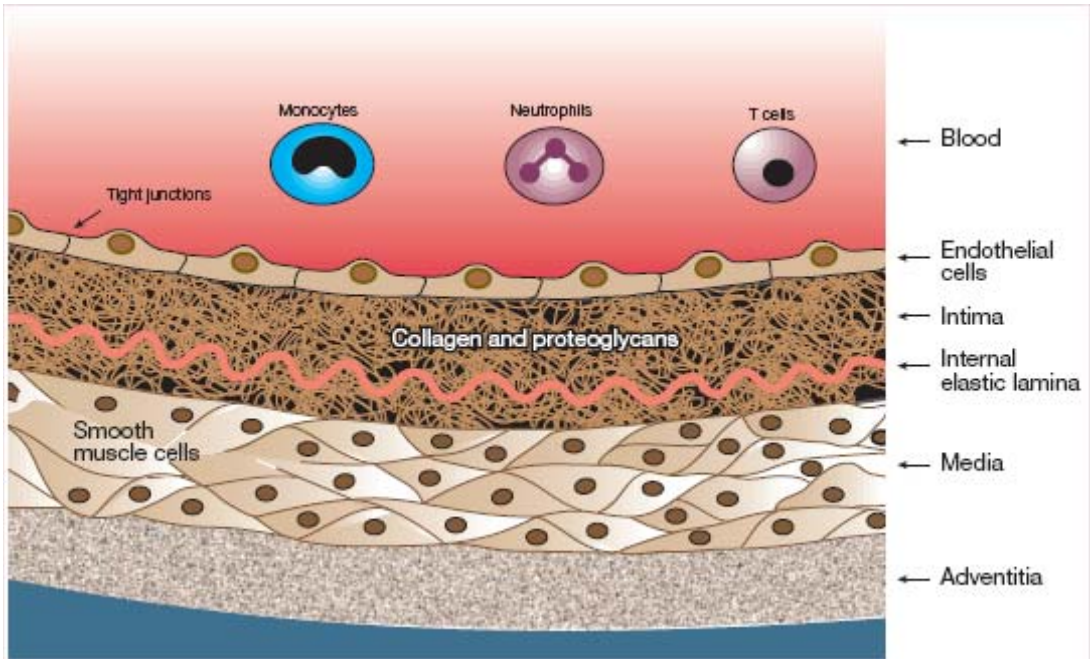

Fig. 1. Structure of a normal large artery
Reprinted by permission from Macmillan Publishers Ltd: Nature; Lusis, 2000, © 2000

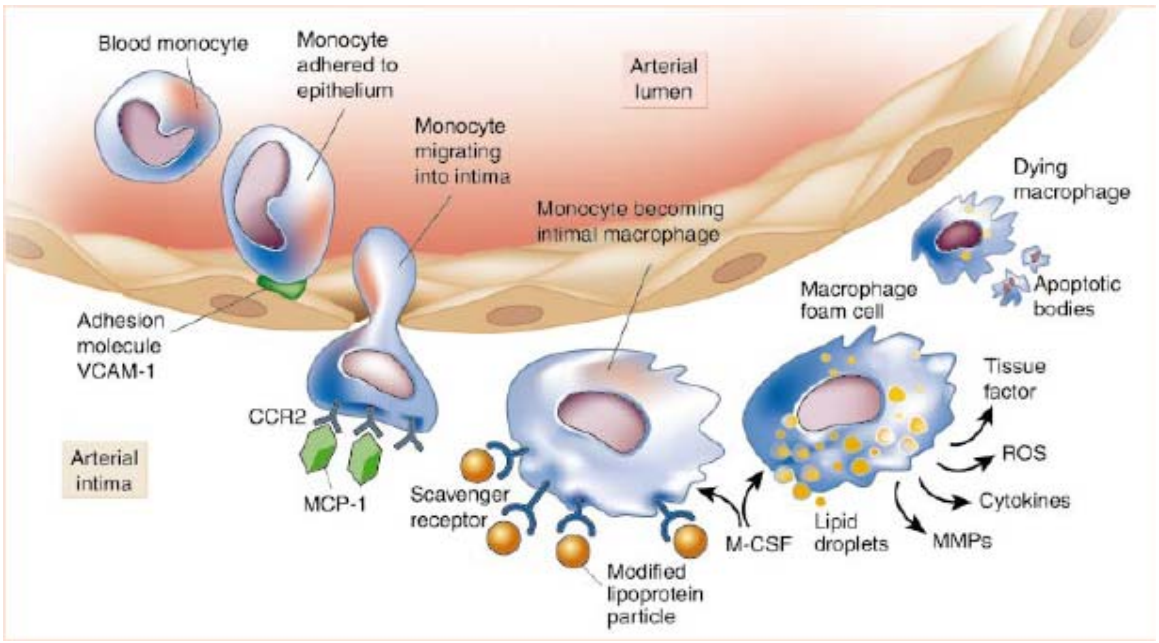

Fig. 2. Development of atherosclerotic lesion.
Reprinted by permission from Macmillan Publishers Ltd: Nature; Libby, 2002, © 2002

Accordingly, it has been observed that stimulation of endothelial cells from different vascular beds such as human aortic endothelial cells (HAEC), human coronary artery endothelial cells (HCAEC) or human heart microvascular endothelial cells (HHMEC) with proinflammatory cytokines, TNFα and IL-1β, upregulates the expression of VCAM-1 (McDouall et al., 2001). Co-culture experiments of endothelial cells with human peripheral blood mononuclear cells (PBMC) revealed increased binding of PBMC to TNFα stimulated endothelial cells, implying that the increased expression of VCAM-1 may increase adhesion to the endothelium and transmigration of monocytes into the blood vessel intima during inflammatory conditions (McDouall et al., 2001). Consistent with this, using an en face imaging technique, Nakashima et al. (1998) reported that in apolipoprotein E deficient (ApoE-/-) mice, VCAM-1 is upregulated at the lesion-prone sites by hypercholesterolemia. The authors concluded that VCAM-1 expression is an early event that precedes fatty streak formation and may play a critical role in monocyte recruitment from the blood. Also, elevated levels of soluble VCAM-1 have been detected in the plasma of patients with coronary heart disease and myocardial infarction compared to healthy subjects (Zeitler et al., 1997).

During the progression of an atherosclerotic lesion there is accumulation of excessive lipid, multiplying SMCs and SMC-derived extracellular matrix, especially collagen. The developing plaque consists of a core, fibrous cap covering the plaque and the shoulder region (Lusis, 2000). Composition of the plaque determines its stability. Vulnerable plaques generally have thin fibrous cap, decreased collagen content and increased number of lipid laden macrophages in the shoulder region. The matrix metalloproteinases (MMP), collagenase, gelatinase and stromolysin, secreted by the

activated macrophages can cause thinning of the fibrous cap by degrading the collagen content of the extracellular matrix. This can make the atherosclerotic plaques more vulnerable to rupture. Inflammatory cytokines also play a significant role in plaque instability and rupture. Cytokines such as TNFα and IL-1β have been shown to stimulate the production of 92 kDa gelatinase in macrophages without affecting tissue inhibitor of metalloproteinases-1 (TIMP-1), which is their natural inhibitor (Saren et al., 1996).

Increased IL-6 levels have been strongly correlated with atherosclerotic plaque instability and rupture in human subjects. In the left anterior descending coronary artery obtained from patients with ischemic cardiomyopathy, atherosclerotic plaques showed co-localization of IL-6 with macrophages in the shoulder region (Schieffer et al., 2000). The lipid-rich shoulder areas of plaques are the most vulnerable sites of plaque rupture (van der Wal et al., 1994, Schieffer et al., 2000). Similarly, Cheng et al. (2006) demonstrated increased expression of IL-6 in macrophage-rich areas of atherosclerotic plaques in ApoE-/- mice along with increased MMP activity. The authors suggested that IL-6 causes the increase in macrophage MMP activity that contributes to weakening of the fibrous cap and increased potential of plaque rupture. Increased plasma levels of IL-6 have been detected in patients with acute myocardial infarction, coronary artery disease and peripheral artery disease (Erren et al., 1999, Ikeda et al., 1992). Rupture of plaques can generate circulating blood clots, when blood coming in contact with the tissue factor in the plaque coagulates (Libby, 2002). These clots can result in occlusion of blood vessels leading to ischemia, myocardial infarction or stroke.

1.2.4 Mouse models of Atherosclerosis

Numerous animal species have been used to study the pathogenesis of atherosclerosis. These include pigeons, hamsters, rabbits, pigs and monkeys. However, several factors such as costs of maintenance and/or dissimilar disease progression status compared to humans have limited their use (Jaweiń et al., 2004). In recent years, the mouse has become a most useful model in the study of atherosclerosis. The low cost of maintenance, ease of breeding and genetic manipulation have made it the model of choice among biomedical researchers.

The most commonly used mouse models in the study of atherosclerosis are low density lipoprotein receptor deficient mice (LDLr-/-), the ApoE-/- mice, and the apolipoprotein E and low density lipoprotein receptor (ApoE-/- /LDLr-/-) double knockout mice (Jaweiń et al., 2004, Daugherty, 2002). Mice are highly resistant to atherosclerosis and the lipid profile differs from that in humans. Mice carry most of the plasma cholesterol on high density lipoprotein (HDL), whereas humans carry 75% of cholesterol on low density lipoprotein (LDL) (Jaweiń et al., 2004). However, targeted gene deletion has enabled the generation of mouse models that develop atherosclerosis and have lipid profiles similar to humans.

ApoE is a 34 kD glycoprotein that is synthesized mainly by the liver. It is also produced by other tissues such as brain, spleen, lung, ovary, adrenal gland, kidney and muscles, and by cells types such as macrophages (Greenow et al., 2005). There are 3 isoforms of ApoE; ApoE2, E3 and E4. The e3 allele is present in the majority of population. People with familial hypercholesterolemia have two copies of the e2 allele. ApoE is a major constituent of very low density lipoprotein (VLDL), but is also present

in HDL and chylomicron remnants. It promotes hepatic clearance of cholesterol by acting as a high affinity ligand for the hepatic LDL receptor. ApoE also binds another hepatic receptor, LDL receptor related protein (LRP), and has been implicated in the clearance of chylomicron remnants (Greenow et al., 2005). Other anti-atherogenic functions of ApoE include inhibition of LDL oxidation, inhibition of platelet aggregation, inhibition of SMC and endothelial cell proliferation and cholesterol efflux from macrophages. The hepatic LDL receptor, in addition to recognizing lipoproteins containing ApoE, is also responsible for the uptake of LDLs via interaction with ApoB-100. The ApoB-100 is an exclusive apolipoprotein associated with LDLs (Olofsson and Boren, 2005). Thus, the LDL receptor plays an important role in removal of excessive blood cholesterol. The increase in circulating LDLs is a risk factor for CVD.

The ApoE-/- mice develop atherosclerotic lesions/plaques that closely resemble the human condition. The development of plaques in the innominate artery of this mouse model has been well characterized and has been shown to closely resemble that of human condition with events such as intraplaque hemorrhage and loss of fibrous cap or plaque rupture (Rosenfeld et al., 2000). A major limitation of the ApoE-/- mouse model is that the lipid profiles are dissimilar from that of human subjects. In these mice, the plasma cholesterol is carried on VLDL (Ishibashi et al., 1994, Daugherty, 2002, Ohashi et al., 2004), whereas in human subjects with atherosclerosis the majority of plasma cholesterol is carried on LDLs. On the other hand, the lipid profiles of LDLr-/- mouse model are more similar to that of human subjects with the majority of plasma cholesterol being carried on LDL and VLDL (Ishibashi et al., 1994, Jaweiń et al., 2004, Ohashi et al., 2004). However, these mice develop lesions that consist of primarily lipid-laden

macrophages and lack advanced atherosclerotic lesions. Only when fed with high fat diet for longer periods do these mice develop advanced atherosclerotic lesions (Daugherty, 2002, Ohashi et al., 2004). Compared to ApoE-/- or LDLr-/- mice alone, the ApoE-/-/LDLr-/- mice develop more marked atherosclerotic plaques (Jaweiń et al., 2004). The lipid profiles of this mouse model are more similar to that of humans as compared to either ApoE-/- or LDLr-/- mice, with the majority of plasma cholesterol being carried on LDLs when fed with normal mouse chow (Ishibashi et al., 1994). This makes the ApoE-/-/LDLr-/- mouse an ideal model to study the progression of atherosclerosis.

1.3 Arsenic

1.3.1 Environmental Significance of Arsenic

Arsenic is a ubiquitous element in the environment present in rocks and soil, air and natural water. Exposure to arsenic via drinking water poses a significant threat to human health. Contamination of ground water occurs by mobilization of arsenic under natural conditions. Arsenic occurs as a major constituent in several minerals such as sulphides and oxides. Three mechanisms have been identified that result in arsenic mobilization under geochemical conditions (Smedley and Kinniburgh, 2002, Delemos et al., 2006). First, in arid or semi-arid environments, mineral weathering and high evaporation rates can result in development of high pH (>8.5) conditions that can cause desorption of adsorbed arsenic from mineral oxides or prevent it from being adsorbed. Second, strong reducing conditions result in the reductive dissolution of oxides such as iron and manganese, and release of arsenic by desorption. Third, competitive desorption

of arsenic by the presence of large concentrations of phosphate, bicarbonate and silicates can lead to increased ground water contamination with arsenic.

In addition to the natural existence, arsenic is also widely distributed in the environment by human activities such as mining, smelting, pesticide application and manufacturing and use of products such as wood preservatives and dyes. In the United States, improper waste management from industrial and municipal sources, has created contaminated areas termed as 'Superfund Sites' that contain extremely high and dangerous levels of several environmental contaminants including arsenic. About 30% of the Superfund Sites in United States have excessive arsenic levels (Welch et al., 2000). Some of the sites have arsenic contamination introduced from human activities but many of the sites do not have a known source of contamination. A recent study performed at the Coakley Landfill Superfund Site in New Hampshire, a site contaminated with arsenic, chromium, lead, nickel, zinc and aromatic hydrocarbons, has reported that the concentrations of most of the contaminants diminished as a result of treatment by monitored natural attenuation that began in 1998, but the levels of dissolved arsenic increased over the same time interval (Delemos et al., 2006). This was due to the reductive release of arsenic from iron oxides. Natural biogeochemical processes are used to degrade contaminants. However, reducing environments created due to biodegradation of organic waste can cause the release of adsorbed arsenic from mineral oxides (Delemos et al., 2006). Although, this problem has only been identified in New Hampshire thus far, it could be a major problem all across the United States or in other countries where arsenic concentration in ground water is higher than the standard implemented by World Health Organization (WHO).

In the United States, the western regions have higher arsenic contamination of ground water (10 to >50 ppb) than the eastern regions (<10 ppb). However, there may be geographic 'hotspots' in the regions that have higher arsenic levels. In February 2002, the United States Environmental Protection Agency implemented the maximum contaminant limit (MCL) of 10 ppb for arsenic. The public water supply systems had to comply with this new standard by January 2006. Arsenic contamination of ground water is a worldwide problem. In 1993, the WHO also implemented the MCL of 10 ppb. In addition to the United States, Taiwan, Bangladesh, India (West Bengal), China, Vietnam, Hungary, Mexico, Romania and Argentina have high levels of arsenic in ground water ranging from 10-14,000 ppb (Wang and Wai, 2004, Smedley and Kinniburgh, 2002).

1.3.2 Metabolism of Arsenic

Exposure to arsenic can occur via food, water and air, of which drinking water (ground water) is a significant source of arsenic exposure in humans. Natural waters including drinking water mostly contain inorganic arsenic species; trivalent arsenite [As(III)] and pentavalent arsenate [As(V)] (Smedley and Kinniburgh, 2002). Concentrations of organic forms of arsenic are generally low or negligible in drinking water, but may occur in waters severely affected by industrial pollution (Smedley and Kinniburgh, 2002). The metabolism of arsenic in most mammals involves a series of reduction and oxidative methylation reactions during which As(V) is reduced to As(III) that is further metabolized to methylated species (Abernathy et al., 1999). The major site of arsenic methylation is the liver and the route of excretion is via the kidneys. There is considerable variation in arsenic methylation among mammalian species (Vahter, 2000).

As(V) and As(III) are the major forms of inorganic arsenic present in drinking water. The mechanism of cellular uptake of arsenic varies with the valence state. As(V) is structurally similar to phosphate and its uptake into the cells is mediated through the phosphate carrier system (Huang and Lee, 1996). Two different mechanisms have been proposed for the cellular uptake of As(III); simple diffusion (Huang and Lee, 1996) and transport by mammalian aquaglyceroporins (Liu et al., 2002). As(V) has been shown to compete with phosphate and can deplete cellular energy levels by preventing the incorporation of phosphate into adenosine 5'-triphosphate (ATP). As(III) on the other hand is extremely thiol reactive and can affect the activities of several enzymes (Aposhian et al., 2004). The first step in the metabolism of arsenic involves the reduction of As(V) to As(III) by arsenate reductase in the presence of glutathione (GSH). The sulfhydryl-containing tripeptide, GSH, forms As(III)-$(GS)_3$ complexes that may be substrates for methylating enzymes (Scott et al., 1993). Recent *in vitro* and *in vivo* studies using a rat model suggest that the key glycolytic enzyme, glyceraldehyde-3-phosphate dehydrogenase (GAPDH), is the arsenate reductase enzyme in mammals (Neméti and Gregus, 2005, Gregus and Neméti, 2005, Neméti et al., 2006). However, further studies are needed to confirm this observation.

The next step in the metabolism of arsenic consists of a series of methylation reactions. As(III) is methylated to the pentavalent species, monomethyl arsonic acid [MMA(V)], by arsenite/MMA(III) methyltransferase in the presence of GSH. S-adenosylmethionine (SAM) is the methyl donor in the methylation reactions (Buchet and Lauwerys, 1988). Using methyltransferases of rabbit liver, it has been shown that the arsenite methyltransferase and MMA(III) methyltransferase appear to have common

properties or may be part of the same protein or multienzyme complex (Zakharyan et al., 1995). Furthermore, studies have reported that rat liver arsenite methyltransferase is a homologue of human cyt19 (Lin et al., 2002, Thomas et al., 2004). Recombinant rat and human cyt19 has been shown to methylate inorganic arsenite in *in vitro* conditions (Waters et al., 2004, Hayakawa et al., 2005). However, the expression and enzymatic activity of cyt19 in human liver has yet to be confirmed (Aposhian and Aposhian, 2006).

The first methylation step is followed by alternating reduction of pentavalent arsenic to trivalent arsenic with the addition of a methyl group (Fig. 3). MMA(V) reductase in the presence of GSH catalyzes the reduction of MMA(V) to monomethylarsonous acid [MMA(III)] (Zakharyan and Aposhian, 1999) that is further oxidatively methylated to dimethylarsinic acid [DMA(V)] in the presence of arsenite/MMA (III) methyltransferase.

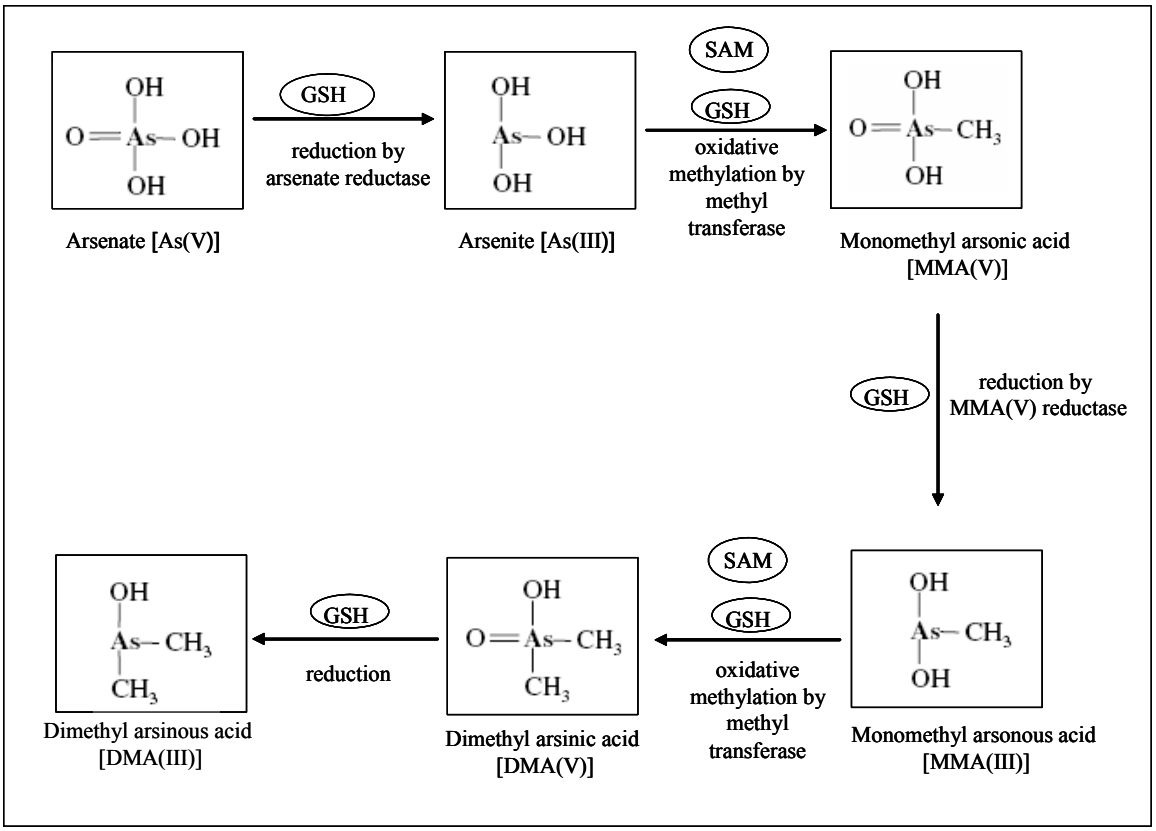

Fig. 3. Classical metabolic pathway of inorganic arsenic.
Adapted from Hayakawa et al., 2005.

In vitro studies have proposed the existence of As(III)-$(GS)_3$ complexes (Scott et al., 1993). Kala et al. (2000) showed that arsenic-glutathione complexes are excreted in bile using the rat as *in vivo* animal model. This study detected the presence of arsenic triglutathione (ATG) and methylarsonic diglutathione (MADG) in bile samples. Based on these studies, a new metabolic pathway for inorganic arsenic has been proposed (Hayakawa et al., 2005) (Fig. 4). According to this pathway, As(V) is reduced to As(III) as described previously in the original pathway. As(III) complexes with GSH in the presence of SAM and cyt19 to form ATG that in turn acquires 2 methyl groups forming MADG and dimethylarsinic glutathione (DMAG), respectively. MADG is then hydrolyzed to MMA(III), which is further oxidized to MMA(V). Similarly, DMAG is converted to DMA(V). This new pathway is in its infancy and additional studies will be needed to confirm the reaction steps. Also, the formation of various intermediates in this pathway has been demonstrated in *in vitro* conditions and needs further *in vivo* confirmation (Thomas et al., 2007, Aposhian and Aposhian, 2006).

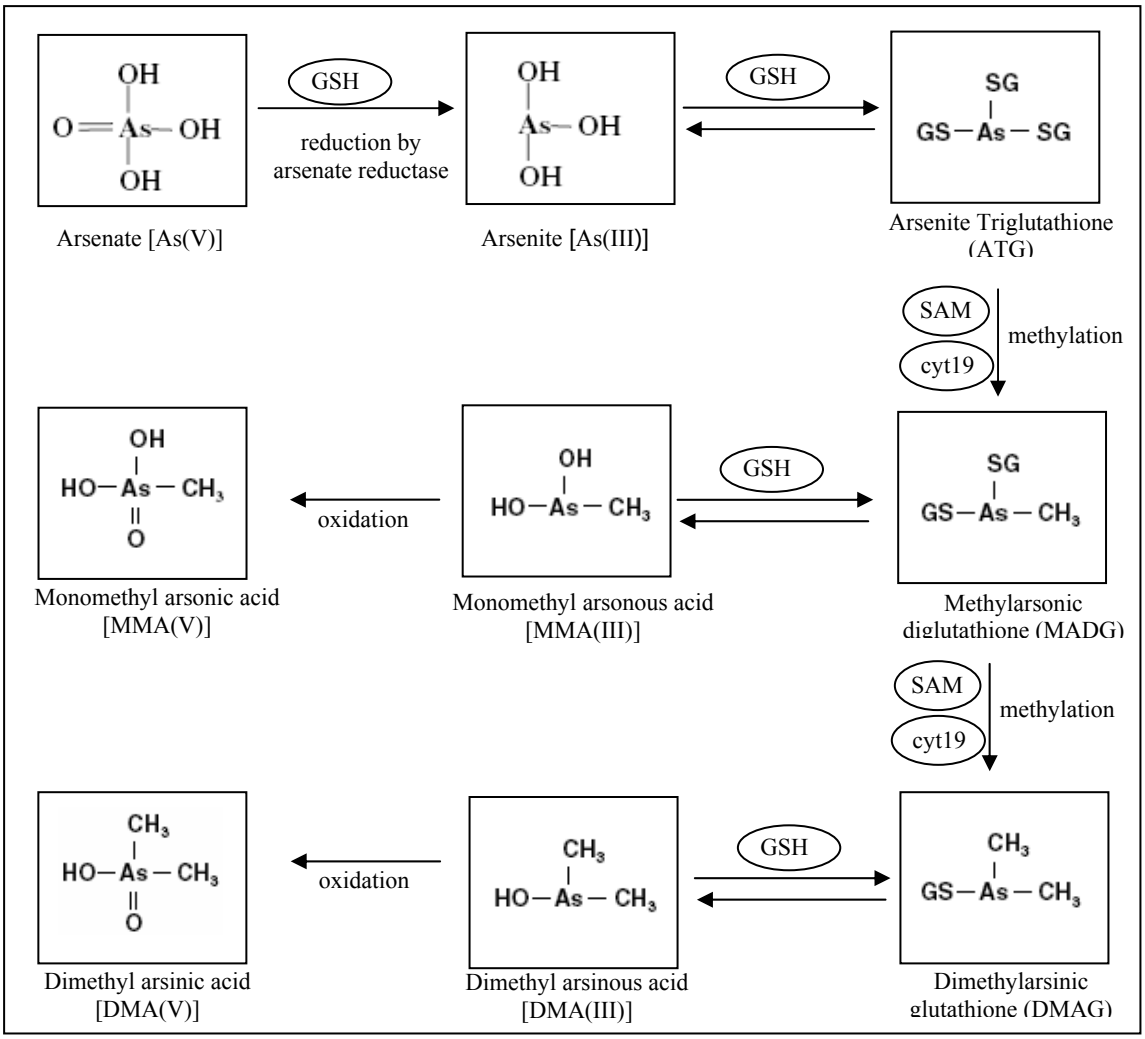

Fig. 4. New metabolic pathway of inorganic arsenic
Adapted from Hayakawa et al., 2005.

The bulk of data on metabolism of arsenic has been obtained from *in vitro* cell-free studies using rat liver cytosol, purified arsenic methyltransferase enzyme or rat hepatocytes. Styblo et al. (1999) documented the metabolism of arsenic using primary human hepatocytes. According to this study, human hepatocytes exposed to As(III) showed a steady decline in As(III) in the culture medium with simultaneous increase in MMA and DMA species. The formation of DMA accounted for 60% of the arsenic in the culture medium. In contrast, exposure of human hepatocytes to As(V) resulted in the total methylation yield (MMAs and DMAs) of less than 3%, probably due to the lower uptake of As(V) by hepatocytes (Styblo et al., 1999). However, it has been shown that majority of the ingested As(V) is rapidly reduced to As(III), probably in the blood (Vahter, 2002). Therefore, As(III) could be the major inorganic arsenic species metabolized by liver hepatocytes.

In mammals, liver is the primary organ for arsenic methylation. Other organs such as kidneys, lungs and testes also have arsenic methylating activity (Vahter, 2002). The major route of arsenic excretion is via the kidneys. MMA(V) and DMA(V) are the main metabolites found in the urine of humans exposed to arsenic. Variation in arsenic methylation between different populations groups have been reported based on the metabolites analyzed in urine samples (Vahter, 2002). Several factors such as age, gender, nutrition and polymorphisms in genes regulating the methyltransferases have been suggested to play a role in the inter-individual variation in arsenic metabolism. Irrespective of the arsenic concentration and the extent of exposure, on average, the human urine contains 10-30% inorganic arsenic, 10-20% MMA(V) and 60-80% DMA(V) (Vahter, 2000, Vahter, 2002). Considerable variation in the methylation of

arsenic has been reported among other mammalian species (Vahter, 1994). Compared to human subjects, animal species such as rat, mouse, dog, rabbit and hamster excrete very little MMA(V). The excretion of DMA(V) and inorganic arsenic also differs between species. Interestingly, the marmoset monkey and the chimpanzee lack the ability to methylate arsenic (Vahter, 1994, Vahter, 2000). This points out the species specific differences in the arsenic methylating enzymes and therefore, the results of arsenic metabolism studied using different species should be interpreted with caution.

1.3.3 Arsenic and Reactive Species

As(III) ($\leq$5 μM) has been shown to produce reactive oxygen species (ROS) including superoxide anion and hydrogen peroxide, but not reactive nitrogen species (RNS) such as nitric oxide in porcine aortic endothelial cells (Barchowsky et al., 1999). Increased levels of plasma superoxide have been positively correlated with arsenic concentration in whole blood of human subjects exposed to high arsenic levels in northeastern Taiwan (Wu et al., 2001). As(III) (>5 μM) has been shown to increase levels of nitric oxide in bovine aortic endothelial cells (Lynn et al., 1998; Liu and Jan, 2000). Furthermore, As(III) (>0.25 μM) has been shown to generate the RNS, peroxynitrite, in bovine aortic endothelial cells (Bunderson et al., 2002). Peroxynitrite is formed by the rapid reaction of superoxide with nitric oxide and is a strong oxidizing and nitrating molecule. Peroxynitrite can induce protein modifications via oxidation/nitration of cysteine, tyrosine, methionine and tryptophan residues (Pryor and Squadrito, 1995, Radi et al., 2001, Beckman, 1996). Formation of peroxynitrite can cause lipid peroxidation (Radi et al., 1991), generate oxLDLs (Keaney, 2000) and activate nuclear factor-kappa B

(NF-κB) (Cooke and Davidge, 2002, Matata and Galinanes, 2002). Peroxynitrite has been reported to interfere with cellular processes and signal transduction pathways by oxidation as well as nitration of proteins (Klotz et al., 2002). The detection of nitrotyrosine in biological samples has been used as a marker for the presence of peroxynitrite (Ischiropoulos, 1998, Beckman and Koppenol, 1996). The presence of nitrotyrosine has been observed in human atherosclerotic plaques (Beckman et al., 1994, Cromheeke et al., 1999). Also, nitrotyrosine formation has been detected in the atherosclerotic plaques of ApoE-/- /LDLr-/- mice exposed to As(III) in drinking water (Bunderson et al., 2004).

Contradictory to the increase in nitric oxide production in endothelial cells, it was observed that Chinese individuals exposed to arsenic in drinking water had reduced serum levels of nitric oxide metabolites indicating impaired nitric oxide generation (Pi et al., 2000). This observation was confirmed in rabbits exposed to 5 ppm As(V) in drinking water for 18 weeks (Pi et al., 2003). As(V) or As(III) (100 μM) were shown to suppress the activity of endothelial nitric oxide synthase (eNOS), the enzyme responsible for catalyzing production of nitric oxide, in the homogenates of human umbilical vein endothelial cells (HUVEC) (Pi et al., 2000). It was also observed that treatment of HAECs with As(III) ($\geq$10 μM) reduced eNOS activity, thereby suppressing nitric oxide production (Lee et al., 2003). However, Kao et al. (2003) demonstrated that As(III) (<5 μM) induces an increase in eNOS protein synthesis and production of nitric oxide in HUVECs. Therefore, it appears that the production of reactive species with arsenic treatment differs with the experimental conditions such as cell line in consideration and concentration of arsenic.

1.3.4 Arsenic and Cardiovascular Disease

Epidemiological studies have associated arsenic exposure with the development of CVDs. In the United States, a study conducted in 30 counties investigated the ecological relationship between population-weighted mean arsenic concentration in public water supplies and mortality from vascular disease from 1968 to 1984 (Engel and Smith, 1994). According to this study, exposure to arsenic levels greater than 20 ppb were associated with increased mortality from various CVDs such as coronary heart disease, peripheral arterial diseases and stroke (Engel and Smith, 1994, Navas-Acien et al., 2005). In Bangladesh, where the arsenic concentration is ground water ranges from 10-14,000 ppb (Wang and Wai, 2004), a study was conducted to determine the relationship between arsenic exposure and development of hypertension. After adjusting for age, sex and body mass index, a significant dose-response relationship was observed between concentration of arsenic in drinking water and prevalence of hypertension (Rahman et al., 1999). Arsenic exposure through drinking water has also been associated with the development of ischemic heart disease and carotid atherosclerosis based on studies conducted in Taiwan, where arsenic levels range from 100-1810 ppb (Wang and Wai, 2004). Wang et al. (2002) documented the effect of long-term arsenic exposure and extent of carotid atherosclerosis. By adjusting for the risk factors of atherosclerosis including age, sex, hypertension, diabetes mellitus, cigarette smoking, alcohol consumption, waist-to-hip ratio and cholesterol, a significant association was observed between arsenic exposure and prevalence of carotid atherosclerosis. A dose-response relationship was observed between the prevalence of carotid atherosclerosis and each of the three indices of arsenic exposure; duration of consumption of arsenic contaminated

water, average arsenic concentration in water and cumulative arsenic exposure (Wang et al., 2002). Atherosclerosis is the underlying cause of CVDs including ischemic heart disease. Tseng et al. (2003) documented the association of long-term arsenic exposure with ischemic heart disease. After adjusting for risk factors, prevalence rates for ischemic heart disease positively correlated with cumulative arsenic exposure (arsenic concentration in drinking water and duration of exposure) of 0.1 to $\geq$ 15 mg/l-year. Thus, epidemiological studies strongly associate arsenic exposure with development of CVD.

Several confounding factors can obscure or underestimate the severity of arsenic effects. For example, a majority of epidemiological studies have taken into account arsenic exposure through drinking water, but have not accounted for exposure due to other sources such as contaminated food or cooking water (Navas-Acien et al., 2005). Controlled animal studies have helped eliminate the confounding factors and confirm the association between high levels of arsenic exposure and development of CVD. It has been observed that exposure to 20 and 100 ppm As(III) in drinking water for 24 weeks accelerates atherogenesis in ApoE-/- mice (Simeonova et al., 2003). Our laboratory has previously demonstrated that chronic exposure (18 weeks) to 10 ppm As(III) in drinking water exacerbates atherosclerotic plaque formation in ApoE-/- /LDLr-/- mice (Bunderson et al., 2004). In addition, As(III) exposure has been documented to cause blood vessel dysfunction in a rat model. It was observed that intravenous injection of 1 mg/kg As(III) solution suppressed the acetylcholine-induced reduction of blood pressure (Lee et al., 2003) and augmented the phenylephrine-induced increase in blood pressure (Lee et al., 2005) in conscious male Sprague-Dawley rats. Thus, As(III) exposure possibly impairs vascular homeostasis and thereby contributes to the development of CVDs.

The vascular endothelium plays a critical role in the atherosclerotic disease process. *In vitro* and *in vivo* studies suggest that arsenic can modulate the inflammatory mediators involved in the process of atherosclerosis, generate oxidative and nitrosative stress and cause transcription factor activation and gene expression relevant to endothelial dysfunction. It has been observed that treatment of HAECs with 5 or 50 μM As(III) induces IL-8 gene expression with simultaneous increase in AP-1 and NF-κB DNA binding activity (Simeonova et al., 2003). Expression of the inflammatory mediator, IL-8, is regulated by the transcription factors AP-1 and NF-κB. Oxidant-sensitive activation of NF-κB has been documented in porcine aortic endothelial cells exposed to 2-5 μM As(III) (Barchowsky et al., 1996). In addition, As(III) (>5 μM) has been shown to increase the expression of inflammatory mediators such as cyclooxygenase-2 (Bunderson et al., 2002) and leukotriene E_4 (Bunderson et al., 2004) in bovine aortic endothelial cells as well as ApoE-/- /LDLr-/- mice exposed to 10 ppm As(III) for 18 weeks. As(V) and As(III) have also been related to the impairment of nitric oxide production in the vasculature as described previously in section 1.3.3 (Lee et al., 2003, Pi et al., 2003). Nitric oxide plays an important role in vascular homeostasis. This may contribute to arsenic-related hypertension as well as atherosclerosis. As(III) ($\geq$10 μM) has also been shown to cause platelet aggregation and thrombus formation (Lee et al., 2002). Thrombus formation could result in fatal consequences such as ischemic heart disease, myocardial infarction as well as stroke.

1.4 The Endothelium

1.4.1 Endothelial Junctions

Endothelial cells form two major types of cell-cell adhesion complexes, adherens junctions and tight junctions. In addition, endothelial cells have gap junctions that mediate cell-cell communication. The adherens junctions and tight junctions exist intermingled with each other at the boundaries of endothelial cells (Bazzoni and Dejana, 2004). The adherens junctions are thought to organize before the tight junctions and regulate the assembly of tight junctions (Liebner et al., 2006). The junctional complexes are in part responsible for maintaining vascular homeostasis. Endothelial cells are a heterogeneous population and there are differences in the cell-cell junctions between endothelial cells from different vascular beds. For example, the tight junctions in brain endothelial cells are well developed and maintain strict control of permeability. The venous endothelial cells on the other hand have poorly organized tight junctions to allow dynamic movement of plasma proteins. The arterial endothelial cells have well developed tight junctions and adherens junctions to maintain a semipermeable barrier. Accordingly, it has been observed that HAEC and HUVEC show different permeability levels when exposed to histamine (Ikeda et al., 1999). The authors showed that treatment of HAECs with various concentrations of histamine showed no difference in permeability as compared to untreated cells, whereas HUVECs showed a significant concentration-dependent increase in permeability. Under normal physiological conditions arterial endothelial cells allow the passage of molecules smaller than 4 nm through the intercellular junctions (Tedgui, 1996).

1.4.2 Adherens Junction of Endothelial Cells

The molecular components of adherens junction includes the endothelial cell specific vascular endothelial (VE)-cadherin and the catenins. VE-cadherin belongs to the cadherin family of transmembrane glycoproteins. It consists of a cytoplasmic domain and an extracellular region with five domains (EC1-EC5) (Fig. 5). VE-cadherin promotes homotypic adhesion between cells via its extracellular domains in a calcium (Ca^{2+}) dependent manner. The EC1 domain of the extracellular region is proposed to participate in the formation of cis/trans dimers and promote stable homophilic cell-cell adhesion (Ivanov et al., 2001, Bazzoni and Dejana, 2004, Steinberg and McNutt, 1999). The homophilic adhesion characteristics of cadherins were discovered when it was observed that co-culture of cells expressing different types of cadherins results in aggregation of cells with identical cadherins (Nose et al., 1988, Ivanov et al., 2001). The intercellular adhesion mediated by VE-cadherin is Ca^{2+} sensitive. It has been observed that exposure of HUVECs to 3 mM Ca^{2+} chelator, EGTA, causes the loss of VE-cadherin immunostaining. Also, exposure of HUVECs to low Ca^{2+} ($<10^{-7}$ M) in serum free medium was observed to induce intercellular gaps that were reversible with the introduction of medium containing serum and Ca^{2+} (Schnittler et al., 1997). VE-cadherin along with other cadherins such as epithelial (E), neural (N), placental (P) and retinal (R) belongs to the class of type I classical cadherins. The type II classical cadherins include the recently discovered cadherins that are yet to be characterized (Ivanov et al., 2001).

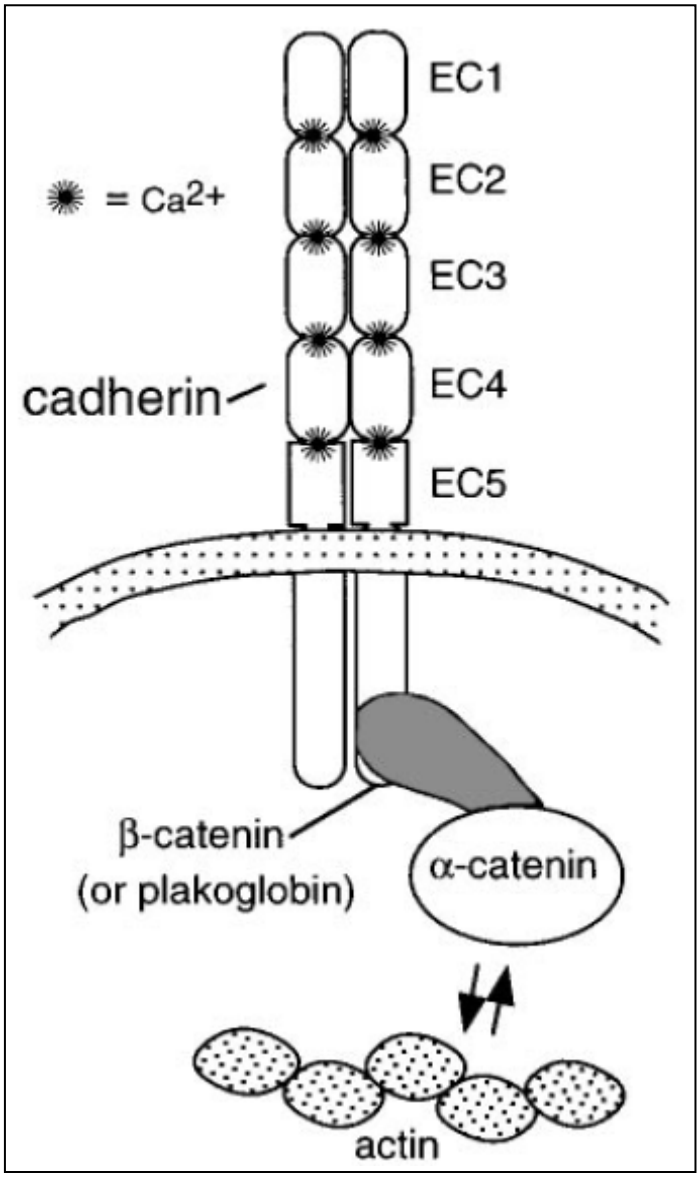

Fig. 5. The cadherin-catenin complex and actin cytoskeleton.
Reprinted, with permission, from the Annual Review of Cell and Developmental Biology, Volume 13 ©1997 by Annual Reviews www.annualreviews.org

The cytoplasmic domain of VE-cadherin associates with β-catenin that in turn is linked to the actin cytoskeleton via α-catenin (Ivanov et al., 2001) (Fig. 3). This association is extremely important to maintain endothelial monolayer integrity. It has been observed that mutant VE-cadherin with a truncated cytoplasmic domain, promotes cell-cell adhesion via the extracellular domains but the association with β-catenin and actin cytoskeleton is severely impaired (Navarro et al., 1995). As a result, the junctional stability is compromised with increased endothelial permeability. The formation of a stable cadherin-catenin complex has also been shown to be important for endothelial cell survival as it activates phosphoinositide 3-kinase (PI3K) and Akt phosphorylation (Carmeliet et al., 1999, Liebner et al., 2006). Other catenins such as γ-catenin (also known as plakoglobin) and p120 catenin have been shown to associate with the adherens junction complex. γ-Catenin has been shown to associate with the VE-cadherin in HUVECs after formation of stable cell-cell adhesions and is proposed to strengthen the adherens junction complex (Lampugnani et al., 1995, Schnittler et al., 1997). p120 catenin associates with the membrane proximal region of the cytoplasmic domain of VE-cadherin and does not interact with any of the other catenins. Its role in cell-cell adhesion has yet to be elucidated (Bazzoni and Dejana, 2004, Anastasiadis and Reynolds, 2000).

The tyrosine phosphorylation of adherens junction proteins plays a critical role in the formation and maintenance of stable cell-cell adhesions. Tyrosine phosphorylation of VE-cadherin and β-catenin is a normal physiological process. It has been observed using HUVECs that loosely or recently confluent cells have increased tyrosine phosphorylation of VE-cadherin and β-catenin (Lampugnani et al., 1997). The tyrosine phosphorylation levels decrease when endothelial cells reach the fully confluent state. Furthermore, if the

confluent endothelial monolayer is damaged, the cells at the migrating front show increased tyrosine phosphorylation of VE-cadherin and β-catenin (Lampugnani et al., 1997). The tyrosine phosphorylation of VE-cadherin and/or β-catenin can alter their interaction with each other as well as the actin cytoskeleton. Association of adherens junction proteins with the actin cytoskeleton is extremely important for maintaining the mechanical strength and stability of the endothelial monolayer. The endogenous mediator, histamine (10^{-4} M), has been shown to increase tyrosine phosphorylation of both β-catenin and VE-cadherin in HUVECs or human dermal microvascular endothelial cells (HMEC). This was accompanied by a decrease in the association of VE-cadherin with the actin cytoskeleton as analyzed by the reduced distribution of VE-cadherin in the detergent insoluble fraction (Andriopoulou et al., 1999). Intercellular gaps with increased permeability were also observed with histamine treatment, implying that the VE-cadherin mediated adhesion was compromised (Andriopoulou et al., 1999). Vascular endothelial growth factor (VEGF) (50-100 ng/ml) has been shown to increase tyrosine phosphorylation of VE-cadherin and β-catenin causing the loosening of adherens junctions and increased permeability in HUVECs (Esser et al., 1998). The increase in permeability due to disruption of the endothelial monolayer could accelerate atherogenesis by increasing the transmigration of oxLDLs and monocytes into the intima of blood vessels. Accordingly, it has been observed that injection of anti-VE-cadherin blocking antibody into the tail vein of mice increased vascular permeability with damage to the endothelial lining and deposition of monocytes and neutrophils in the areas of exposed basement membrane (Corada et al., 1999). Similarly, another study documented that intravenous injection of anti-VE-cadherin antibody increases vascular permeability

and accelerates neutrophil entry into chemically inflamed mouse peritoneum (Gotsch et al., 1997).

There are several protein tyrosine kinases such as Fyn, Fer, cMet, Abl and Src as well as protein tyrosine phosphatases such as PTP1B, SHP1, SHP2 and VE-PTP that have been shown to associate with and modulate the phosphorylation state of the cadherin-catenin complex (Lilien and Balsamo, 2005, Yuan, 2003, Bogatcheva et al., 2003, Xu et al., 2004, Daniel and Reynolds, 1997). The exact role of each of the tyrosine kinases and phosphatases has yet to be elucidated, but each of these might act in an unique temporal and spatial context to maintain stable cadherin-catenin mediated cell-cell adhesion. It has been observed that the endothelial cell-specific protein tyrosine phosphatase, VE-PTP, reduces the tyrosine phosphorylation of VE-cadherin induced by VEGF and strengthens the cell-cell adhesion (Nawroth et al., 2002, Bazzoni and Dejana, 2004). Phosphorylation of β-catenin at tyrosine 654 by Src has been shown to cause a fivefold reduction in its affinity for E-cadherin (Roura et al., 1999), which belongs to the same class of type I classical cadherins as VE-cadherin (Ivanov et al., 2001). Therefore, the phosphorylation/dephosphorylation states of the cadherin-catenin complex may be modulated by complex interplay between tyrosine kinase and phosphatase activities.

1.5 Stress Fibers

Endothelial cells contain two pools of actin. Globular actin (G-actin) is the monomeric form, which can undergo polymerization to form filamentous actin (F-actin) (DuBose and Haugland, 1993, Oosawa, 2001). In nonmuscle cells such as endothelial cells and fibroblasts, F-actin is involved in cell activities such as locomotion, cell

adhesion, cytokinesis and maintenance of cell shape. Under normal physiological conditions and in confluent endothelial cell culture, F-actin forms the dense peripheral band (DPB) that is a thin layer of actin microfilaments near the plasma membrane (Wong and Gotlieb, 1990, Guyton et al., 1989, Colangelo et al., 1998). F-actin also forms the cytoplasmic stress fibers that extend from the cells periphery towards the central regions or in some cases crossing the entire cell. Very few stress fibers may be visible in normal endothelial cells, but can be dramatically increased in pathological conditions such as hypertension and atherosclerosis (White et al., 1983, Guyton et al., 1989, Colangelo et al., 1998). F-actin of the DPB is linked to the cadherin-catenin complex and plays a critical role in maintaining endothelial monolayer integrity. Actin reorganization associated with disruption of the endothelial barrier is characterized by increased stress fiber density and reduction or loss of the DPB (Lum and Roebuck, 2001).

Stress fibers consist of several proteins such as myosin, tropomyosin and α-actinin intermittently associated with the F-actin filaments (Byers et al., 1984). Stress fibers are contractile elements. Stress fibers isolated from cultured human foreskin fibroblast and bovine aortic endothelial cells have been shown to contract/shorten to approximately 23% of the initial length (Katoh et al., 1998). Mitogenic stimulation of 3T3 fibroblast with 10% serum or 10 nM thrombin has been shown to induce contraction of stress fibers accompanied by retraction of cell edges (Giuliano and Taylor, 1990).

The formation of stress fibers is regulated by the phosphorylation of myosin light chain (MLC) of myosin II. Phosphorylation of MLC causes a conformational change in the myosin molecule and promotes its association with actin, resulting in the assembly of stress fibers (van Nieuw Amerongen and van Hinsbergh, 2001). The Ca^{2+}/calmodulin-

dependent myosin light chain kinase (MLCK) is considered to be the primary regulator of MLC phosphorylation, since the K_m of MLCK for MLC is 52 μM/L. The small GTPase, Rho, has also been shown to modulate phosphorylation of MLC and development of stress fibers by several mechanisms (van Nieuw Amerongen and van Hinsbergh, 2001). Rho GTPase has been shown to phosphorylate MLC through Rho kinase. The K_m of Rho kinase for MLC is 0.91 μM/L. Rho GTPase has also been shown to inhibit the myosin phosphatase type 1 (PP1M) responsible for dephosphorylation of MLC. In addition, Rho GTPase has been proposed to induce stress fiber formation by induction of actin polymerization and inhibition of actin depolymerization (van Nieuw Amerongen and van Hinsbergh, 2001).

Disruption of endothelial monolayer integrity and increased endothelial permeability have been associated with the development of stress fibers. It has been shown that exposure of endothelial cells to apolipoprotein(a) component of lipoprotein(a), a risk factor for atherosclerotic disorders, induces cytoplasmic stress fibers with simultaneous loss of the DPB and VE-cadherin dispersion. This was accompanied by cell retraction, intercellular gap formation and increased endothelial permeability in HUVEC as well as HCAECs (Pellegrino et al., 2004). The formation of stress fibers was shown to be dependent on increased phosphorylation of MLC by Rho GTPase and Rho-kinase. Inhibition of Rho GTPase and Rho-kinase by pretreating HUVECs with C3 transferase and Y-27632, respectively, inhibited MLC phosphorylation, abolished the formation of stress fibers and restored VE-cadherin at the cell-cell junctions. The phosphorylation of MLC was also found to be Ca^{2+} dependent, although no increase in intracellular Ca^{2+} was observed (Pellegrino et al., 2004). Other mediators of vascular

permeability such as thrombin and histamine have also been shown to induce formation of stress fibers. It has been observed that treatment of HUVECs with 1 μM α-thrombin or histamine increases intracellular Ca^{2+} levels and formation of stress fibers with a simultaneous increase in endothelial permeability (Ehringer et al., 1996, Ehringer et al., 1999). Sandoval et al. (2001) further demonstrated that exposure of HUVECs to 10 nM thrombin increases intracellular Ca^{2+} levels and MLC phosphorylation with a concomitant increase in stress fibers. An increase in endothelial permeability was also recorded. The authors suggest the involvement of Rho GTPase mediated signaling in the observed effects.

The *in vivo* presence of stress fibers has been reported during hypertension and atherosclerosis. It was observed that the aortic endothelium of spontaneously hypertensive rats had more than a twofold higher proportion of endothelial cells containing stress fibers than the age and sex-matched Wistar-Kyoto normotensive rats (White et al., 1983). The stress fibers in the Wistar-Kyoto normotensive rats were also thinner as compared to those in spontaneously hypertensive rats. The development of stress fibers in atherosclerotic conditions was demonstrated using New Zealand white rabbits. Guyton et al. (1989) demonstrated that 80% of the endothelial cells from control aortas had either no stress fibers or were narrow, thin and no more than 1/3 the length of the cell, if present. The same pattern of expression was also found in nonlesioned areas of experimental cholesterol fed animals. The stress fibers in endothelial cells near and over the atherosclerotic lesions were much more numerous than those observed in control animals and extended the entire length of the endothelial cells. Furthermore, Colangelo et al. (1998) characterized the stress fibers in early, minimal, intermediate and advanced

lesions in rabbits fed with a high fat diet. The early lesions were characterized by adhesion of leukocytes to the endothelium, minimal lesions consisted of few cells in the subendothelium, intermediate lesions had numerous subendothelial leukocytes and the advanced lesions consisted of several layers of leukocytes. The endothelial areas with early lesions showed normal actin distribution as DPB. The minimal lesion areas showed few cytoplasmic stress fibers whereas the intermediate lesion areas showed a decrease of DPB and prominent cytoplasmic stress fibers. Isolated thick bundles of stress fibers were also observed. Interestingly, the areas of advanced lesions showed no or few cytoplasmic stress fibers (Colangelo et al., 1998). The authors suggested that the pattern of expression of stress fibers signifies their involvement in the early stages of atherogenesis by increasing endothelial permeability and transmigration of monocytes.

1.6 Protein Kinase C

1.6.1 Structure of Protein Kinase C

The protein kinase C (PKC) family members are serine/threonine kinases and have been grouped into 3 classes based on their structural and enzymatic properties: classical or conventional, novel and atypical PKC isotypes (Mellor and Parker, 1998, Newton, 2001). The classical PKC (cPKC) includes α, the alternatively spliced β_1 and β_2, and γ subtypes. The β_1 and β_2 isoforms differ at the C-terminal kinase domain; PKCβ_1 has 50 residues and PKCβ_2 has 52 residues (Kawakami et al., 2002). The novel PKC (nPKC) consist of η, ε, δ and θ subtypes, and the ι and ζ subtypes belong to the atypical class of PKC (aPKC). All members contain a regulatory region and a kinase domain that are connected with each other by a proteolytically labile hinge region. The regulatory region

consists of the pseudosubstrate site, and C1 and C2 domains. The kinase domain consists of binding sites for ATP and substrate. The pseudosubstrate site of the regulatory region interacts with the kinase domain and is responsible for suppression of PKC catalytic activity. The C1 and C2 domains are the membrane-targeting modules. The C1 domain binds diacylglycerol (DAG) and phosphatidyl serine (PS), and the C2 domain binds Ca^{2+}. The regulatory region of the cPKCs includes the C1 and C2 domains and requires Ca^{2+}, DAG and PS for activation. The nPKCs also consist of C1 and C2 domains in the regulatory region but the C2 domain does not bind Ca^{2+} and therefore requires only DAG and PS for activation. The aPKCs possess only the C1 domain and require only PS for activation (Mellor and Parker, 1998, Newton, 2001).

1.6.2 Regulation of Classical Protein Kinase C isoforms

The activation and physiological function of cPKC isoforms is strictly regulated by phosphorylation, binding of cofactors and subcellular localization (Newton, 2001). Phosphorylation is the first step that primes newly synthesized cPKCs for catalytic activity. cPKC isoforms are phosphorylated at one serine and two threonine residues in the kinase domain. Phosphoinositide dependent kinase-1 (PDK-1) phosphorylates a threonine residue (T497 in case of PKCα, T500 for PKC β_1 and β_2 and T514 for PKCγ), following which the other threonine and serine residues are autophosphorylated. The phosphorylation by PDK-1 is proposed to be constitutive, but dependent on a specific conformation of cPKC (Newton, 2001, Sonnenburg et al., 2001, Newton, 2003). The phosphorylated PKC molecule remains inactive in the cytosol until activated by cofactors (Ca^{2+}, DAG and PS). An increase in intracellular Ca^{2+} promotes its binding to

phosphorylated PKC in the cytosol. Ca^{2+} binding triggers translocation of phosphorylated PKC to the membrane and binding of DAG and PS for complete activation. Phorbol esters that mimic DAG, are extremely potent activators of cPKCs and can cause membrane translocation and activation without the need for PS or increased intracellular Ca^{2+} (Newton, 2001). Apart from the cofactor based activation of cPKCs, their activity has also been shown to be modulated by tyrosine phosphorylation (Konishi et al., 1997), oxidative modification of the regulatory region (Gopalakrishna and Anderson, 1989), and proteolysis at the hinge region (Kishimoto, et al., 1989).

The subcellular localization of the PKC isoforms plays a critical role in their biological activity. Several proteins have been identified that interact with the different PKC isoforms and position them in specific intracellular compartments or in close proximity to the substrates, phosphatases or other kinases (Ron and Kazanietz, 1999). For example, it has been observed that syndecan-4, a member of the transmembrane matrix binding proteoglycans, associates with PMA activated PKCα and potentiates its activity. This complex may colocalize to the focal adhesions (Oh et al., 1997). Another anchoring protein, receptor for activated C kinase 1 (RACK1), has been shown to associate only with activated $PKC\beta_2$ and regulate its intracellular localization (Newton, 2001, Ron and Kazanietz, 1999). Interestingly, it was observed that the association of activated PKC with RACK1 promotes the binding of RACK1 with Src tyrosine kinase (Chang et al., 2001). Thus, RACK1 possibly mediates the cross talk between serine/threonine and tyrosine kinase signaling pathways (Bauman and Scott, 2002, Chang et al., 2001). Further identification and characterization of PKC binding proteins will aid in our understanding of the complex regulation of PKC activities. Also, depending on cell types and

experimental conditions, the activation and translocation of PKCs may differ. It was observed that in response to different stimulating agents, PKCα translocation varies within the same cell type and experimental conditions. Treatment of A7r5 smooth muscle cells with 10^{-8} M phorbol 12, 13 dibutyrate, 10^{-5} M thapsigargin, 2 x 10^{-5} M A23187 or 10^{-6} M angiotensin II induced a varied spatial and temporal response in PKCα translocation (Li et al., 2002). Furthermore, varying subcellular localization of the different PKC isoforms (α, β_1, β_2, γ, δ, ε, ζ and η) was observed when NIH 3T3 fibroblasts were stimulated with 100 nM 12-O-tetradecanoylphorbol-13-acetate (TPA) (Goodnight et al., 1995).

1.6.3 Classical Protein Kinase C and Regulation of the Endothelial barrier

Tyrosine phosphorylation of adherens junction proteins as well as development of stress fibers could adversely affect the endothelial barrier. The cPKC isoforms, α and β, have been implicated in the modulation of the endothelial barrier. It has been observed that activation of PKCα by 50 nM α-thrombin activates Rho GTPase by dissociating it from guanine dissociation inhibitor (GDI) in HUVECs (Mehta et al., 2001). The GDI sequesters Rho in its GDP bound form and thereby prevents its activation (Rolfe et al., 2005). Activated PKCα was also found to associate with Rho GTPase (Mehta et al., 2001). Activation of Rho GTPase has been shown to induce stress fiber formation. Also, activation of PKCα in HUVECs by 10 nM thrombin has been shown to cause MLC phosphorylation with concomitant increase in stress fibers and endothelial permeability (Sandoval et al., 2001). VEGF (100 ng/ml) has been shown to induce tyrosine phosphorylation of β-catenin in a PKC dependent manner in bovine pulmonary artery

endothelial cells, although the exact PKC isoform involved was not determined (Cohen et al., 1999). Wang et al. (2004) further showed that 100 ng/ml VEGF mediates activation of PKCβ_1 and β_2 isoforms in HUVECs and disrupts the association of VE-cadherin with β-catenin. Inhibition of PKCα has been demonstrated to inhibit the ischemia-induced endothelial permeability in porcine endothelial cells (Hempel et al., 1999). *In vivo* use of PKCβ inhibitors in the treatment of vascular complications in diabetes mellitus has been reported (Meier and King, 2000). Therefore, PKCs play a significant role in regulation of the endothelial barrier.

1.7 Summary

Arsenic exposure has been associated with the development of CVD including atherosclerosis. During the atherosclerotic process, the semipermeable property of the endothelium is severely impaired. The endothelium is the most important barrier between the blood and vessel wall, and adherens junction proteins play a significant role in the maintenance of this barrier. The cadherin-catenin complex of the adherens junction associates with the actin cytoskeleton that provides the strength and stability to the endothelial barrier. The effects of arsenic on the proteins involved in maintaining endothelial integrity remain unknown. Endogeneous mediators have implicated cPKCs in the modulation of endothelial integrity. However, the effects of arsenic on PKC activation vary with the experimental conditions. Arsenic has been shown to induce peroxynitrite generation that can modulate signaling pathways. Controversial data exist regarding the effects of peroxynitrite in activation of PKCs. Using human aortic endothelial cells (HAECs), our laboratory tested the hypothesis that arsenic, via

generation of peroxynitrite, induces the activation of cPKC (α and β) isotypes resulting in the loss of endothelial monolayer integrity characterized by formation of actin stress fibers, disruption of adherens junctions and increased endothelial permeability. Epidemiological and animal studies have established the relationship between arsenic exposure and atherosclerosis. But the time- and concentration-dependent effects of arsenic in the development of atherosclerosis remain unknown. Therefore, we analyzed the effects of low and environmentally relevant concentrations of arsenic on atherogenesis using the ApoE-/- /LDLr-/- mouse model.

1.8 References

1. Abernathy, C.O., Liu, Y.P., Longfellow, D., Aposhian, H.V., Beck, B., Fowler, B., Goyer, R., Menzer, R., Rossman, T., Thompson, C., Waalkes, M., 1999. Arsenic health effects, mechanisms of action, and research issues. Environ. Health Perspect. 107, 593-597.
2. Anastasiadis, P.Z., Reynolds, A.B., 2000. The p120 catenin family: complex roles in adhesion, signaling and cancer. J. Cell Sci. 113, 1319-1334.
3. Andriopoulou, P., Navarro, P., Zanetti, A., Lampugnani, M.G., Dejana, E., 1999. Histamine induces tyrosine phosphorylation of endothelial cell-to-cell adherens junctions. Arterioscler. Thromb. Vasc. Biol. 19, 2286-2297.
4. Aposhian, H.V., Aposhian, M.M., 2006. Arsenic toxicology: five questions. Chem. Res. Toxicol. 19(1), 1-15.
5. Aposhian, H.V., Zakharyan, R.A., Avram, M.D., Sampayo-Reyes, A., Wollenberg, M.L., 2004. A review of enzymology of arsenic metabolism and a new potential role of hydrogen peroxide in the detoxification of the trivalent arsenic species. Toxicol. Appl. Pharmacol. 198, 327-335.
6. Barchowsky, A., Dudek, E.J., Treadwell, M.D., Wetterhahn, K.E., 1996. Arsenic induces oxidant stress and NF-κB activation in cultured aortic endothelial cells. Free Radic. Biol. Med. 21(6), 783-790.
7. Barchowsky, A., Klei, L.R., Dudek, E.J., Swartz, H.M., James, P.E., 1999. Stimulation of reactive oxygen, but not reactive nitrogen species, in vascular endothelial cells exposed to low levels of arsenite. Free Radic. Biol. Med. 27(11/12), 1405-1412.

8. Bauman, A.L., Scott, J.D., 2002. Kinase- and phosphatase-anchoring proteins: harnessing the dynamic duo. Nat. Cell Biol. 4, E203-E206.
9. Bazzoni, G., Dejana, E., 2004. Endothelial cell-to-cell junctions: molecular organization and role in vascular homeostasis. Physiol. Rev. 84, 869-901.
10. Beckman, J.S., 1996. Oxidative damage and tyrosine nitration from peroxynitrite. Chem. Res. Toxicol. 9, 836-844.
11. Beckman, J.S., Koppenol, W.H., 1996. Nitric oxide, superoxide and peroxynitrite: the good, the bad, and the ugly. Am. J. Physiol. 271, C1424-C1437.
12. Beckman, J.S., Ye, Y.Z., Anderson, P.G., Chen, J., Accavitti, M.A., Tarpey, M.M., White, R., 1994. Extensive Nitration of protein tyrosines in human atherosclerosis detected by immunohistochemistry. Biol. Chem. Hoppe Seyler. 375, 81-88.
13. Bogatcheva, N.V., Garcia, J.G.N., Verin, A.D., 2003. Role of tyrosine kinase signaling in endothelial cell barrier regulation. Vascul. Pharmacol. 39, 201-212.
14. Buchet, J.P., Lauwerys, R., 1988. Role of thiols in the in-vitro methylation of inorganic arsenic by rat liver cytosol. Biochem. Pharmacol. 37(16), 3149-3153.
15. Bunderson, M., Brooks, D.M., Walker, D.L., Rosenfeld, M.E., Coffin, D.J., Beall, H.D., 2004. Arsenic exposure exacerbates atherosclerotic plaque formation and increases nitrotyrosine and leukotriene biosynthesis. Toxicol. Appl. Pharmacol. 201, 32-39.
16. Bunderson, M., Coffin, D.J., Beall, H.D., 2002. Arsenic induces peroxynitrite generation and cyclooxygenase-2 protein expression in aortic endothelial cells: possible role in atherosclerosis. Toxicol. Appl. Pharmacol. 184, 11-18.

17. Byers, H.R., White, G.E., Fujiwara, K., 1984. Organization and function of stress fibers in cells in vitro and in situ. Cell Muscle Motil. 5, 83-137.

18. Carmeliet, P., Lampugnani, M-G., Moons, L., Breviario, F., Compernolle, V., Bono, F.O., Balconi, G., Spagnuolo, R., Oosthuyse, B., Dewerchin, M., Zanetti, A., Angellilo, A., Mattot, V., Nuyens, D., Lutgens, E., Clotman, F., de Ruiter, M-C., Gittenberger-de Groot, A., Poelmann, R., Lupu, F., Herbert, J.M., Collen, D., Dejana, E., 1999. Targeted deficiency or cytosolic truncation of the VE-cadherin gene in mice impairs VEGF-mediated endothelial survival and angiogenesis. Cell. 98, 147-157.

19. Chang, B.Y., Chiang, M., Cartwright, C.A., 2001. The interaction of Src and RACK1 is enhanced by activation of protein kinase C and tyrosine phosphorylation of RACK1. J. Biol. Chem. 276(23), 20346-20356.

20. Cheng, C., Tempel, D., van Haperen, R., van der Baan, A., Grosveld, F., Daemen, M.J.A.P., Krams, R., de Crom, R., 2006. Atherosclerotic lesion size and vulnerability are determined by patterns of fluid shear stress. Circulation. 113, 2744-2753.

21. Cohen, A.W., Carbajal, J.M., Schaeffer JR, R.C., 1999. VEGF stimulates tyrosine phosphorylation of β-catenin and small-pore endothelial barrier dysfunction. Am. J. Physiol. 277, H2038-H2049.

22. Colangelo, S., langille, B.L., Steiner, G., Gotlieb, A.L., 1998. Alterations in endothelial F-actin microfilaments in rabbit aorta in hypercholesterolemia. Arterioscler. Thromb. Vasc. Biol. 18, 52-56.

23. Cooke, C.L., Davidge, S.T., 2002. Peroxynitrite increases iNOS through NF-kappaB and decreases prostacyclin synthase in endothelial cells. Am. J. Physiol. Cell Physiol. 282(2), C395-402.

24. Corada, M., Mariotti, M., Thurston, G., Smith, K., Kunkel, R., Brockhaus, M., Lampugnani, M.G., Martin-Padura, I., Stoppacciaro, A., Ruco, L., McDonald, D.M., Ward, P.A., Dejana, E., 1999. VE-cadherin is an important determinant of microvascular permeability in vivo. Proc. Natl. Acad. Sci. 96, 9815-9820.

25. Cromheeke, K. M., Kockx, M.M., De Meyer G, R.Y., Bosmans, J.M., Bult, H., Beelaerts, W.J.F., Vrints, C.J., Herman, A.G., 1999. Inducible nitric oxide synthase colocalizes with signs of lipid oxidation/peroxidation in human atherosclerotic plaques. Cardiovasc. Res. 43, 744–754.

26. Cybulsky, M.I., Iiyama, K., Li, H., Zhu, S., Chen, M., Iiyama, M., Davis, V., Gutierrez-Ramos, J-C., Connelly, P.W., Milstone, D.S., 2001. A major role for VCAM-1 but not ICAM-1 in early atherosclerosis. J. Clin. Invest. 107, 1255-1262.

27. Daniel, J.M., Reynolds, A.B., 1997. Tyrosine phosphorylation and cadherin/catenin function. Bioessays. 19(10), 883-891.

28. Daugherty, A., 2002. Mouse models of atherosclerosis. Am. J. Med. Sci. 323(1), 3-10.

29. Delemos, J.L., Bostick, B.C., Renshaw, C.E., Stürup, S., Feng, X., 2006. Landfill-stimulated iron reduction and arsenic release at the coakley superfund site. Environ. Sci. Technol. 40, 67-73.

30. DuBose, D.A., Haugland, R., 1993. Comparison of endothelial cell G-and F-actin distribution in situ and in vitro. Biotech. Histochem. 6(1), 8-16.

31. Ehringer, W.D., Edwards, M.J., Miller, F.N., 1996. Mechanisms of α-thrombin, histamine and bradykinin induced endothelial permeability. J. Cell. Physiol. 176, 562-569.

32. Ehringer, W.D., Yamany, S., Steier, K., Farag, A., Roisen, F.J., Dozier, A., Miller, F.N., 1999. Quantitative image analysis of F-actin in endothelial cells. Microcirculation. 6, 291–30.

33. Engel, R.R., Smith, A.H., 1994. Arsenic in drinking water and mortality from vascular disease: an ecologic analysis in 30 counties in the United States. Arch. Environ. Health. 49, 418-427.

34. Erren, M., Reinecke, H., Junker, R., Fobker, M., Schulte, H., Schurek, J.O., Kropf, J., Kerber, S., Breithardt, G., Assmann, G., Cullen, P., 1999. Systemic inflammatory parameters in patients with atherosclerosis of the coronary and peripheral arteries. Arterioscler Thromb Vasc Biol. 19, 2355-2363.

35. Esser, S., Lampugnani, M.G., Corada, M., Dejana, E., Risau, W., 1998. Vascular endothelial growth factor induces VE-cadherin tyrosine phosphorylation in endothelial cells. J.Cell Sci. 111, 1853-1865.

36. Giuliano, K.A., Taylor, D.L., 1990. Formation, transport, contraction and disassembly of stress fibers in fibroblast. Cell Motil. Cytoskeleton. 16(1), 14-21.

37. Goodnight, J., Mischak, H., Kolch, W., Mushincki, J.F., 1995. Immunocytochemical localization of eight protein kinase C isozymes overexpressed in NIH 3T3 fibroblast. J. Biol. Chem. 270(17), 9991-10001.

38. Gopalakrishna, R., Anderson, W.B., 1989. Ca^{2+} - and phospholipid-independent activation of protein kinase C by selective oxidative modification of the regulatory domain. Proc. Natl. Acad. Sci. U.S.A. 86, 6758-6762.

39. Gotsch, U., Borges, E., Bosse, R., Boggemeyer, E., Simon, M., Mossmann, H., Vestweber, D., 1997. VE-cadherin antibody accelerates neutrophil recruitment in vivo. J. Cell Sci. 110, 583-588.

40. Greenow, K., Pearce, N.J., Ramji, D.P., 2005. The key role of apolipoprotein E in atherosclerosis. J. Mol. Med. 83, 329-342.

41. Gregus, Z., Neméti, B., 2005. The glycolytic enzyme glyceraldehydes-3-phosphate dehydrogenase works as an arsenate reductase in human red blood cells and rat liver cytosol. Toxicol. Sci. 85, 859-869.

42. Guyton, J.R., Shaffer, D.R., Henry, P.D., 1989. Stress fibers in endothelial cells overlaying atherosclerotic lesions in rabbit aorta. Am. J. Med. Sci. 298(2), 79-82.

43. Hayakawa, T., Kobayashi, Y., Hirano, X.C.S., 2005. A new metabolic pathway of arsenite: arsenic-glutathione complexes are substrates for human arsenic methytransferase cyt19. Arch. Toxicol. 79, 183-191.

44. Hempel, A., Lindschau, C., Maasch, C., Mahn, M., Bychkov, R., Noll, T., Luft, F.C., Haller, H., 1999. Calcium antagonist ameliorate ischemia-induced endothelial cell permeability by inhibiting protein kinase C. Circulation. 99, 2523-2529.

45. Huang, R., Lee, T., 1996. Cellular uptake of trivalent arsenite and pentavalent arsenate in KB cells cultured in phosphate-free medium. Tox. Appl. Pharmacol. 136, 243-249.

46. Ikeda, K., Utoguchi, N., Makimoto, H., Mizuguchi, H., Nakagawa, S., Mayumi, T., 1999. Different reactions of aortic and venular endothelial cell monolayers to histamine on macromolecular permeability: Role of cAMP, Cytosolic Ca^{2+} and F-actin. Inflammation 23(1), 87-97.

47. Ikeda, U., Ohkawa, F., Seino, Y., Yamamoto, K., Hidaka, Y., Kasahara, T., Kawai, T., Shimada, K., 1992. Serum interleukin 6 levels become elevated in acute myocardial infarction. J. Mol. Cell. Cardiol. 24(6), 579-584.

48. Ischiropoulos, H., 1998. Biological tyrosine nitration: a pathophysiological function of nitric oxide and reactive oxygen species. Arch. Biochem. Biophys. 356, 1-11.

49. Ishibashi, S., Herz, J., Maeda, N., Goldstein, J.L., Brown, M.S., 1994. The two-receptor model of lipoprotein clearance: Test of the hypothesis in "knockout" mice lacking the low density lipoprotein receptor, apolipoprotein E, or both proteins. Proc. Natl. Acad. Sci. USA 91, 4431-4435.

50. Ivanov, D.B., Philippova, M.P., Tkachuk, V.A., 2001. Structure and functions of classical cadherins. Biochemistry 66(10), 1174-1186.

51. Jaweiń, J., Nastalek, P., Korbut, R., 2004. Mouse models of experimental atherosclerosis. J. Physiol. Pharmacol. 55(3), 503-517.

52. Kala, S.V., Neely, M.W., Kala, G., Prater, C.I., Atwood, D.W., Rice, J.S., Lieberman, M.W., 2000. The MRP2/cMOAT transporter and arsenic-glutathione complex formation are required for biliary excretion of arsenic. J. Biol. Chem. 275(43), 33404-33408.

53. Kao, Y-H., Yu, C-L., Chang, L-W., Yu, H-S., 2003. Low concentrations of arsenic induce vascular endothelial growth factor and nitric oxide release and stimulate angiogenesis in vitro. Chem. Res. Toxicol. 16, 460-468.

54. Katoh, K., Kano, Y., Masuda, M., Inishi, H., Fujiwara, K., 1998. Isolation and contraction of the stress fibers. Mol. Biol. Cell. 9, 1919-1938.

55. Kawakami, T., Kawakami, Y., Kitaura, J., 2002. Protein kinase Cβ (PKCβ): normal finctions and diseases. J. Biochem. 132, 677-682.

56. Keaney, J.F. Jr., 2000. Atherosclerosis: from lesion formation to plaque activation and endothelial dysfunction. Mol. Aspects Med. 21, 99-166.

57. Kishimoto, A., Mikawa, K., Hashimoto, K., Yasuda, I., Tanaka, S., Tominaga, M., Kuroda, T., Nishizuka, Y., 1989. Limited proteolysis of protein kinase C subspecies by calcium-dependent neutral protease (calpain). J. Biol. Chem. 264, 4088-4092.

58. Klotz, L.O., Schroeder, P., Sies, H., 2002. Peroxynitrite signaling: receptor tyrosine kinases and activation of stress-responsive pathways. Free Radic. Biol. Med. 33(6), 737–743.

59. Konishi, H., Tanaka, M., Takemura, Y., Matsuzaki, H., Ono, Y., Kikkawa, U., Nishizuka, Y., 1997. Activation of protein kinase C by tyrosine phosphorylation in response to H2O2. Proc. Natl. Acad. Sci. U.S.A. 94, 11233–11237.

60. Lampugnani, M-G., Corada, M., Andriopoulou, P., Esser, S., Risau, W., Dejana, E., 1997. Cell confluence regulates tyrosine phosphorylation of adherens junction components in endothelial cells. J. Cell Sci. 110, 2065-2077.

61. Lampugnani, M-G., Corada, M., Caveda, L., Breviario, F., Ayalon O., Geiger, B., Dejana, E., 1995. The molecular organization of endothelial cell to cell junctions: differential association of plakoglobin, β-catenin, and α-catenin with vascular endothelial cadherin (VE-cadherin). J. Cell Biol. 129(1), 203-217.
62. Lee, M-Y., Bae, O-N., Chung, S-M., Kang, K-T., Lee, J-Y., Chung, J-H., 2002. Enhancement of platelet aggregation and thrombus formation by arsenic in drinking water: a contributing factor to cardiovascular disease. Toxicol. Appl. Pharmacol. 179, 83-88.
63. Lee, M-Y., Jung, B-I., Chung, S-M., Bae, O-N., Lee, J-Y., Park, J-D., Yang, J-S., Lee, H., Chung, J-H., 2003. Arsenic-induced dysfunction in relaxation of blood vessels. Environ. Health Perspect. 111, 513-517.
64. Lee, M-Y., Lee, Y-H., Lim, K-M., Chung, S-M., Bae, O-N., Kim, H., Lee, C-R., Park, J-D., Chung, J-H., 2005. Inorganic arsenite potentiates vasoconstriction through calcium sensitization in vascular smooth muscle. Environ. Health Perspect. 113, 1330-1335.
65. Li, C., Fultz M.E., Wright, G.L., 2002. PKC-α shows variable patterns of translocation in response to different stimulatory agents. Acta. Physiol. Scand. 174, 237-246.
66. Libby, P., 2002. Inflammation in atherosclerosis. Nature. 420, 868-874.
67. Liebner, S., Cavallaro, U., Dejana, E., 2006. The multiple languages of endothelial cell-to-cell communication. Arterioscler. Thromb. Vasc. Biol. 26, 1431-1438.

68. Lilien, J., Balsamo, J., 2005. The regulation of cadherin-mediated adhesion by tyrosine phosphorylation/dephosphorylation of β-catenin. Curr. Opin. Cell Biol. 17, 459-465.

69. Lin, S., Shi, Q., Nix, F.B., Styblo, M., Beck, M.A., Herbin-Davist, K.M., Hall, L.L., Simeonsson, J.B., Thomas, D.J., 2002. A novel S-adenosyl-L-methionine: arsenic(III) methytransferase from rat liver cytosol. J. Biol. Chem. 277, 10795-10803.

70. Liu, F., Jan, K.Y., 2000. DNA damage in arsenite and cadmium treated bovine aortic endothelial cells. Free Radic. Biol. Med. 28, 55-63.

71. Liu, Z., Shen, J., carbrey, J.M., Mukhopadhyay, R., Agre, P., Rosen, B.P., 2002. Arsenite transport by mammalian aquaglyceroporins AQP7 and AQP9. Proc. Natl. Acad. Sci. 99(9), 6053-6058.

72. Lum, H., Roebuck, K.A., 2001. Oxidant stress and endothelial cell dysfunction. Am. J. Physiol. Cell Physiol. 280, C719-C741.

73. Lusis, A.J., 2000. Atherosclerosis. Nature. 407, 233-241.

74. Lynn, S., Shiung, J.N., Gurr, J.R., Jan, K.Y., 1998. Arsenite stimulates poly (ADP-ribosylation) by generation of nitric oxide. Free Radic. Biol. Med. 24, 442-449.

75. Matata, B.M., Galinanes, M., 2002. Peroxynitrite is an essential component of cytokines production mechanism in human monocytes through modulation of nuclear factor-κB DNA binding activity. J. Biol. Chem. 277(3), 2330-2335.

76. McDouall, R.M., Farrar, M.W., Khan, S., Yacoub, M.H., Allen, S.P., 2001. Unique sensitivities to cytokine regulated expression of adhesion molecule in human heart-derived endothelial cells. Endothelium. 8(1), 25-40.

77. Mehta, D., Rahman, A., Malik, A.B., 2001. Protein kinase C-α signals Rho-guanine nucleotide dissociation inhibitor phosphorylation and Rho activation and regulates the endothelial cell barrier function. J. Biol. Chem. 276(25), 22614-22620.

78. Meier, M., King, G.L., 2000. Protein kinase C activation and its pharmacological inhibition in vascular disease. Vasc. Med. 5, 173-185.

79. Mellor, H., Parker, P.J., 1998. The extended protein kinase C superfamily. Biochem. J. 332, 281-292.

80. Nakashima, Y., Raines, E.W., Plump, A.S., Breslow, J.L., Ross, R., 1998. Upregulation of VCAM-1 and ICAM-1 at atherosclerosis-prone sites on the endothelium in ApoE-deficient mouse. Arterioscler. Thromb. Vasc. Biol. 18, 842-851.

81. Navarro, P., Caveda, L., Breviario, F., Mandoteanu, I., Lampugnani, M-G., Dejana, E., 1995. Catenin-dependent and –independent functions of vascular endothelial cadherin. J. Biol. Chem. 270(52), 30965-30972.

82. Navas-Acien, A., Sharrett, A.R., Silbergeld, E.K., Schwartz, B.S., Nachman, K.E., Burke, T.A., Guallar, E., 2005. Arsenic exposure and cardiovascular disease: A systematic review of epidemiologic evidence. Am. J. Epidemiol. 162(11), 1037-1049.

83. Nawroth, R., Poell, G., Ranft, A., Kloep, S., Samulowitz, U., Fachinger, G., Golding, M., Shima, D.T., Deutsch, U., Vestweber, D., 2002. VE-PTP and VE-cadherin ectodomains interact to facilitate regulation of phosphorylation and cell contacts. EMBO J. 21(18), 4885-4895.

84. Neméti, B., Csanaky, I., Gregus, Z., 2006. Effect of an inactivator of glyceraldehydes-3-phosphate dehydrogenase, a fortuitous arsenate reductase, on disposition of arsenate in rats. Toxicol. Sci. 90(1), 49-60.

85. Neméti, B., Gregus, Z., 2005. Reduction of arsenate to arsenite by human erythrocyte lysate and rat liver cytosol – characterization of a glutathione- and NAD-dependent arsenate reduction linked to glycolysis. Toxicol. Sci. 85, 847-858.

86. Newton, A.C., 2001. Protein Kinase C: Structural and Spatial Regulation by Phosphorylation, Cofactors, and Macromolecular interactions. Chem. Rev. 101, 2353-2364.

87. Newton, A.C., 2003. Regulation of the ABC kinases by phosphorylation: protein kinase C as a paradigm. Biochem. J. 370, 361-371.

88. Nose, A., Nagafuchi, A., Takeichi, M., 1988. Expressed recombinant cadherins mediate cell sorting in model systems. Cell. 54(7), 993-1001.

89. Oh, E.S., Woods, A., Couchman, J.R., 1997. Syndecan-4 proteoglycan regulates the distribution and activity of protein kinase C. J. Biol. Chem. 273, 10914-10918.

90. Ohashi, R., Mu, H., Yao, Q., Chen, C., 2004. Cellular and molecular mechanisms of atherosclerosis with mouse models. Trends Cardiovasc. Med. 14, 187-190.

91. Olofsson, S-O., Borèn, J., 2005. Apolipoprotein B: a clinically important apolipoprotein which assembles atherogenic lipoproteins and promotes the development of atherosclerosis. J. Intern. Med. 258, 395-410.

92. Oosawa, F., 2001. A historical perspective of actin assembly and its interactions. Results Probl. Cell Differ. 32, 9-21.

93. Pellegrino, M., Kazmierczak, E.F., LeBlanc, J.C., Cho, T., Cao, K., Marcovina, S.M., Boffa, M.B., Cote, G.P., Koschinsky, M.L., 2004. The apolipoprotein(a) component of lipoprotein(a) stimulates actin stress fiber formation and loss of cell-cell contact in cultured endothelial cells. J. Biol. Chem. 279(8), 6526-6533.

94. Pi, J., Horiguchi, S., Sun, Y., Nikaido, M., Shimojo, N., Hayashi, T., Yamauchi, H., Itoh, K., Yamamoto, M., Sun, G., Waalkes, M.P., Kumagai, Y., 2003. A potential mechanism for the impairment of nitric oxide formation caused by prolonged oral exposure to arsenate in rabbits. Free Radic. Biol. Med. 35(1), 102-113.

95. Pi, J., Kumagai, Y., Sun, G., Yamauchi, H., Yoshida, T., Iso, H., Endo, A., Yu, L., Yuki, K., Miyauchi, T., Shimojo, N., 2000. Decreased serum concentrations of nitric oxide metabolites among Chinese in an endemic area of chronic arsenic poisoning in inner Mongolia. Free Radic. Biol. Med. 28(7), 1137-1142.

96. Pryor, W.A., Squadrito, G.L., 1995. The chemistry of peroxynitrite: a product from the reaction of nitric oxide with superoxide. Am. J. Physiol. Lung Cell Mol. Physiol. 268, L699-L722.

97. Radi, R., Beckman, J.S., Bush, K.M., Freeman, B.A., 1991. Peroxynitrite-induced membrane lipid peroxidation: the cytotoxic potential of superoxide and nitric oxide. Arch. Biochem. Biophys. 288(2), 481-7.

98. Radi, R., Peluffo, G., Alvarez, M.N., Naviliat, M., Cayota, A., 2001. Unraveling peroxynitrite formation in biological systems. Free Radic. Biol. Med. 30(5), 463-488.

99. Rahman, M., Tondel, M., Ahmad, S. A., Chowdhury, I. A., Faruquee, M. H., and Axelson, O., 1999. Hypertension and arsenic exposure in Bangladesh. Hypertension. 33(1), 74-78.

100. Rolfe, B.E., Worth, N.F., World, C.J., Campbell, J.H., Campbell, G.R., 2005. Rho and Vascular disease. Atherosclerosis. 183, 1-16.

101. Ron, D., Kazanietz, M.G., 1999. New insights into the regulation of protein kinase C and novel phorbol ester receptors. FASEB J. 13, 1658-1676.

102. Rosenfeld, M.E., Polinsky, P., Virmani, R., Kauser, K., Rubanyi, G., Schwartz, S.M., 2000. Advanced atherosclerotic lesions in the innominate artery of the ApoE knockout mouse. Arterioscler Thromb Vasc Biol. 20, 2587-2592.

103. Roura, S., Miravet, S., Piedra, J., Herreros, A.G., Dunach, M., 1999. Regulation of E-cadherin/catenin association by tyrosine phosphorylation. J. Biol. Chem. 274(51), 36734-36740.

104. Sandoval, R., Malik, A.B., Minshall, R.D., Kouklis, P., Ellis, C.A., Tiruppathi, C., 2001. Ca^{2+} signaling and PKCα activate increased endothelial permeability by disassembly of VE-cadherin junctions. J. Physiol. 533(2), 433-445.

105. Saren, P., Welgus, H.G., Kovanen, P.T., 1996. TNF-alpha and IL-1beta selectively induce expression of 92-kDa gelatinase by human macrophages. J. Immunol. 157(9), 4159-4165.

106. Schieffer, B., Schieffer, E., Hilfiker-Kleiner, D., Hilfiker, A., Kovanen, P.T., Kaartinen, M., Nussberger, J., Harringer, W., Drexler, H., 2000. Expression of angiotensin II and interleukin 6 in human coronary atherosclerotic plaques. Potential implications for inflammation and plaque instability. Circulation. 101, 1372-1378.

107. Schnittler, H-J., Puschel, B., Drenckhahn, D., 1997. Role of cadherins and plakoglobin in interendothelial adhesion under resting conditions and sheer stress. Am. J. Physiol. 273, H2396-H2405.

108. Scott, N., Hatlelid, K.M., MacKenzie, N.E., Carter, D.E., 1993. Reactions of arsenic(III) and arsenic(V) species with glutathione. Chem. Res. Toxicol. 6, 102-106.

109. Simeonova, P.P., Hulderman, T., Harki, D., Luster, M.I., 2003. Arsenic exposure accelerates atherogenesis in apolipoprotein $E^{-/-}$ mice. Environ. Health Perspect. 111, 1744-1748.

110. Smedley, P.L., Kinniburgh, D.G., 2002. A review of the source, behaviour and distribution of arsenic in natural waters. Appl. Geochem. 17, 517-568.

111. Sonnenburg, E.D., Gao, T., Newton, A.C., 20001. The phosphoinositide dependent kinase, PDK-1, phosphorylates conventional protein kinase C isozymes by a mechanism that is independent of phosphoinositide-3-kinase. J. Biol. Chem. 276, 45289-45297.

112. Steinberg, M.S., McNutt, P.M., 1999. Cadherins and their connections: adhesion junctions have border functions. Curr. Opin. Cell Biol. 11, 554-560.

113. Styblo, M., Razo, L.M.D., Leclusye, E.L., Hamilton, G.A., Wang, C., Cullen, W.R., Thomas, D.J., 1999. Metabolism of arsenic in primary cultures of human and rat hepatocytes. Chem. Res. Toxicol. 12, 560-565.

114. Tedgui, A., 1996. Endothelial permeability under physiological and pathological conditions. Prostaglandins Leukot. Essent. Fatty Acids. 54, 27-29.

115. Tedgui, A., Mallat, Z., 2006. Cytokines in atherosclerosis: Pathogenic and regulatory pathways. Physiol. Rev. 86, 515-581.

116. Thomas, D.J., Li, J., Waters, S.B., Xing, W., Adair, B.M., Drobna, Z., Devesa, V., Styblo, M. 2007. Arsenic (+3 oxidation state) methyltransferase and the methylation of arsenicals. Exp. Biol. Med. 222, 3-13.

117. Thomas, D.J., Waters, S.B., Styblo, M., 2004. Elucidating the pathway for arsenic methylation. Toxico. Appl. Pharmacol. 198, 319-326.

118. Tseng, C.H., Chong, C.K., Tseng, C.P., Hsueh, Y.M., Chiou, H.Y., Tseng, C.C., Chen, C.J., 2003. Long-term arsenic exposure and ischemic heart disease in arseniasis-hyperendemic villages in Taiwan. Toxicol. Lett. 137(1-2), 15-21.

119. Vahter, M., 1994. Species differences in the metabolism of arsenic compounds. Appl. Organomet. Chem. 8(3), 175-182.

120. Vahter, M., 2000. Genetic polymorphism in the biotransformation of inorganic arsenic and its role in toxicity. Toxicol. Lett. 112-113, 209-217.

121. Vahter, M., 2002. Mechanisms of arsenic biotransformation. Toxicology. 181-182, 211-217.

122. van der Wal, A.C., Becker, A.E., van der Loos, C.M., Das, P.K., 1994. Site of intimal rupture or erosion of thrombosed coronary atherosclerotic plaques is characterized by an inflammatory process irrespective of the dominant plaque morphology. Circulation. 89, 36-44.

123. van Nieuw Amerongen, G.P., van Hinsbergh, V.M.N., 2001. Cytoskeletal effects of Rho-like small guanine nucleotide–binding proteins in the vascular system. Arterioscler. Thromb. Vasc. Biol. 21, 300-311.

124. Wang, C.H., Jeng, J.S., Yip, P.K., Chen, C.L., Hsu, L.I., Hsueh, Y.M., Chiou, H.Y., Wu, M.M., Chen, C.J., 2002. Biological gradient between long-term arsenic exposure and carotid atherosclerosis. Circulation 105(15), 1804-1809.

125. Wang, J.S., Wai, C.M., 2004. Arsenic in drinking water-A global environmental problem. J. Chem. Educ. 81(2), 207-13.

126. Wang, Y., Pampou, S., Fujikawa, K., Varticovski, L., 2004. Opposing effect of angiopoietin-1 on VEGF-mediated disruption of endothelial cell-cell interactions requires activation of PKCβ. J. Cell. Physiol. 198, 53-61.

127. Waters, S.B., Devesa, V., Razo, L.M.D., Styblo, M., Thomas, D.J., 2004. Endogeneous reductants support the catalytic function of recombinant rat cyt19, an arsenic methytransferase. Chem. Res. Toxicol. 17, 404-409.

128. Welch, A.H., Westjohn, D.B., Helsel, D.R., Wanty, R.B., 2000. Arsenic in ground water of United States – occurrence and geochemistry. Ground Water. 38(4), 589-604.

129. White, G.E., Gimbrone, M.A Jr., Fujiwara, K., 1983. Factors influencing the expression of stress fibers in vascular endothelial cells in situ. J. Cell Biol. 97, 416-424.

130. Wong, M.K.K., Gotlieb, A.I., 1990. Endothelial monolayer integrity: perturbation of F-actin filaments and the dense peripheral band-vinculin network. Arteriosclerosis. 10, 76-84.

131. Wu, M-M., Chiou, H-Y., Wang, T-W., Hsueh, Y-M., Wang, I-H., Chen, C-J., Lee, T-C., 2001. Association of blood arsenic levels with increased reactive oxidants and decreased antioxidant capacity in a human population of northeastern Taiwan. Environ. Health Perspect. 109, 1011-1017.

132. Xu, G., Craig, A.W.B., Greer, P., Miller, M., Anastasiadis, P.Z., Lilien, J., Balsamo, J., 2004. Continuous association of cadherin with β-catenin requires the non-receptor tyrosine-kinase Fer. J. Cell Sci. 117, 3207-3219.

133. Yap, A.S., Brieher, W.M., Gumbiner, B.M., 1997. Molecular and functional analysis of cadherin-based adherens junctions. Annu. Rev. Cell Dev. Biol. 13, 119-146.

134. Yuan, S.Y., 2003. Protein kinase signaling in the modulation of microvascular permeability. Vascul. Pharmacol. 39, 213-223.

135. Zakharyan, R., Aposhian, H.V., 1999. Enzymatic reduction of arsenic compounds in mammalian systems: the rate-limiting enzyme of rabbit liver arsenic biotransformation is MMA^{V} reductase. Chem. Res. Toxicol. 12, 1278-1283.

136. Zakharyan, R., Wu, Y., Bogdan, G.M., Aposhian, H.V., 1995. Enzymatic methylation of arsenic compounds: assay, partial purification, and properties of arsenite methytransferase and monomethylarsonic acid mathyltransferase of rabbit liver. Chem. Res. Toxicol. 8, 1029-1038.

137. Zeitler, H., Ko, Y., Zimmermann, C., Nickenig, G., Glanzer, K., Walger, P., Sachinidis, A., Vetter, H., 1997. Elevated serum concentrations of soluble adhesion molecules in coronary artery disease and acute myocardial infarction. Eur. J. Med. Res. 2, 389-94.

Chapter 2

Time- and Concentration-Dependent Effects of Arsenic on Atherogenesis in ApoE-/- /LDLr-/- Mice

2.1 Abstract

Exposure to arsenic through drinking water has been associated with cardiovascular disease. In the present study, the effects of environmentally relevant concentrations of arsenic in the development of atherosclerosis were investigated using the well-established animal model of human atherosclerosis, mice deficient in apolipoprotein E and low density lipoprotein receptor (ApoE-/- /LDLr-/-). The temporal effects of arsenic were determined by exposing the mice to 10 ppm sodium arsenite [As(III)] in drinking water for 5 or 10 weeks. Histology revealed that mice treated with As(III) showed an increasing trend in atherosclerotic plaque formation within the innominate arteries compared to the controls at both 5 and 10 weeks. Analysis of interleukin-6 (IL-6) levels in the serum obtained from mice treated with As(III) for 10 weeks showed an increasing trend compared to the control mice. These results suggest that As(III) contributes to atherogenesis at an early stage of the disease. The concentration-dependent effects of arsenic were analyzed by exposing the ApoE-/- /LDLr-/- mice to 1, 5 and 10 ppm As(III) in drinking water for 20 weeks. A significant increase in occlusion of the innominate arteries was observed with 1 and 5 ppm As(III). An increasing trend in occlusion was observed with 10 ppm As(III), and serum IL-6 levels were significantly elevated in this group. These results demonstrate the

significance of low levels of arsenic in both the onset and progression of atherosclerosis in this animal model.

2.2 Introduction

Arsenic contamination of ground water is a global problem. In addition to the United States, Taiwan, Bangladesh, India, China, Vietnam and Argentina have high levels of arsenic in ground water ranging from 50-14,000 ppb (Wang and Wai, 2004). Epidemiological evidence suggests that arsenic levels exceeding 20 ppb in drinking water are associated with increased mortality from various cardiovascular diseases (Engel and Smith, 1994). Atherosclerosis is the most important contributing factor to other cardiovascular diseases and can lead to serious clinical manifestations such as ischemic heart disease, myocardial infarction and stroke. Epidemiological studies have linked arsenic exposure via drinking water to diseases such as carotid atherosclerosis (Wang et al., 2002), ischemic heart disease (Tseng et al., 2003) and hypertension (Rahman et al., 1999). Atherosclerosis is a multifactorial disease. The hallmark of atherosclerosis is inflammation, characterized by the increased expression of cell adhesion molecules, proinflammatory cytokines and chemokines (Tedgui and Mallat, 2006, Blankenberg et al., 2003, Reape and Groot, 1999, Zeitler et al., 1997, Libby, 2002, Lusis, 2000). In particular, increased levels of the proinflammatory cytokine, interleukin-6 (IL-6), have been observed in patients with acute myocardial infarction (Erren et al., 1999, Ikeda et al., 1992), and it has been implicated in smooth muscle cell proliferation, formation of atherosclerotic lesions and instability of the atherosclerotic plaques (Ikeda, 2003, Rattazzi et al., 2003). Also, elevated levels of soluble vascular cell adhesion molecule-1 (sVCAM-

1) have been observed in patients with coronary heart disease and myocardial infarction (Zeitler et al., 1997), although its pathological role is unclear.

In addition to the epidemiological evidence, controlled animal studies have confirmed the association between arsenic exposure and development of atherosclerosis. It has been shown that exposure to 20 and 100 ppm arsenic in drinking water for 24 weeks accelerates atherogenesis in apolipoprotein E knockout (ApoE-/-) mice (Simeonova et al., 2003). Furthermore, we showed that chronic exposure (18 weeks) to 10 ppm arsenic in drinking water exacerbates atherosclerotic plaque formation in apolipoprotein E and low density lipoprotein receptor double knockout (ApoE-/- /LDLr-/-) mice (Bunderson et al., 2004). The ApoE-/- /LDLr-/- mouse is a well established model of human atherosclerosis. Mice are resistant to the development of atherosclerosis, but targeted gene deletion of ApoE and LDLr in mice results in hyperlipidemia and atherosclerosis that resembles human disease (Ishibashi et al., 1994, Jawein et al., 2004).

While, the animal studies have helped to clearly establish the link between arsenic exposure and atherosclerosis by eliminating the confounding factors that obscure epidemiological studies, the temporal effects of arsenic exposure in the development of atherosclerosis have not been identified. Also, the effects of arsenic concentrations lower than 10 ppm on atherogenesis have yet to be determined. In the present study, we investigated the time- and concentration-dependent effects of arsenic on the development of atherosclerosis in the ApoE-/- /LDLr-/- mouse.

2.3 Materials and Methods

2.3.1 Experimental animals. ApoE-/- /LDLr-/- mice were obtained from Jackson Laboratories (Bar Harbor, ME). All the animals were housed under specific pathogen-free conditions according to IACUC protocols with 12 h light/dark cycle and controlled temperature. The animals receiving arsenic treatment were given either 10 ppm As(III) (GFS Chemicals, Columbus, OH) for 5 or 10 weeks or 1, 5 and 10 ppm As(III) for 20 weeks ad libitum via drinking water. The control group received ddH_2O. The mice were fed a commercial mouse chow diet. Male and female animals were evenly distributed between treatment and control groups and were 4-7 weeks of age at the beginning of the study. Mice were weighed at the beginning and termination of the study.

2.3.2 Dissection procedures and quantification of atherosclerotic plaques. At the termination of treatments, blood was collected from each animal and the mice were perfused with 1% paraformaldehyde/PBS. The dissection of the innominate artery and quantification of the atherosclerotic plaques were done as described by Bunderson et al. (2004) with slight modifications. Briefly, cross sections of 10 μm thickness were obtained from paraffin-embedded innominate arteries of control and As(III)-treated mice. To ensure that the majority of plaque expanse was analyzed, the fifth, tenth and fifteenth sections of each sample, beginning from the base of the innominate artery, were stained with Movat's pentachrome. The sections were examined using blinded methods. Image analysis was done using NIH ImageJ software.

2.3.3 Enzyme-linked immunosorbent assay. Blood collected from ApoE-/- /LDLr-/- mice treated with 10 ppm As(III) for 10 or 20 weeks was used to analyze serum IL-6 and sVCAM-1 levels. Serum was obtained by centrifugation of the blood at 1,600 rpm for 5 min at 4 ^{0}C and was stored at -80 ^{0}C until analysis. Serum IL-6 and sVCAM-1 levels were analyzed by ELISA kits from BD Biosciences (San Diego, CA) and R&D Systems (Minneapolis, MN), respectively, according to the manufacturer's instructions.

2.3.4 Statistical analysis. Results are presented as mean ± standard error of the mean (SEM). Statistical analysis was performed using Student's *t* test when comparing two groups or Bonferroni method for comparing three groups or more. When using the Bonferroni method, the alpha level of each individual test was adjusted downwards to ensure that the overall experiment wise-risk remains at 0.05. Statistical analysis was performed using GraphPad Prism, version 4.00. Alpha error was set at $p<0.05$.

2.4 Results and Discussion

Epidemiological studies have associated arsenic exposure with the development of cardiovascular diseases such as carotid atherosclerosis and ischemic heart disease (Wang et al., 2002, Tseng et al., 2003). Previous studies, using animal models of atherosclerosis, have shown that exposure of mice to 10, 20 and 100 ppm arsenic exacerbates the process of atherosclerosis (Bunderson et al., 2004, Simeonova et al., 2003). This is the first study to show that low and environmentally relevant concentrations of arsenic (1 and 5 ppm) significantly increase atherosclerotic plaque

formation in the ApoE-/- /LDLr-/- mice. Analysis of the temporal effects of arsenic suggests that it may also contribute to the initiation of atherosclerosis.

The concentration-dependent effects of As(III) in the development of atherosclerosis were determined by exposing ApoE-/- /LDLr-/- mice to 1, 5 and 10 ppm As(III) in drinking water for 20 weeks (Fig. 6). Atherosclerotic plaque development was determined by measuring the percent occlusion of the innominate artery, which is a small vessel that connects the aortic arch to the right subclavian and right carotid arteries. Development of atherosclerotic lesions in this artery has been shown to progress at a highly consistent rate and closely resemble that of human condition, with events such as intraplaque hemorrhage and loss of fibrous cap or plaque rupture (Rosenfeld et al., 2000). The innominate arteries obtained from mice exposed to 1, 5 and 10 ppm As(III) were stained with Movat's pentachrome (Fig. 6A). The percent occlusion of the innominate artery was determined by dividing the plaque area by the lumen area plus the plaque area. Histology revealed a significant increase in plaque formation with 1 and 5 ppm As(III) treatment compared to the control group (Fig. 6B).

These concentrations of arsenic are well within the range encountered in the water supplies of the aforementioned countries having 0.05-14 ppm of arsenic contamination in drinking water (Wang and Wai, 2004). This finding is remarkable when considering that the toxicity of arsenic in humans could be much greater than that in mice at equivalent concentrations. Mice excrete approximately 90% of ingested arsenic in 2 days, whereas the biological half-time of arsenic in humans is on the order of 4 days (Vahter, 2000). Therefore, human subjects could be even more susceptible to arsenic-induced cardiovascular toxicity.

Our lab has previously shown that exposure to 10 ppm As(III) for 18 weeks significantly increases atherosclerotic plaque formation in ApoE-/- /LDLr-/- mice (Bunderson et al., 2004). In the present study, however, only an increasing trend in plaque formation was observed with 10 ppm As(III) treatment for 20 weeks (Fig. 6B) along with a significant increase in IL-6 levels (Fig. 8B). Increases in IL-6 levels have been strongly correlated with atherosclerotic plaque instability and rupture in human subjects (Schieffer et al., 2000) as well as a mouse model (Cheng et al., 2006). IL-6 is an important factor for increased plaque vulnerability because it stimulates the matrix degrading enzymes such as metalloproteinases (Cheng et al., 2006, Schieffer et al., 2000, Lin et al., 2007). In addition, studies have demonstrated the expression of IL-6 in the lipid-rich shoulder areas of plaques that are the most vulnerable sites of plaque rupture (van der Wal et al., 1994, Schieffer et al., 2000, Cheng et al., 2006). Therefore, it is possible that plaque rupture might have contributed to the statistically non-significant increase in atherosclerotic plaques observed with 10 ppm As(III) treatment for 20 weeks compared to our previous finding at 18 weeks of As(III) treatment (Bunderson et al., 2004). To ensure that the mice were sufficiently hydrated and healthy, all the animals were weighed at the beginning (initial weight) and at the termination (final weight) of the study. Final and initial weights were not significantly different between the control group and the As(III) treated groups (Table 1). In addition, visual inspection of the animals revealed no apparent adverse effects related to As(III) treatment on the general health of the animals.

The temporal effects of As(III) on atherogenesis were determined by exposing the ApoE-/- /LDLr-/- mice to 10 ppm As(III) via drinking water for 5 or 10 weeks (Fig. 7).

The innominate arteries obtained from mice exposed to As(III) for 5 weeks (Fig. 7A) and 10 weeks (Fig. 7C) were stained with Movat's pentachrome. Histology revealed an increasing trend in plaque formation with As(III) treatment at 5 weeks (Fig. 7B) and 10 weeks (Fig. 7D) compared to the control mice. These results suggests that As(III) may affect the initiation of atherosclerosis since an increasing trend in plaque formation was observed as early as 5 weeks. An initiating event in the development of atherosclerosis is increased accumulation of oxidized low density lipoproteins (LDLs) and monocytes within the blood vessel intima that leads to the formation of foam cells and ultimately culminates with the development of plaques (Lusis, 2000, Libby, 2002). Damage to the endothelium can result in increased permeability/passage of oxidized LDLs and monocytes across the endothelial monolayer. Consistent with this, we have recently documented that arsenic treatment induces intercellular gaps and increases permeability in cultured human aortic endothelial cells (Pereira et al., 2007), and *in situ* arsenic treatment has been shown to increase vascular permeability in rodents (Chen et al., 2004, Tsai et al., 2005). In addition, IL-6 has been shown to increase endothelial permeability (Desai et al., 2002). We observed that with 10 ppm As(III) treatment, serum IL-6 levels showed an increasing trend at 10 weeks (Fig. 8A) and a significant increase at the 20 week time point (Fig. 8B). Therefore, arsenic could potentially affect the initiation of atherosclerosis by increasing vascular permeability and the accumulation of oxidized LDLs and monocytes within the neo-intima of the blood vessel.

Surprisingly, a significant decrease was observed in sVCAM-1 levels at both 10 week (Fig. 9A) and 20 week (Fig. 9B) time points with 10 ppm As(III) treatment. The expression of VCAM-1 by endothelial cells is an early event in the development of

atherosclerosis (Nakashima et al., 1998). The role of VCAM-1 expressed by endothelial cells in atherogenesis is well characterized and is known to mediate transmigration of monocytes into the blood vessel intima (Cybulsky et al., 2001, Nakashima et al., 1998, Lusis, 2000). The soluble form of VCAM-1 has been proposed to be a prognostic factor in clinical manifestations such as myocardial infarction, coronary artery disease and unstable angina. However, contradictory results have been documented regarding the correlation of sVCAM-1 with cardiovascular events. Rohde et al. (1998) and Zeitler et al. (1997) demonstrated a correlation between increased serum levels of sVCAM-1 with carotid atherosclerosis and myocardial infarction, whereas Hwang et al. (1997) and Saku et al. (1999) found no such correlation. Furthermore, the clinical relevance of the sVCAM-1 is unclear (Blakenberg et al., 2003, Lind, 2003). The genesis of soluble form of VCAM-1 is also not certain. The most widely accepted theory is the proteolytic cleavage of cell surface expressed VCAM-1 molecule by an unidentified metalloprotease (Leca et al., 1995) and the relation between cellular expression and amount of soluble forms has yet to be elucidated (Blakenberg et al., 2003). This study does not suggest that there is reduced expression of endothelial VCAM-1. One possible interpretation for the reduced sVCAM-1 is that the increased interaction of the leukocytes with endothelial VCAM-1 may inhibit the proteolytic cleavage. Another possibility is increased clearance of these plasma proteins, although the mechanism of clearance or catabolism remains unknown. As mentioned above, it might also be possible that arsenic exacerbates the process of atherosclerosis by damaging the endothelial monolayer and not by modulating all of the classical mediators.

Atherosclerosis is a multifactorial disease with complex interplay between various signaling pathways and inflammatory mediators. Arsenic is a versatile molecule, and several mechanisms have been proposed by which it might modulate vascular homeostasis and influence the development of atherosclerosis (reviewed in Navas-Acien et al., 2005). Therefore, it is possible that arsenic affects atherogenesis by triggering multiple mediators. In summary, this study showed that environmentally relevant concentrations of arsenic induce significant increases in atherosclerotic plaque formation in the ApoE-/- /LDLr-/- mouse. Furthermore, the process of atherosclerosis is plausibly initiated or accelerated by arsenic at an early stage. Additional mechanistic studies are needed to elucidate how arsenic contributes to the onset and progression of atherosclerosis.

2.5 Figures

Fig. 6. Concentration-dependent effect of As(III) in the development of atherosclerosis

A.

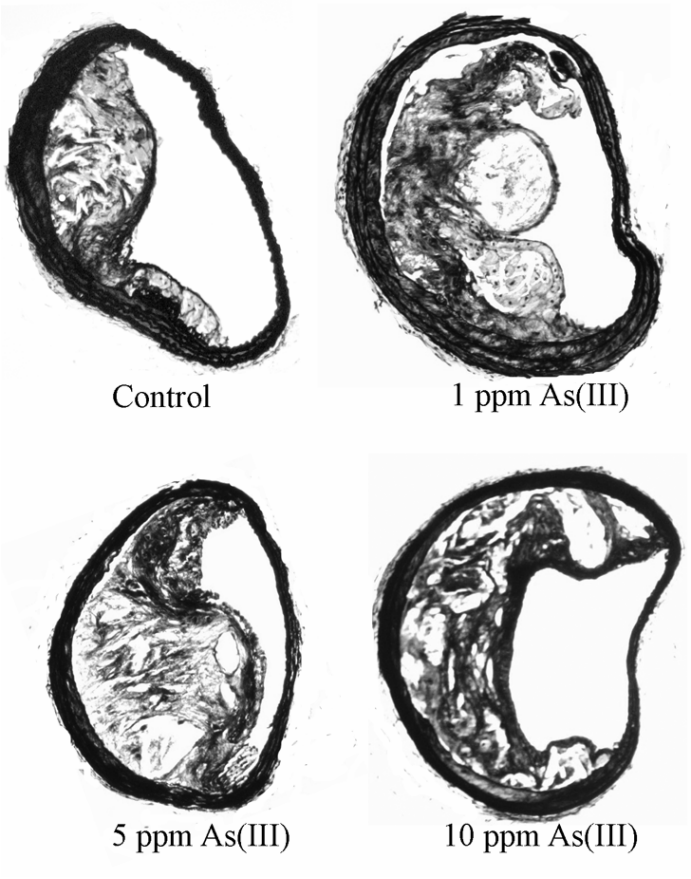

B.

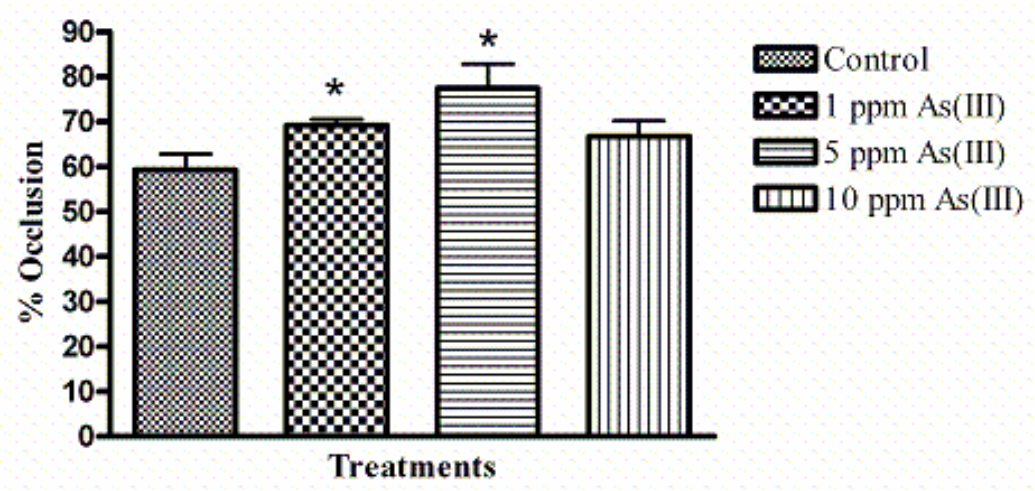

Fig. 6. Concentration-dependent effect of As(III) in the development of atherosclerosis. ApoE-/- /LDLr-/- mice were given either ddH_2O (control) or 1, 5 and 10 ppm As(III) in drinking water for 20 weeks and the concentration-dependent effects of As(III) in the development of atherosclerotic plaque within the innominate arteries were analyzed (A); magnification=10X. Percent occlusion of the innominate arteries was analyzed (B) with n=10-19 mice per group and the treatment groups marked with asterisk were significantly different from the control (*, $p<0.01$).

Fig. 7. Temporal effect of As(III) in the development of atherosclerosis

A.

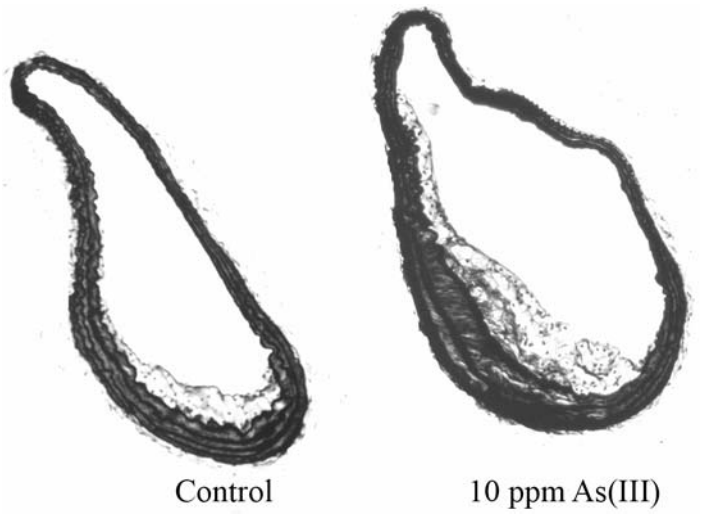

B.

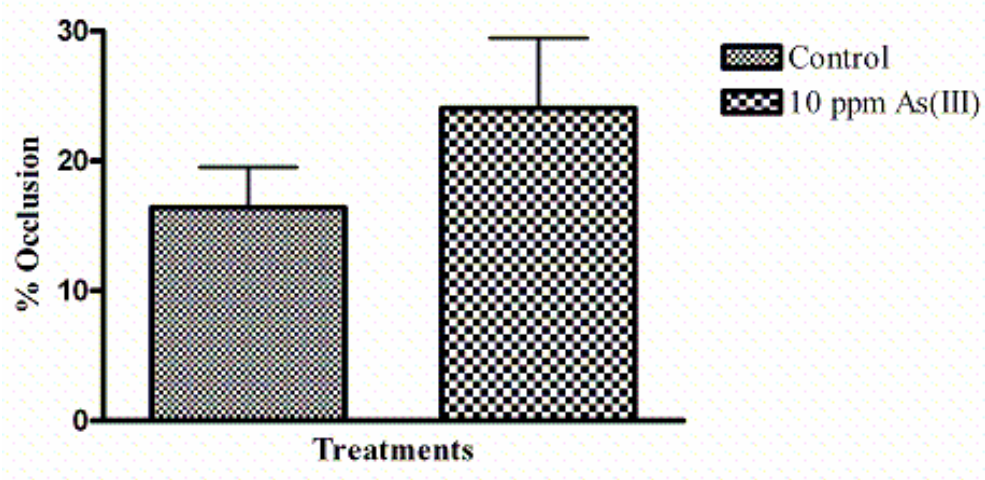

C.

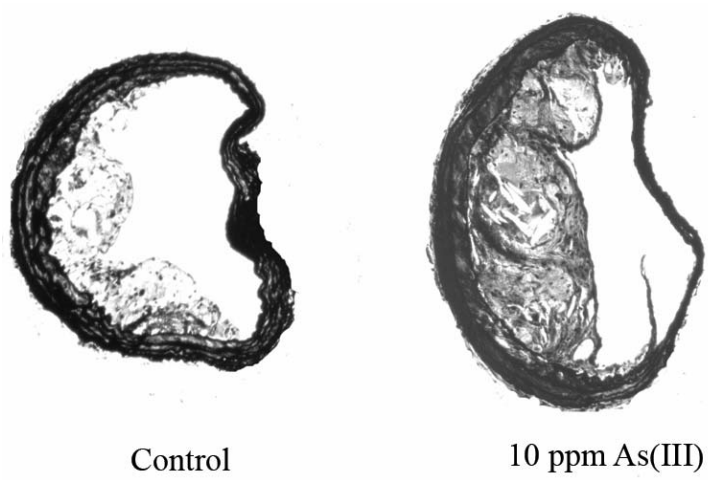

D.

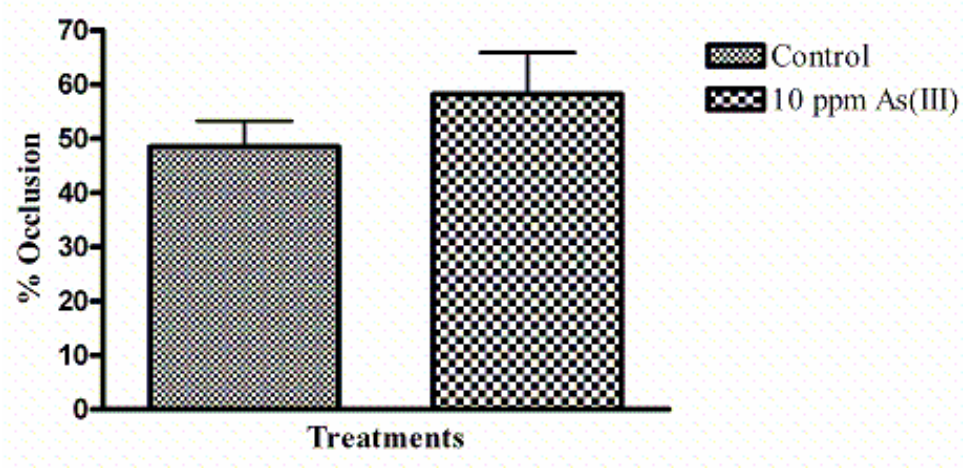

Fig. 7. Temporal effect of As(III) in the development of atherosclerosis. ApoE-/- /LDLr-/- mice were given either ddH_2O (control) or 10 ppm As(III) in drinking water and the temporal effects of As(III) in the development of atherosclerotic plaques within the innominate arteries were analyzed at 5 week (A) or 10 week (C) time points; magnification=10X. Percent occlusion of the innominate arteries was analyzed at 5 weeks (B) with 11-14 mice per group and 10 weeks (D) with 7-12 mice per group.

Fig. 8. Effect of As(III) treatment on serum IL-6 levels

A.

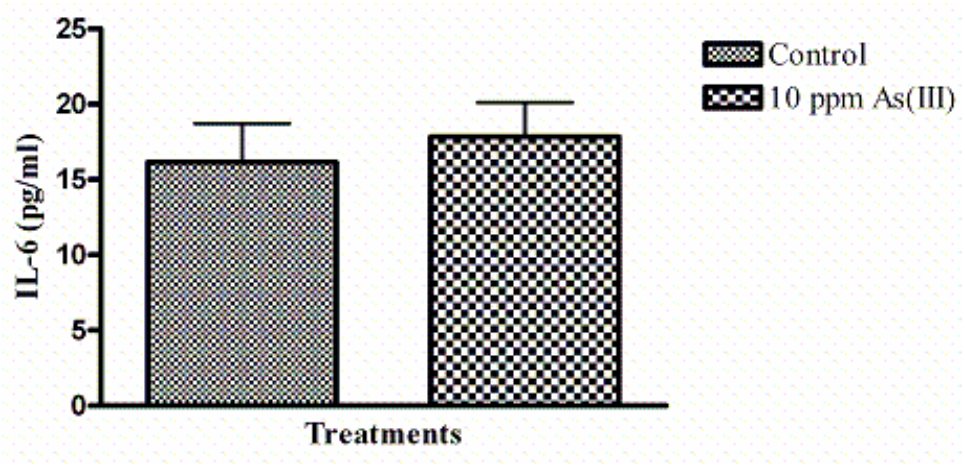

B.

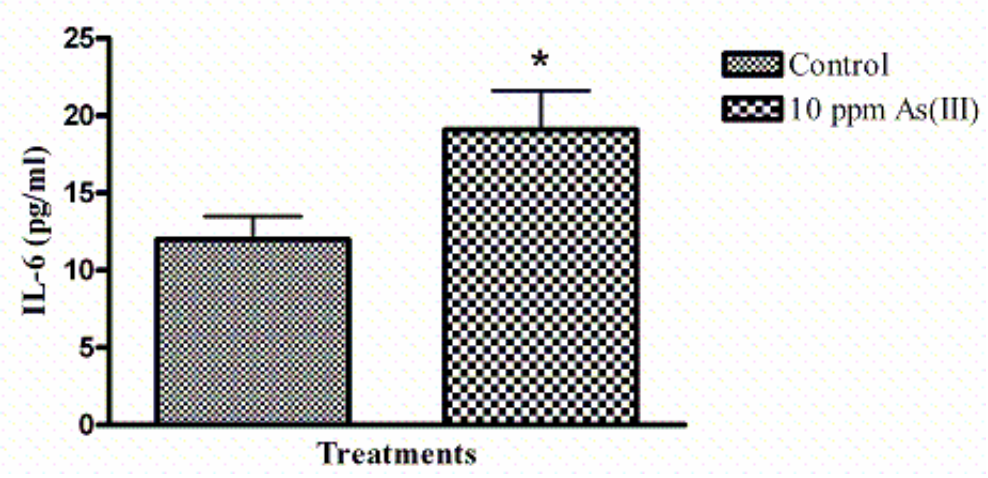

Fig. 8. Effect of As(III) treatment on serum IL-6 levels. IL-6 levels were measured by ELISA in the serum of ApoE-/- /LDLr-/- mice given either ddH2O (control) or 10 ppm As(III) for (A) 10 weeks or (B) 20 weeks (n=6-7 mice per group). Treatment group marked with asterisk was significantly different from the respective control (*, $p<0.05$).

Fig. 9. Effect of As(III) treatment on serum levels of sVCAM-1

A.

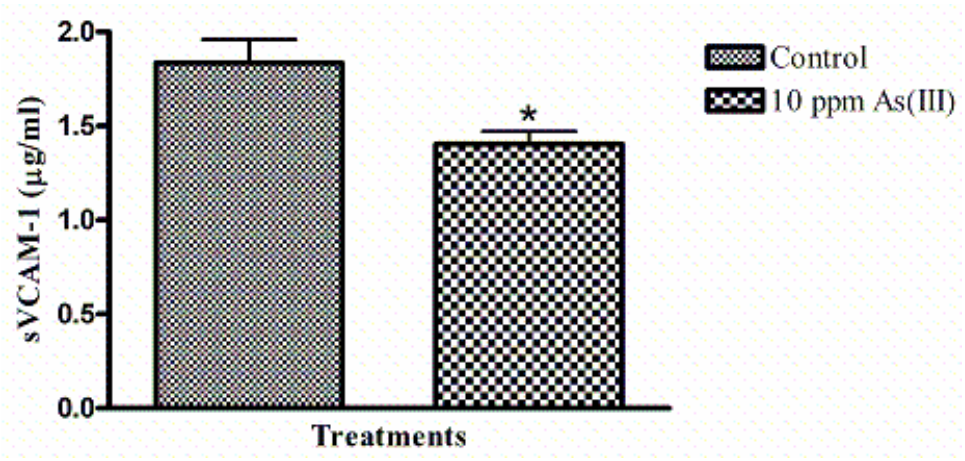

B.

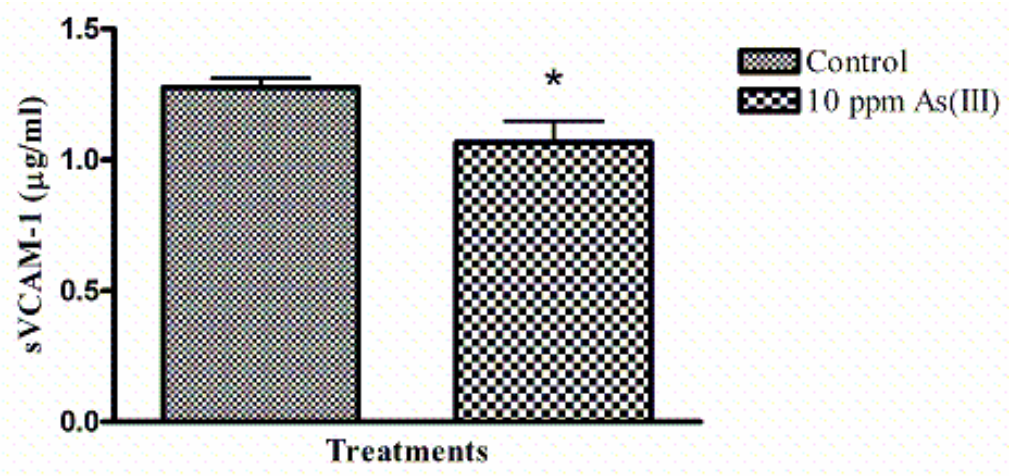

Fig. 9. Effect of As(III) treatment on serum levels of sVCAM-1. sVCAM-1 levels were measured by ELISA in the serum of ApoE-/- /LDLr-/- mice given either ddH2O (control) or 10 ppm As(III) for (A) 10 weeks or (B) 20 weeks (n=7 mice per group). Treatment group marked with asterisk were significantly different from the respective control (*, $p<0.05$).

Table 1. Body weight of mice exposed to As(III) for 20 weeks.

	Initial weight (g)	Final weight (g)	Difference (g)
Control	17.59 ± 0.44	19.93 ± 0.43	2.35 ± 0.27
1 ppm As(III)	19.54 ± 0.35	21.3 ± 0.37	1.76 ± 0.18
5 ppm As(III)	17.61 ± 0.59	20.08 ± 0.56	2.47 ± 0.16
10 ppm As(III)	20.91 ± 0.60	23.04 ± 0.63	2.14 ± 0.20

Each value represents mean ± SEM; no significant differences observed between groups.

2.6 References

1. Blankenberg, S., Barbaux, S., Tiret, L., 2003. Adhesion molecules and atherosclerosis. Atherosclerosis. 170, 191-203.
2. Bunderson, M., Brooks, D.M., Walker, D.L., Rosenfeld, M.E., Coffin, D.J., Beall, H.D., 2004. Arsenic exposure exacerbates atherosclerotic plaque formation and increases nitrotyrosine and leukotriene biosynthesis. Toxicol. Appl. Pharmacol. 201**,** 32-39.
3. Chen, S-C., Tsai, M-H., Wang, H-J., Yu, H-S., Chang, L.W., 2004. Vascular permeability alterations induced by arsenic. Hum Exp Toxicol. 23, 1-7.
4. Cheng, C., Tempel, D., van Haperen, R., van der Baan, A., Grosveld, F., Daemen, M.J.A.P., Krams, R., de Crom, R., 2006. Atherosclerotic lesion size and vulnerability are determined by patterns of fluid shear stress. Circulation. 113, 2744-2753.
5. Cybulsky, M.I., Iiyama, K., Li, H., Zhu, S., Chen, M., Iiyama, M., Davis, V., Gutierrez-Ramos, J-C., Connelly, P.W., Milstone, D.S., 2001. A major role for VCAM-1 but not ICAM-1 in early atherosclerosis. J. Clin. Invest. 107, 1255-1262.
6. Desai, T.R., Leeper, N.J., Hynes, K.L., Gewertz, B.L., 2002. Interleukin-6 causes endothelial barrier dysfunction via the protein kinase C pathway. J. Surg. Res. 104(2), 118-123.
7. Engel, R.R., Smith, A.H., 1994. Arsenic in drinking water and mortality from vascular disease: an ecologic analysis in 30 counties in the United States. Arch. Environ. Health. 49, 418-427.

8. Erren, M., Reinecke, H., Junker, R., Fobker, M., Schulte, H., Schurek, J.O., Kropf, J., Kerber, S., Breithardt, G., Assmann, G., Cullen, P., 1999. Systemic inflammatory parameters in patients with atherosclerosis of the coronary and peripheral arteries. Arterioscler Thromb Vasc Biol. 19, 2355-2363.
9. Hwang, S-J., Ballantyne, C.M., Sharrett, A.R., Smith, L.C., Davis, C.E., Gotto, A.M., Boerwinkle, E., 1997. Circulating Adhesion Molecules VCAM-1, ICAM-1, and E-selectin in Carotid Atherosclerosis and Incident Coronary Heart Disease Cases. Circulation. 96, 4219-4225.
10. Ikeda, U., 2003. Inflammation and coronary artery disease. Curr. Vasc. Pharmacol. 1, 65-70.
11. Ikeda, U., Ohkawa, F., Seino, Y., Yamamoto, K., Hidaka, Y., Kasahara, T., Kawai, T., Shimada, K., 1992. Serum interleukin 6 levels become elevated in acute myocardial infarction. J. Mol. Cell. Cardiol. 24(6), 579-584.
12. Ishibashi, S., Herz, J., Maeda, N., Goldstein, J.L., Brown, M.S., 1994. The two-receptor model of lipoprotein clearance: Test of the hypothesis in "knockout" mice lacking the low density lipoprotein receptor, apolipoprotein E, or both proteins. Proc. Natl. Acad. Sci. USA. 91, 4431-4435.
13. Jawein, J., Nastalek, P., Korbut, R., 2004. Mouse models of experimental atherosclerosis. J. Physiol. Pharmacol. 55(3), 503-517.
14. Leca, G., Mansur, S.E., Bensussan, A., 1995. Expression of VCAM-1 (CD 106) by a subset of TCR gamma delta-bearing lymphocyte clones, Involvement of a metalloprotease in the specific hydrolytic release of the soluble isoform. J. Immunol. 154, 1069-1077.

15. Libby, P., 2002. Inflammation in atherosclerosis. Nature. 420, 868-874.

16. Lin, T., Zhang, W., Fan, Y., Mulholland, M., 2007. Interleukin-1β and interleukin-6 stimulate matrix metalloproteinase-9 secretion in cultured myenteric glia. J. Surg. Res. 137, 38-45.

17. Lind, L., 2003. Circulating markers of inflammation and atherosclerosis. Atherosclerosis. 169, 203-214.

18. Lusis, A.J., 2000. Atherosclerosis. Nature. 407, 233-241.

19. Nakashima, Y., Raines, E.W., Plump, A.S., Breslow, J.L., Ross, R., 1998. Upregulation of VCAM-1 and ICAM-1 at atherosclerosis-prone sites on the endothelium in ApoE-deficient mouse. Arterioscler. Thromb. Vasc. Biol. 18, 842-851.

20. Navas-Acien, A., Sharrett, A.R., Silbergeld, E.K., Schwartz, B.S., Nachman, K.E., Burke, T.A., Guallar, E., 2005. Arsenic exposure and cardiovascular disease: A systematic review of epidemiologic evidence. Am. J. Epidemiol. 162(11), 1037-1049.

21. Pereira, F.E., Coffin, D.J., Beall, H.D., 2007. Activation of protein kinase C and disruption of endothelial monolayer integrity by sodium arsenite—potential mechanism in the development of atherosclerosis. Toxicol. Appl. Pharmacol., 220(2), 164-177.

22. Rahman, M., Tondel, M., Ahmad, S.A., Chowdhury, I.A., Faruquee, M.H., Axelson, O., 1999. Hypertension and arsenic exposure in Bangladesh. Hypertension. 33(1), 74-78.

23. Rattazzi, M., Puato, M., Faggin, E., Bertipaglia, B., Zambon, A., Pauletto, P., 2003. C-reactive protein and interleukin-6 in vascular disease: culprits or passive bystanders? J. Hypertens. 21, 1787-1803.

24. Reape, T.J., Groot, P.H.E., 1999. Chemokines and atherosclerosis. Atherosclerosis. 147, 213-225.

25. Rohde, L.E., Lee, R.T., Rivero, J., Jamacochian, M., Arroyo, L.H., Briggs, W., Rifai, N., Libby, P., Creager, M.A., Ridker, P.M., 1998. Circulating cell adhesion molecules are correlated with ultrasound-based assessment of carotid atherosclerosis. Arterioscler. Thromb. Vasc. Biol. 18, 1765-1770.

26. Rosenfeld, M.E., Polinsky, P., Virmani, R., Kauser, K., Rubanyi, G., Schwartz, S.M., 2000. Advanced atherosclerotic lesions in the innominate artery of the ApoE knockout mouse. Arterioscler Thromb Vasc Biol. 20, 2587-2592.

27. Saku, K., Zhang, B., Ohta, T., Shirai, K., Tsuchiya, Y., Arakawa, K., 1999. Levels of soluble cell adhesion molecules in patients with angiographically defined coronary atherosclerosis. Jpn. Circ. J. 63, 19-24.

28. Schieffer, B., Schieffer, E., Hilfiker-Kleiner, D., Hilfiker, A., Kovanen, P.T., Kaartinen, M., Nussberger, J., Harringer, W., Drexler, H., 2000. Expression of angiotensin II and interleukin 6 in human coronary atherosclerotic plaques. Potential implications for inflammation and plaque instability. Circulation. 101, 1372-1378.

29. Simeonova, P.P., Hulderman, T., Harki, D., Luster, M.I., 2003. Arsenic exposure accelerates atherogenesis in apolipoprotein $E^{-/-}$ mice. Environ. Health Perspect. 111, 1744-1748.

30. Tedgui, A., Mallat, Z., 2006. Cytokines in atherosclerosis: Pathogenic and regulatory pathways. Physiol. Rev. 86, 515-581.

31. Tsai, M-H., Chen, S-C., Wang, H-J., Yu, H-S., Chang, L.W., 2005. A mouse model for study of vascular permeability changes induced by arsenic. Toxicol. Mech. Methods. 15, 433-437.

32. Tseng, C.H., Chong, C.K., Tseng, C.P., Hsueh, Y.M., Chiou, H.Y., Tseng, C.C., Chen, C.J., 2003. Long-term arsenic exposure and ischemic heart disease in arseniasis-hyperendemic villages in Taiwan. Toxicol. Lett. 137(1-2), 15-21.

33. Vahter, M., 2000. Genetic polymorphism in the biotransformation of inorganic arsenic and its role in toxicity. Toxicol. Lett. 112-113, 209-217.

34. van der Wal, A.C., Becker, A.E., van der Loos, C.M., Das, P.K., 1994. Site of intimal rupture or erosion of thrombosed coronary atherosclerotic plaques is characterized by an inflammatory process irrespective of the dominant plaque morphology. Circulation. 89, 36-44.

35. Wang, C.H., Jeng, J.S., Yip, P.K., Chen, C.L., Hsu, L.I., Hsueh, Y.M., Chiou, H.Y., Wu, M.M., Chen, C.J., 2002. Biological gradient between long-term arsenic exposure and carotid atherosclerosis. Circulation 105(15), 1804-1809.

36. Wang, J.S., Wai, C.M., 2004. Arsenic in drinking water-A global environmental problem. J. Chem. Educ. 81(2), 207-13.

37. Zeitler, H., Ko, Y., Zimmermann, C., Nickenig, G., Glanzer, K., Walger, P., Sachinidis, A., Vetter, H., 1997. Elevated serum concentrations of soluble adhesion molecules in coronary artery disease and acute myocardial infarction. Eur J Med Res. 2, 389-94.

Chapter 3

Activation of Protein Kinase C and Disruption of Endothelial Monolayer Integrity by Sodium Arsenite

3.1 Abstract

The endothelium maintains a semipermeable barrier between the blood and vessel wall. The objective of the present study was to determine whether arsenic treatment induces activation of protein kinase C (PKC) isoforms, α and β, by generation of the reactive nitrogen species, peroxynitrite, and thereby causes endothelial disruption. Human aortic endothelial cells (HAECs) were exposed to 1, 5 and 10 μM sodium arsenite [As(III)] for 1, 6, 12 and 24 h. Western blotting revealed that As(III) treatment induced a concentration-dependent increase in activation of PKCα with no change in PKCβ levels. The activation of PKCα was found to be calcium-dependent. Peroxynitrite formation was not observed with As(III) treatment. Endothelial barrier integrity is maintained by proteins of the adherens junction, vascular endothelial (VE)-cadherin and β-catenin, and their association with the actin cytoskeleton. Immunofluorescence studies revealed reorganization of actin filaments into stress fibers and non-uniform staining of VE-cadherin and β-catenin at cell-cell junctions that were concentration- and time-dependent. Intercellular gaps were observed with a measured increase in endothelial permeability. In addition, a concentration-dependent increase in tyrosine phosphorylation of β-catenin was detected by Western blotting. Inhibition of PKCα using the classical PKC inhibitor, Gö 6979, restored VE-cadherin and β-catenin staining at cell-cell junctions and abolished the As(III) induced formation of intercellular gaps and actin stress fibers. Endothelial

permeability and tyrosine phosphorylation of β-catenin were also reduced to basal levels. These results suggest that As(III) induces activation of PKCα, which leads to increased tyrosine phosphorylation of β-catenin and formation of actin stress fibers downstream of PKCα activation. Phosphorylation of β-catenin plausibly severs the association of VE-cadherin and β-catenin, which along with formation of actin stress fibers, results in intercellular gap formation and increased endothelial permeability. As(III)-induced loss of endothelial monolayer integrity may contribute to the development of atherosclerosis by accelerating the accumulation of oxidized low density lipoproteins and monocytes within the blood vessel intima.

3.2 Introduction

Arsenic, an element present in the earth's crust, has been widely distributed in the environment by human activities such as mining, smelting, pesticide application and manufacturing and use of products such as wood preservatives and dyes. Epidemiological studies analyzing the correlation between cardiovascular diseases and arsenic exposure have linked arsenic to atherosclerosis (Wang et al., 2002), ischemic heart disease (Tseng et al., 2003) and hypertension (Rahman et al., 1999). Drinking water is a significant source of arsenic exposure to humans. Using mouse models of atherosclerosis, we and others have demonstrated that chronic exposure to arsenic through drinking water exacerbates atherosclerotic plaque formation (Bunderson et al., 2004, Simeonova et al., 2003). Atherosclerosis can lead to serious clinical manifestations such as heart attack and stroke.

Arsenic has been shown to generate reactive oxygen species such as superoxide anion and hydrogen peroxide (Barchowsky et al., 1999a) in porcine aortic endothelial cells and reactive nitrogen species such as nitric oxide and peroxynitrite in bovine aortic endothelial cells (Bunderson et al., 2002, Lynn et al., 1998, Liu and Jan, 2000). Peroxynitrite is a strong oxidizing and nitrating molecule formed by the rapid reaction of superoxide with nitric oxide. Peroxynitrite has been reported to interfere with cellular processes and signal transduction pathways by oxidation as well as nitration of proteins (Klotz et al., 2002). Amino acids such as cysteine, tyrosine, methionine and tryptophan are known to be modified by peroxynitrite via oxidation or nitration (Pryor and Squadrito, 1995, Radi et al., 2001, Beckman, 1996). In particular, 3-nitrotyrosine is a stable product that is formed by the attack of peroxynitrite on protein tyrosine residues. The detection of 3-nitrotyrosine in biological samples has been used as a marker for the presence of peroxynitrite (Ischiropoulos, 1998, Beckman et al., 1994, Beckman and Koppenol, 1996, Beckman, 1996).

There are numerous regulatory points in the vascular system that may be disrupted and lead to atherogenesis. The integrity of the vascular endothelium is maintained by proteins of the adherens junctions that includes the transmembrane protein vascular endothelial (VE)-cadherin linked to the cytoplasmic protein β-catenin, which in turn is linked to the actin cytoskeleton through α-catenin (Ivanov et al., 2001). This association is critical to maintaining cell-cell adhesion and structural integrity. The tyrosine phosphorylation of adherens junction proteins can alter their interaction with each other and the cytoskeleton. Endogenous mediators such as histamine have been shown to increase tyrosine phosphorylation of both β-catenin and VE-cadherin, resulting

in dissociation of VE-cadherin from the actin cytoskeleton with a subsequent increase in vascular permeability (Andriopoulou et al., 1999). The tyrosine phosphorylation of β-catenin has been shown to cause a fivefold reduction in its affinity for E-cadherin (Lilien and Balsamo, 2005, Roura et al., 1999). Accordingly, vascular endothelial growth factor (VEGF) induced tyrosine phosphorylation of VE-cadherin and β-catenin has been implicated in the loosening of cell-cell contacts and increased vascular permeability (Esser et al., 1998).

The association of cadherin-catenin complex with the actin cytoskeleton is also very important for maintaining junctional stability. Reorganization of the actin filaments into stress fibers can compromise the stability of the endothelial monolayer. Stress fibers consist of proteins such as myosin, tropomyosin and α-actinin intermittently associated with the actin filaments (Byers et al., 1984). Stress fibers are contractile elements and have been shown to develop *in vivo* during endothelial cell adaptation to unfavorable or pathological situations such as atherosclerosis and hypertension (White et al., 1983, Guyton et al., 1989, Colangelo et al., 1998). It has been observed that the apolipoprotein(a) component of lipoprotein(a), a risk factor for atherosclerotic disorders, induces stress fiber formation and VE-cadherin dispersion accompanied by cell retraction, intercellular gap formation and increased endothelial permeability (Pellegrino et al., 2004). Thus, development of stress fibers in endothelial cells adversely affects monolayer integrity. Treatment with peroxynitrite or the peroxynitrite donor, 3-morpholinosydnonimine hydrochloride (SIN-1), has been shown to induce actin stress fibers and nitration of tyrosine residues on actin and β-catenin in porcine aortic endothelial cells with an increase in permeability (Knepler et al., 2001). Nitration of these

proteins was proposed to be the cause of endothelial disruption. However, the effects of arsenic on the proteins involved in maintaining endothelial monolayer integrity remain unknown.

Several signaling intermediates have been implicated in the regulation of endothelial barrier function. In particular, the various protein kinase C (PKC) isotypes have a host of cellular substrates and are involved in numerous biological processes. PKCs are serine/threonine kinases and have been grouped into 3 subfamilies: classical, novel and atypical PKCs (Newton, 2001). The classical PKCs (cPKC), which consists of α, β and γ subtypes, are activated in calcium (Ca^{2+})-dependent manner and require diacylglycerol and phosphatidylserine. The PKCβ gene is alternatively spliced into PKCβ_1 and β_2 isoforms that differ by 2 amino acids in the C-terminal kinase domain. The PKCβ_1 isoform consists of 50 residues and the β_2 isoform has 52 residues (Kawakami et al., 2002). Among the cPKCs, endothelial cells express α and β isotypes (Mattila et al., 1994). The cPKCs have been implicated in the modulation of endothelial barrier function (Yuan, 2003). Activation of PKCα by thrombin has been shown to induce actin stress fibers and increase endothelial permeability (Sandoval et al., 2001). VEGF has been shown to activate PKCα, PKCβ_1 and β_2, and inhibition of the PKCβ isoforms was demonstrated to inhibit the dissociation of β-catenin from VE-cadherin and reduce endothelial permeability observed with PKC activation (Wang et al., 2004). Nagpala et al. (1996) have demonstrated that overexpression of PKCβ_1 in endothelial cells increases permeability when stimulated with phorbol ester. Conflicting data exist regarding the effects of arsenic on the modulation of intracellular Ca^{2+} levels and cPKCs; effects that

are dependent on the cell line studied and the duration of arsenic treatment (Chen et al., 2000, Liu and Huang, 1997).

Peroxynitrite has been implicated in the modulation of cPKC activity. It has been shown that treatment of endothelial cells with peroxynitrite results in an increase in Ca^{2+}-dependent PKCα activity that was inhibited by the intracellular Ca^{2+} chelator, BAPTA-AM, and the cPKC inhibitor, Gö 6976. Peroxynitrite treatment also induced tyrosine nitration of PKCα (Chakraborti et al., 2005). Conversely, peroxynitrite treatment has been shown to nitrate tyrosine residues and inactivate PKCα and β isoforms in hippocampal homogenates and rat brain purified PKC (Knapp et al., 2001). The effect of arsenic-induced peroxynitrite formation in the modulation of cPKC activation remains unknown.

Various mechanisms for arsenic-induced atherosclerosis have been proposed including activation of the endothelium that is characterized by up-regulation of adhesion molecules and inflammatory mediators (Simeonova and Luster, 2004). In particular, *in situ* arsenic exposure through intradermal injections on the dorsal surface of rats has been shown to induce vascular permeability (Chen et al., 2004). However, the mechanism of increased vascular permeability remains unknown. The endothelium maintains a semipermeable barrier and damage to the endothelial lining can result in increased permeability. This could lead to subsequent recruitment and migration of monocytes and oxidized low density lipoproteins (oxLDL) into the intima of the blood vessel, thereby promoting the development of atherosclerotic lesions. Hence, the objective of this study was to determine the effects of arsenic on endothelial barrier integrity and characterize

the pathways for arsenic-induced increases in vascular permeability. We also analyzed whether the effects of arsenic were mediated through formation of peroxynitrite.

3.3 Materials and Methods

3.3.1 Cell culture. Human aortic endothelial cells (HAECs) were purchased from Cambrex Bio Science (Walkersville, MD) and were grown in the supplier's formulated medium: EBM-2 medium supplemented with EGM-2 SingleQuots (0.04% hydrocortisone, 0.4% hFGF-B, 2% FBS and 0.1% each of VEGF, R^3-IGF-1, ascorbic acid, heparin, hEGF and GA-1000). Bovine aortic endothelial cells (BAECs) were provided by Dr. J. Douglas Coffin of The University of Montana, Missoula and were originally a gift from Dr. Steve Schwartz of The University of Washington. Cells were grown in Dulbecco's Modified Eagle Medium (DMEM) with penicillin/streptomycin and L-glutamine, and supplemented with 15% FBS (Mediatech, Inc., Herndon, VA). The HAECs and BAECs were incubated at 37 ^{0}C under a humidified atmosphere containing 5% CO_2. Cells were used between passages 2 and 10.

3.3.2 Cell viability assay. The viability of HAECs was determined using the 3-(4,5-dimethythiazol-2-yl)2,5-diphenyltetrazolium bromide (MTT) assay described by Bunderson et al. (2002) with some modifications. HAECs were seeded at a density of $1x10^4$ cells/well in 96-well plates. At 24 h post seeding, cells were treated with 0.5, 1, 2.5, 5, 10, 25, 50, 100, 250 or 500 μM concentrations of sodium arsenite [As(III)] (GFS Chemicals, Columbus, OH) for 12, 24 and 48 h. The treatment solutions were removed and replaced with medium alone for 24 h. MTT/medium solution (50 μg) was added to

each well and cells were incubated for another 4 h. The MTT/medium solution was carefully removed and the formazan crystals were dissolved in 100 µl DMSO/well. Absorbance was determined using the VersaMax microplate reader (Molecular Devices Corporation, Sunnyvale, CA) at 560 nm. The effect of Gö 6976 (Calbiochem, San Diego, CA), nitro-L-arginine methyl ester (L-NAME) (Sigma-Aldrich, Saint Louis, MO) and 5,10,15,20-Tetrakis-[4-sulfonatophenyl]-porphyrinato-iron[III], Chloride (FeTPPS) (Calbiochem, San Diego, CA) on cell viability for 24 h was also determined.

3.3.3 Detection of Peroxynitrite. Generation of peroxynitrite with As(III) treatment was determined in HAECs and BAECs by analyzing nitrotyrosine formation. Cells were grown on 18-mm round coverslips inserted into 12-well plates. For HAECs 0.1 mg/ml solution of Poly-D-Lysine hydrobromide (Sigma-Aldrich, Saint Louis, MO) was used to coat the coverslips. HAECs and BAECs were seeded at a density of $2x10^5$-$3x10^5$ cells/well in 12-well plates and were grown to confluence for 48-72 h. Cells were then treated with As(III) for specified time periods. Cells were fixed with 1% paraformaldehyde/phosphate-buffered saline (PBS) for 30 min at room temperature (RT), permeabilized using 0.1% saponin solution/ PBS for 10 min at RT and then blocked with 5% goat serum/PBS (Sigma-Aldrich, Saint Louis, MO) for 30 min at RT. Cells were then incubated with 20 µg/ml rabbit anti-nitrotyrosine polyclonal antibody for 24 h at 4 ^{0}C followed by incubation with 10 µg/ml Alexa Fluor 594-conjugated goat anti-rabbit secondary antibody (Molecular Probes, Inc. Eugene, OR) for 1 h at RT in the dark. Cells were counterstained with Hoechst 33342 stain for 5 min at RT, coverslipped with Fluorosave (EMD Biosciences, San Diego, CA) and stored in the dark until imaged.

Fluorescence was quantitated using a Laser Scanning Cytometer (CompuCyte Corporation, Cambridge, MA).

Generation of peroxynitrite with As(III) treatment was also determined in HAECs by analyzing the oxidation of hydroethidine to its fluorescent form ethidium (Zhao et al., 2005, Zhao et al., 2003). HAECs were grown in 24-well plates coated with 0.1 mg/ml solution of Poly-D-Lysine hydrobromide. Cells were seeded at a density of $1x10^5$ cells/well and grown to confluence for 48-72 h. Cells were incubated with 20 μM hydroethidine/PBS for 30 min at 37 ^{0}C. PBS was supplemented with 1 mM $CaCl_2$, 0.5 mM $MgCl_2$ and 2% fetal bovine serum and was used for rinsing cells and preparing all the solutions for this experiment. Cells were rinsed twice with PBS and then incubated with As(III)/PBS with or without the peroxynitrite decomposition catalyst, FeTPPS, for 1 h at 37 ^{0}C. The total volume of solution in each well was 1 ml at all times except during fluorescence measurement when the volume was reduced to 200 μl. Fluorescence intensity was analyzed using the SpectraMax GeminiXS fluorescence plate reader (Molecular Devices Corporation, Sunnyvale, CA) at 510 nm excitation and 590 nm emission wavelengths (Zhao et al., 2005, Zhao et al., 2003).

3.3.4 Immunofluorescence. HAECs were grown on 18-mm round coverslips inserted into 12-well plates and coated with 0.1 mg/ml solution of Poly-D-Lysine hydrobromide. HAECs were seeded at a density of $2x10^5$-$3x10^5$ cells/well and were grown to confluence for 48-72 h. Cells were treated with As(III) and the cPKC inhibitor, Gö 6976, was added 1 h prior to and during the As(III) treatment wherever applicable. Cells were fixed with 1% paraformaldehyde/PBS for 30 min at RT, permeabilized using 0.1% saponin/PBS for

10 min at RT and then blocked with 5% goat serum/PBS for 30 min at RT. Cells were then incubated with either 2 μg/ml rabbit anti-VE-cadherin polyclonal antibody (Cayman Chemicals, Ann Arbor, MI) or 2 μg/ml rabbit anti-β-catenin polyclonal antibody (Cayman Chemicals, Ann Arbor, MI) or 0.24 μg/ml rabbit polyclonal antibody against cleaved caspase-3 (Cell Signaling Technology, Danvers, MA) in PBS for 2 h at RT or 24 h at 4 ^{0}C followed by incubation with 10 μg/ml Alexa Fluor 488-conjugated goat anti-rabbit secondary antibody (Molecular Probes, Inc. Eugene, OR) for 1 h at RT in the dark. For detection of stress fibers, HAECs were incubated with 16.5 nM Alexa Fluor 568-conjugated phalloidin (Molecular Probes, Inc. Eugene, OR) for 25 min at RT in the dark. Cells were counterstained with Hoechst 33342 stain for 5 min at RT, coverslipped with Fluorosave and stored in the dark until imaged. Slides were photographed with a Nikon Digital Eclipse DXM1200 camera attached to a Nikon E-800 microscope using a 60X oil immersion lens.

3.3.5 Permeability Assay. HAECs ($1x10^5$-$1.5x10^5$) were seeded on 0.4-μm pore polyester membrane transwell inserts (Corning Incorporated, Acton, MA) coated with 0.1 mg/ml solution of Poly-D-Lysine hydrobromide in 12-well plates. Cells were grown to confluence for 48-72 h. The volume of medium in the Transwell was 500 μl with 1.5 ml in the plate well at all times. The As(III) treatments were added to the Transwells and the cPKC inhibitor, Gö 6976, was added 1 h prior to and during the As(III) treatment wherever applicable. At the final 1 h of respective treatments, fluorescein isothiocyanate (FITC)-labeled dextran (average molecular weight 40,000, final concentration of 1 mg/ml; Sigma-Aldrich, Saint Louis, MO) was added to each Transwell including control

wells. After completion of the treatment period, the fluorescence intensity of the medium in the plate well was analyzed using a SpectraMax GeminiXS fluorescence plate reader. For each sample, 5 aliquots of 200 µl each were analyzed using an excitation wavelength of 490 nm and emission wavelength of 520 nm.

3.3.6 Immunoprecipitation of VE-cadherin and β-catenin. To detect tyrosine phosphorylation and tyrosine nitration of VE-cadherin and β-catenin, the proteins were first immunoprecipitated. HAECs were seeded at a density of $7.5x10^5$ cells/25 cm^2 cell culture flask and allowed to reach confluence for 48-72 h. Confluent cells were treated with As(III) and the cPKC inhibitor, Gö 6976 was added 1 h prior to and during As(III) treatment wherever applicable. After completion of treatment, cells were rinsed with cold PBS containing phosphatase inhibitors (1 mM β-glycerophosphate, 1 mM Sodium pyrophosphate and 2.5 mM Sodium orthovanadate). The sodium orthovanadate was activated for maximal inhibition of protein tyrosine phosphatases (activation method obtained from the list of protocols provided by Upstate Cell Signaling Solutions). Cells were harvested using cold 1X RIPA buffer (20 mM Tris, pH 7.5, 5 mM EDTA, 2 mM EGTA, 1% Igepal, 0.1% SDS and 0.5% Deoxycholic acid) containing protease inhibitors (Complete protease inhibitor cocktail tablet; Roche Diagnostics, Indianapolis, IN) and phosphatase inhibitors. Cells were homogenized by sonication and centrifuged at 10,000 rpm for 15 min at 4 ^{0}C. The supernatant was sequentially incubated with 5 µg/ml each of mouse anti-VE-cadherin monoclonal antibody followed by mouse anti-β-catenin monoclonal antibody (Abcam, Cambridge, MA) for 24 h at 4 ^{0}C. Immune complexes were precipitated using immobilized protein G (Pierce, Rockford, IL). After incubation

for 2 h at 4 ^{0}C, the agarose bound immune complexes were washed three times with cold 1X RIPA buffer containing protease and phosphatase inhibitors and then heated at 70 ^{0}C for 10 min in 1X solution of reducing agent and sample buffer (Invitrogen Life Technologies, Carlsbad, CA).

3.3.7 Western blot analysis for VE-cadherin and β-catenin. The tyrosine phosphorylation and tyrosine nitration of VE-cadherin and β-catenin was analyzed by immunoprecipitation followed by Western blot. The immunoprecipitated proteins were resolved using 4-12% NuPAGE Novex Bis-Tris gel (Invitrogen Life Technologies, Carlsbad, CA), transferred to a polyvinylidenedifluoride (PVDF) membrane, blocked with 5% BSA/TBST (TBST: 1.57 gm/l Tris HCl (pH=8), 8.76 gm/l NaCl, 500 µl/l Tween 20) for 1 h at RT and incubated with 2 µg/ml mouse anti-phosphotyrosine monoclonal antibody (BD Transduction Laboratories, San Jose, CA) or 2 µg/ml rabbit anti-nitrotyrosine polyclonal antibody overnight at 4 ^{0}C in 1% BSA/TBST solution. This was followed by incubation of the membrane with 1 µg/ml peroxidase labeled horse anti-mouse or 5 µg/ml goat anti-rabbit secondary antibody (Vector laboratories Inc., Burlingame, CA) for 1 h at RT in 1% BSA/TBST solution. The protein bands were visualized by ECL Western blot detection system (Amersham, Buckinghamshire, England). To quantitate tyrosine phosphorylation and tyrosine nitration, the total protein content of immunoprecipitated VE-cadherin and β-catenin was determined as follows. After analysis of phosphotyrosine and nitrotyrosine content, the membranes were stripped at 60 ^{0}C for 1 h using stripping buffer (100 mM β-mercaptoethanol, 2% SDS and 62.5 mM Tris HCL, pH 6.8), blocked with 5% non-fat milk/TBST for 1 h at RT and

reprobed for VE-cadherin and β-catenin protein using 1.25 μg/ml rabbit anti-VE-cadherin and 1 μg/ml rabbit anti-β-catenin polyclonal antibody (Cayman Chemicals, Ann Arbor, MI) overnight at 4 ^{0}C in 0.4% non-fat milk/TBST. This was followed by incubation with 5 μg/ml peroxidase labeled goat anti-rabbit secondary antibody for 1 h at RT in 0.4% non-fat milk/TBST, and the protein bands were visualized as previously described.

To determine the protein content of VE-cadherin without immunoprecipitation, cells were rinsed with PBS and harvested with 1X RIPA buffer containing protease inhibitors. Cells were homogenized with 18- and 25-gauge needles and boiled for 10 min. Protein concentrations were determined by using the Bradford protein assay (Biorad, Hercules, CA). The proteins were resolved using 4-12% NuPAGE Novex Bis-Tris gel, transferred to PVDF membrane, blocked with 5% non-fat milk/TBST for 2 h at RT and probed for VE-cadherin protein using 1.25 μg/ml rabbit anti-VE-cadherin polyclonal antibody for 2 h at RT or overnight at 4 ^{0}C in 0.4% non-fat milk/TBST. This was followed by incubation with 5 μg/ml peroxidase labeled goat anti-rabbit secondary antibody for 1 h at RT in 0.4% non-fat milk/TBST. The protein bands were visualized by ECL Western blot detection system. Protein loading was normalized using β-actin as loading control. β-actin protein was detected using 0.24 μg/ml mouse anti-β-actin monoclonal antibody (Abcam, Cambridge, MA) and 1 μg/ml peroxidase labeled horse anti-mouse as the secondary antibody.

3.3.8 Western blot analysis for PKCα and β_1. HAECs were seeded at a density of 7.5x10^5 cells in 25 or 75 cm^2 cell culture flasks and after 3-5 days, confluent cells were treated with As(III). Treatments of FeTPPS, L-NAME, Gö 6976 and BAPTA-AM (1,2-

bis(o-aminophenoxy)ethane-N,N,N',N'-tetraacetic acid-acetoxymethyl ester) were applied with or without As(III) wherever applicable. Cells were rinsed with cold PBS, harvested using homogenizing buffer (50 mM Tris HCl, pH 7.5, 1 mM EDTA and protease inhibitors) and sonicated. To separate the membrane and cytosolic fractions, the lysates were centrifuged at 100,000x g for 1 h at 4 ^{0}C. The supernatant was collected as the cytosolic fraction. The pellet was dissolved in 1X RIPA buffer containing protease inhibitors, sonicated and centrifuged again at 100,000x g for 1 h at 4 ^{0}C. The supernatant was the membrane fraction. Protein concentrations were determined by using the Bradford protein assay. The proteins were resolved using 4-12% NuPAGE Novex Bis-Tris gels. To detect good quality protein bands, different amounts of cytosolic and membrane fraction proteins were loaded; 10-20 μg protein for the cytosolic fraction and 40-55 μg protein for the membrane fraction. After separation, the proteins were transferred to PVDF membranes, blocked with 5% non-fat milk/TBST for 1 h at RT and probed for PKCα or PKCβ_1 protein using 0.4 μg/ml mouse anti-PKCα or mouse anti-PKCβ_1 monoclonal antibody (Santa Cruz Biotechnology, Inc., Santa Cruz, CA) overnight at 4 ^{0}C in 0.4% non-fat milk/TBST. This was followed by incubation with 1 μg/ml horse anti-mouse secondary antibody conjugated with horseradish peroxidase for 1 h at RT in 0.4% non-fat milk/TBST. Protein bands were visualized by ECL Western blot detection system. Na^+/K^+ ATPase was used as loading control for the membrane fraction using 0.4 μg/ml mouse anti-Na^+/K^+ ATPase monoclonal antibody (Upstate Cell Signaling Solutions, Lake placid, NY) and GAPDH was used as loading control for the cytosolic fraction using 1 μg/ml mouse anti-GAPDH monoclonal antibody (Chemicon

International, Inc., Temecula, CA). In both cases, 1 μg/ml horse anti-mouse secondary antibody was used.

3.3.9 Statistical analysis. Results are presented as means ± standard error of the mean (SEM). When required, data was normalized with its respective control in order to exclude differences in background conditions. Statistical analysis was performed using Student's *t* test when comparing two groups or Bonferroni method for comparing three groups or more. When using the Bonferroni method, the alpha level of each individual test was adjusted downwards to ensure that the overall experiment wise-risk remains at 0.05. Statistical analysis was performed using GraphPad Prism, version 4.00. Alpha error was set at $p<0.05$.

3.4 Results

3.4.1 Cell viability after As(III) treatment

Cell viability was assessed using the MTT assay that is based on the reduction of yellow MTT to purple formazan by metabolically active cells. The effect of 0.5, 1, 2.5, 5, 10, 25, 50, 100, 250 or 500 μM concentrations of As(III) on HAEC viability was determined at 12, 24 and 48 h. The IC50 and threshold values are represented in Table. 2. IC50 represents the concentration at which cell viability was reduced by 50% and threshold value represents the concentration at which no toxicity was observed at that particular time point. A maximum concentration of 10 μM As(III) was used in all the experiments for a time period not exceeding 24 h. No toxicity was observed at the concentration and time points used in our experiments.

3.4.2 Effect of As(III) on peroxynitrite formation

Peroxynitrite induces nitration of tyrosine residues in proteins resulting in the formation of 3-nitrotyrosine that is a stable adduct (Ischiropoulos, 1998, Beckman et al., 1994, Beckman and Koppenol, 1996, Beckman, 1996). Peroxynitrite generation in HAECs with 1, 5 and 10 μM As(III) treatment was analyzed at 1, 6 and 24-h time points by immunofluorescence detection of 3-nitrotyrosine. No changes in 3-nitrotyrosine levels were observed in the HAECs. The data for the 24-h time point has been shown (Fig. 10A). However, a significant increase in 3-nitrotyrosine was observed in BAECs treated with 10 μM As(III) for 24 h (Fig. 10B).

Our laboratory has previously shown that 1 h As(III) treatment induces peroxynitrite formation in BAECs using the hydroethidine assay (Bunderson et al., 2002). Hydroethidine is oxidized to the fluorescent product ethidium with reactive species such as hydrogen peroxide, hydroxyl radical and peroxynitrite. Reaction of hydroethidine with intracellular superoxide results in the formation of 2-hydroxyethidium, which is very distinct from ethidium (Zhao et al., 2005, Zhao et al., 2003). Treatment of HAECs with 1, 5 and 10 μM As(III) for 1 h showed an increasing trend in peroxynitrite formation with 10 μM As(III), but it was not statistically significant. Exposure of cells to the peroxynitrite decomposition catalyst, FeTPPS (10 μM), during 10 μM As(III) treatment reduced the peroxynitrite formed to basal levels. No change was observed with 1 and 5 μM As(III) treatment (Fig. 10C). The effect of FeTPPS on cell viability was assessed using the MTT assay and no loss of viability was observed at concentrations 1 μM-50 μM up to 24 h (data not shown).

3.4.3 Dose response of HAECs to cPKC inhibitor Gö 6976

The indolocarbazole Gö 6976 has been shown to be a potent and selective inhibitor of cPKCs via interference with binding of ATP to the kinase (Martiny-Baron et al., 1993). Preliminary experiments using HAECs at 5 min, 15 min, 30 min, 1 h, 1.5 h, 2 h and 6 h revealed that 10 μM As(III) induces intercellular gaps beginning at 1 h of treatment that were identified by immunofluorescence staining of VE-cadherin. To determine the effective concentration of Gö 6976 to be used in our experiments, cells were exposed to 10 μM As(III) alone or to 10 nM, 50 nM, 100 nM, 250 nM, 500 nM and 1 μM Gö 6976 in the presence of 10 μM As(III) as depicted in Fig. 11. The duration of As(III) treatment was 1 h and the respective Gö 6976 treatments were applied 1 h prior to and during As(III) treatment. As analyzed by immunofluorescence staining of VE-cadherin, 250 nM-1 μM concentrations of Gö 6976 (Fig. 11F-H) were able to inhibit the As(III) induced gap formation. Therefore, in all the further experiments, 250 nM Gö 6976 was used to inhibit the activity of cPKCs. Also, the effect of Gö 6976 on cell viability was assessed using the MTT assay and no loss of viability was observed at concentrations 10 nM-500 nM up to 24 h (data not shown).

3.4.4 Effect of As(III) on the activation of PKCα

The translocation of PKC from cytosol to the membrane is an important step in its activation process (Newton, 2001). Therefore, the effect of As(III) on the activation of cPKCs in HAECs was analyzed by separation of the cytosolic and membrane fractions and determining the protein content in each fraction by Western blotting technique. Preliminary experiments showed that 10 μM As(III) treatment induced translocation of

PKCα from the cytosolic fraction to the membrane fraction at 1 h, but not with 15 min As(III) treatment. Also, serum starvation of cells (only 1% serum in medium) for 24 h followed by 1 h of 10 μM As(III) treatment showed a similar increase in PKCα levels in the membrane fraction as with 10 μM As(III) treatment without serum starvation. Hence, activation of cPKCs was analyzed at 1 h of As(III) treatment using medium containing serum, which is the normal environment for endothelial cells. As(III) induced damage to the endothelial monolayer was also observed starting at the 1-h time point. Therefore, cells were exposed to 1, 5 and 10 μM As(III) and cPKC activation was analyzed at the 1-h time point (Fig. 12). Treatment with 5 and 10 μM As(III) induced a significant increase in PKCα activation as determined by quantifying the protein content in the membrane fraction (Figs. 12A and B). No change was observed with 1 μM As(III) treatment. In the cytosolic fraction, a decrease in the PKCα content was observed with increasing As(III) concentration indicative of PKCα translocation from the cytosol to the membrane (Figs. 12C and D). Treatment of the cells with 250 nM Gö 6976 for 1 h or with 20 μM BAPTA-AM for 30 min, prior to and during 10 μM As(III) treatment inhibited the PKCα activation as analyzed in the membrane fraction (Figs. 12E and F). The acetoxymethyl (AM) ester derivatives are cell permeable and hence BAPTA-AM was used as an intracellular Ca^{2+} chelator. The cytosolic fraction showed a corresponding change (Figs. 12G and H). An exact proportionate change in the cytosolic fraction was not evident compared to the membrane fraction, but overall, protein levels were much greater in the cytosolic fraction than the membrane fraction. Phorbol esters are very potent activators of PKCs (Newton, 2001) and hence phorbol 12-myristate 13-acetate (PMA) was used as a

positive control. Treatment with 1 μM PMA for 1 h induced a robust activation of PKCα in the membrane fraction (Fig. 13).

PKCα is activated in a Ca^{2+}-dependent manner (Newton, 2001). The effect of Ca^{2+} ionophore, A23187, on PKCα activation was analyzed. Cells were treated with 10 μM A23187 for 10 min or with 20 μM BAPTA-AM for 30 min prior to and during A23187 treatment. Activation of PKCα in the membrane fraction was observed with A23187 that was inhibited by BAPTA-AM (Fig. 14). This also confirmed the function of BAPTA-AM as an intracellular Ca^{2+} chelator.

3.4.5 Effect of L-NAME and FeTPPS on As(III)-induced activation of PKCα

As(III) treatment in HAECs showed no peroxynitrite formation. This was further confirmed by analyzing the effect of the nitric oxide synthase inhibitor, L-NAME, and the peroxynitrite decomposition catalyst, FeTPPS, on activation of PKCα. Peroxynitrite is formed by the reaction between superoxide and nitric oxide. L-NAME impedes the formation of nitric oxide by inhibiting nitric oxide synthase, thereby limiting peroxynitrite formation. Cells were treated with 10 μM As(III) for 1 h or with 50 μM L-NAME for 1 h prior to and during As(III) treatment. Activation of PKCα was observed with As(III) treatment but no change was observed with L-NAME treatment (Figs. 15A and B). The effect of L-NAME on cell viability was assessed using the MTT assay and no loss of viability was observed at concentrations 10 μM-75 μM up to 24 h (data not shown). Treatment with 10 μM FeTPPS during 10 μM As(III) exposure for 1 h also showed no change in PKCα levels in the membrane fraction (Figs. 16A and B).

3.4.6 Effect of As(III) on the activation of PKCβ$_1$

The PKCβ gene consists of alternatively spliced variants, PKCβ$_1$ and β$_2$. Blobe et al. (1996) have demonstrated that the β$_1$ and β$_2$ isoforms display similar requirements for activation cofactors, phosphorylate substrates in an identical manner and are also inhibited to a similar extent. In addition, the kinetics of translocation to the membrane as well as down-regulation with PMA treatment was similar for both isoforms. Therefore, we initially analyzed the effect of As(III) on PKCβ$_1$ activation by determining its translocation from the cytosol to the membrane. Control and 10 μM As(III) treated samples that were used in analyzing PKCα levels were used to detect PKCβ$_1$ activation. The presence of PKCβ$_1$ was only detected in the cytosolic fraction and no protein was detected in the membrane fraction at the 1-h time point (Fig. 17). Since, no activation of PKCβ$_1$ was detected, the effect of As(III) on PKCβ$_2$ was not analyzed.

3.4.7 Effect of As(III) on tyrosine phosphorylation of VE-cadherin and β-catenin

The association of VE-cadherin with β-catenin is critical for the stability of adherens junctions, and tyrosine phosphorylation of either one or both proteins can alter endothelial integrity. As(III)-induced disruption of the endothelial monolayer was evident starting at the 1-h time point. Therefore, the effect of As(III) exposure on tyrosine phosphorylation of VE-cadherin and β-catenin was analyzed at 1 h by immunoprecipitation followed by Western blotting. The phosphorylation of β-catenin was determined by probing the membrane with anti-phosphotyrosine monoclonal antibody following electrophoresis (Fig. 18A). The same membrane was stripped and total β-catenin protein content was analyzed (Fig. 18B). The tyrosine phosphorylation

levels were determined by normalizing with the total β-catenin protein content (Fig. 18C). A concentration-dependent effect of As(III) exposure on tyrosine phosphorylation of β-catenin was observed. Treatment of cells with 1 μM As(III) showed no change in tyrosine phosphorylation as compared to the control (untreated), whereas an increasing trend in tyrosine phosphorylation was observed with 5 μM As(III), and 10 μM As(III) treatment resulted in a significant increase in tyrosine phosphorylation of β-catenin. The increase in tyrosine phosphorylation induced by 10 μM As(III) was completely inhibited by 250 nM Gö 6976 (Fig. 18C).

No tyrosine phosphorylation of VE-cadherin was observed (Fig. 18D). Even a basal level of tyrosine phosphorylation could not be detected. Increasing the concentrations of phosphatase inhibitors in the lysis buffer to confirm that VE-cadherin was not dephosphorylated during harvesting or immunoprecipitation did not yield any positive results. Analysis of the total VE-cadherin protein content established the presence of VE-cadherin and confirmed the adequacy of immunoprecipitation and Western blotting (Fig. 18E).

3.4.8 Effect of As(III) on tyrosine nitration of VE-cadherin and β-catenin

Peroxynitrite has been shown to induce nitration of β-catenin and cause disruption of the endothelial monolayer (Knepler et al., 2001). Although peroxynitrite generation was not observed with As(III) treatment, we analyzed the nitration of VE-cadherin and β-catenin. HAECs were treated with 10 μM As(III) for 1, 6 and 24 h, and tyrosine nitration was determined by immunoprecipitation followed by Western blotting. Tyrosine nitrated bovine serum albumin (BSA) was used as a positive control (Fig 19A). The tyrosine

nitration of VE-cadherin (Fig. 19B) and β-catenin (Fig. 19C) was determined by probing the membrane with anti-nitrotyrosine polyclonal antibody following electrophoresis. The same membranes were stripped and total VE-cadherin and β-catenin protein content was analyzed. No tyrosine nitration of VE-cadherin or β-catenin was detected at any time point. Analysis of the total VE-cadherin and β-catenin protein content established the presence of the proteins and confirmed the adequacy of immunoprecipitation and Western blotting. This further assured that tyrosine phosphorylation and not nitration was the main event following As(III) exposure.

3.4.9 Effect of As(III) on VE-cadherin localization and intercellular gap formation

Based on results from preliminary experiments, the concentration- and time-dependent effects of As(III) on VE-cadherin localization and intercellular gap formation were analyzed by immunofluorescence staining of VE-cadherin. Cells were treated with 1, 5 and 10 μM As(III) for 1, 6, 12 and 24 h. At the 1-h time point (Fig. 20), the frequency of gap formation observed with 10 μM As(III) treatment (Fig. 20D) was much greater than 5 μM As(III) (Fig. 20C) and only a few gaps were observed with 1 μM As(III) treatment (Fig. 20B) as compared to the untreated cells (Fig. 20A). Cells appeared to be pulling apart from the adjacent cells. Some areas of undamaged monolayer could be observed. Also, non-uniform staining of VE-cadherin was observed where the gaps appeared. To corroborate the fact that the observed effects were not due to cells undergoing apoptosis, immunofluorescence staining for cleaved caspase-3 was performed. Figs 20E and F demonstrate little cleaved caspase-3 staining for either untreated or 10 μM As(III) treated cells, respectively. The cPKC inhibitor, Gö 6976, inhibited gap formation at all

concentrations of As(III) treatment and uniform distribution of VE-cadherin could be observed at cell-cell junctions. The images of 250 nM Gö 6976 treatment alone (Fig. 20G) and 10 μM As(III) + 250 nM Gö 6976 treatment (Fig. 20H) are shown. As with As(III) treatment, little and similar cleaved caspase-3 staining was observed for 250 nM Gö 6976 treatment alone and 10 μM As(III) + 250 nM Gö 6976 treatment (data not shown).

At the 6-h time point (Fig. 21), a similar concentration-dependent effect of As(III) was observed but the size and frequency of gaps were greater than that observed at the 1 h time point. Exposure to 1 μM (Fig. 21B) and 5 μM As(III) (Fig. 21C) revealed non-uniform staining of VE-cadherin where the gaps appeared whereas treatment with 10 μM As(III) (Fig. 21D) resulted in loss of VE-cadherin staining at the cell-cell junctions. Immunofluorescence staining of cleaved caspase-3 in untreated (Fig. 21E) and 10 μM As(III) treated cells (Fig. 21F) revealed no differences in apoptosis. Also, Gö 6976 inhibited gap formation at all concentrations of As(III) treatment and restored VE-cadherin staining at the cell-cell junctions. The images of 250 nM Gö 6976 alone (Fig. 21G) and 10 μM As(III) + 250 nM Gö 6976 treatment (Fig. 21H) are shown. As with As(III), little and similar cleaved caspase-3 staining was observed for 250 nM Gö 6976 treatment alone and 10 μM As(III) + 250 nM Gö 6976 treatment (data not shown).

At the 12-h (Fig. 22A-H) and 24-h (Fig. 23A-H) time points, the concentration-dependent effects of As(III) treatment were similar to those seen at earlier time points. However, the frequency and size of gaps observed were maximal at the 6-h time point.

3.4.10 Effect of As(III) treatment on VE-cadherin protein content

The immunofluorescence results in Figs. 20-23 showed that VE-cadherin distribution was altered by As(III) exposure. Therefore, the effects of 1, 5, and 10 μM As(III) treatments on the protein levels of VE-cadherin at the 24-h time point were determined. Western blotting analysis revealed a concentration-dependent effect of As(III) on VE-cadherin protein levels in the HAECs (Figs. 24A and B). Approximately 8, 15 and 30% reductions in VE-cadherin protein were observed with 1, 5 and 10 μM As(III) treatment, respectively, compared to the control (untreated) HAECs (Fig. 24B).

3.4.11 Effect of As(III) exposure on β-catenin localization

The cytoplasmic domain of VE-cadherin is linked with β-catenin, so it was of interest to determine whether As(III) affects β-catenin distribution. Exposure to As(III) for 6 h revealed the most damaging effects on the endothelial monolayer. Hence, the effect of As(III) treatment on β-catenin localization in HAECs was analyzed by immunofluorescence staining at the 6-h time point (Fig. 25). As previously observed with VE-cadherin localization, β-catenin staining showed a corresponding concentration-dependent effect with As(III) treatment. The frequency of gap formation with 10 μM As(III) (Fig. 25D) was greater than 5 μM As(III) (Fig. 25C) and only a few gaps were observed with 1 μM As(III) treatment (Fig. 25B). Non-uniform distribution or loss of β-catenin staining was evident wherever gaps could be observed. Also, 250 nM Gö 6976 treatment inhibited the gap formation induced by 10 μM As(III) (Fig. 25E) and restored the β-catenin staining at cell-cell junctions.

3.4.12 Effect of As(III) exposure on the formation of stress fibers

The cadherin/β-catenin complex is associated with the actin cytoskeleton, and this association is very important for maintaining junctional stability and structural integrity of the endothelial cell monolayer. As previously mentioned, reorganization of actin microfilaments into stress fibers can adversely affect monolayer integrity. Hence, the effects of 1, 5 and 10 μM As(III) on reorganization of actin microfilaments were analyzed at 1, 6, 12 and 24 h by immunofluorescence staining using fluorophore-conjugated phalloidin. A concentration- and time-dependent effect of As(III) treatment was observed. At the 1-h time point (Fig. 26), As(III) induced a concentration-dependent increase in stress fibers with the maximum stress fibers being observed with 10 μM As(III) treatment (Fig. 26D). Treatment with Gö 6976 abolished the stress fiber formation at all concentrations of As(III) treatment. The images of 250 nM Gö 6976 treatment alone (Fig. 26E) and 10 μM As(III) + 250 nM Gö 6976 treatment (Fig. 26F) are shown.

At the 6-h time point (Fig. 27), the frequency and density of stress fibers induced by As(III) was much higher than that observed at the 1-h time point. Also, a concentration-dependent increase in stress fibers was observed with the maximum stress fibers being induced with 10 μM As(III) treatment (Fig. 27D). Treatment with Gö 6976 reduced the stress fibers at all concentrations of As(III) treatment. The images of 250 nM Gö 6976 treatment alone (Fig. 27E) and 10 μM As(III) + 250 nM Gö 6976 treatment (Fig. 27F) are shown.

At the 12-h (Fig. 28A-F) and 24-h (Fig. 29A-F) time points, similar concentration-dependent effects of As(III) treatment were observed. Stress fiber formation, like the intercellular gap formation, was maximal at the 6-h time point.

3.4.13 Effect of As(III) on endothelial permeability

Exposure to As(III) caused detrimental effects on the endothelial monolayer and induced reorganization of actin microfilaments into stress fibers. Therefore, we hypothesized that As(III) would also increase endothelial permeability. The effect of 1, 5 and 10 μM As(III) treatment on endothelial permeability was analyzed at the 6-h time point (Fig. 30). Confluent monolayers of HAECs grown on Transwell inserts were treated with various As(III) concentrations, and the permeability of the monolayer for FITC-dextran was determined by measuring the fluorescence intensity of the medium in the plate well. A 5% increase in permeability was observed with 1 and 5 μM As(III) treatment, whereas 10 μM As(III) induced approximately a 19% increase. Treatment with 250 nM Gö 6976 inhibited the increase in permeability induced by 10 μM As(III).

3.5 Figures

Table. 2. Cell viability after As(III) treatment

Time	12 h	24 h	48 h
IC50	103 μM	40 μM	23 μM
Threshold	50 μM	10 μM	5 μM

Table. 2. Cell viability after As(III) treatment. HAECs were treated with As(III) up to 500 μM for 12, 24 and 48 h. Cell viability was determined using the MTT colorimetric assay.

Fig. 10. Effect of As(III) on peroxynitrite formation

A.

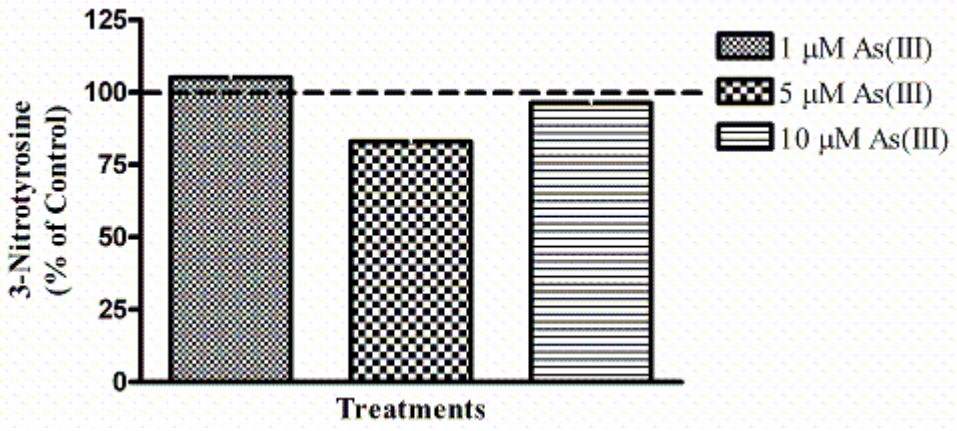

B.

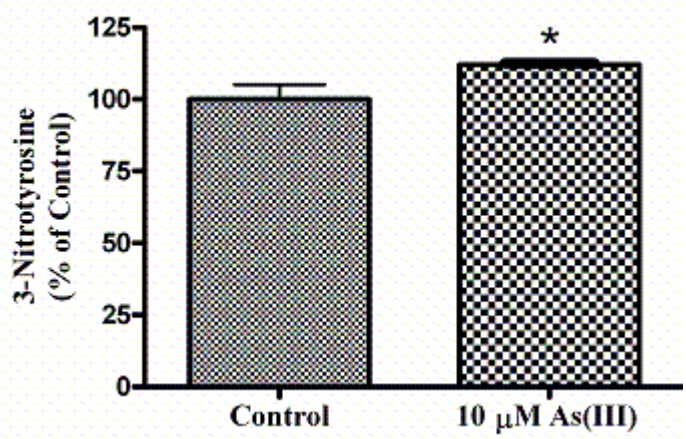

C.

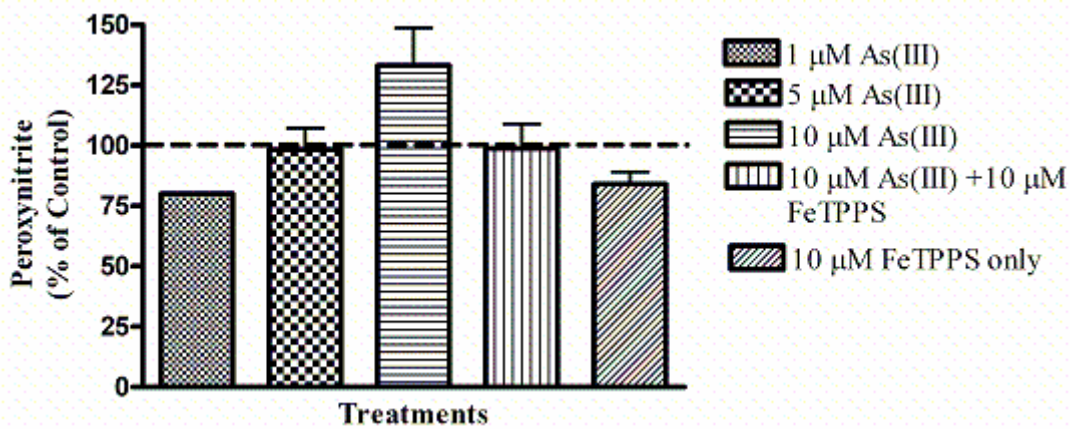

Fig. 10. Effect of As(III) on peroxynitrite formation. (A) Confluent HAECs were treated with 1, 5 and 10 μM As(III) for 24 h and the formation of 3-nitrotyrosine was analyzed by immunofluorescence. The control (100%) is indicated by dotted line and the graph is representative of 2 independent experiments performed. (B) Confluent BAECs were treated with 10 μM As(III) for 24 h and the formation of 3-nitrotyrosine was analyzed by immunofluorescence quantification. Error bars represent mean ± SEM for n=3 and * indicates significantly different from control with $p<0.05$. (C) Confluent HAECs were treated with 1, 5 and 10 μM As(III) or 10 μM FeTPPS in the presence of 10 μM As(III) for 1 h and the formation of peroxynitrite was analyzed based on the oxidation of hydroethidine to ethidium. Error bars represent mean ± SEM for n=4-5.

Fig. 11. Dose response of HAECs to cPKC inhibitor Gö 6976

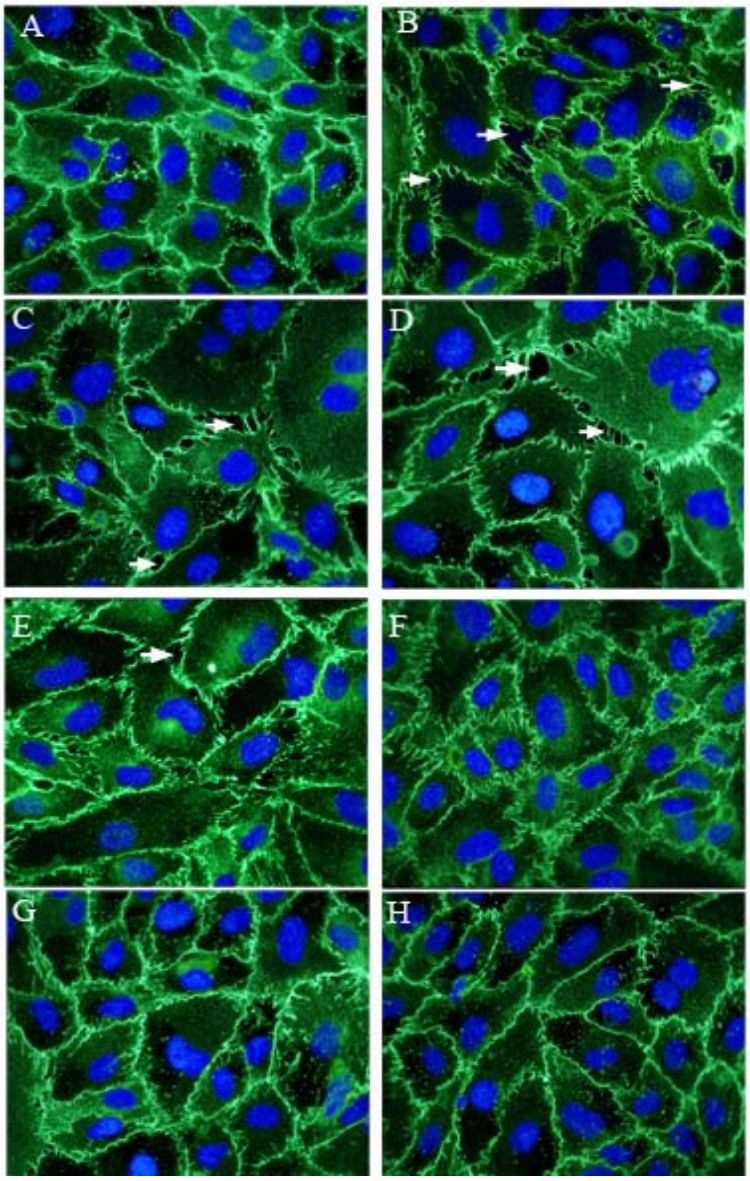

Fig. 11. Dose response of HAECs to cPKC inhibitor Gö 6976. Confluent HAEC monolayers were either untreated (A) or treated with 10 μM As(III) (B) for 1 h and the intercellular gaps (indicated with arrows) were visualized by immunofluorescence staining of VE-cadherin (green). The nuclei were stained with Hoechst (blue). Pretreating the cells with increasing concentration of Gö 6976 for 1 h prior to and during 10 μM As(III) treatment inhibited the gap formation in a concentration-dependent manner: 10 μM As(III) + 10 nM Gö 6976 (C), 10 μM As(III) + 50 nM Gö 6976 (D), 10 μM As(III) + 100 nM Gö 6976 (E), 10 μM As(III) + 250 nM Gö 6976 (F), 10 μM As(III) + 500 nM Gö 6976 (G) and 10 μM As(III) + 1 μM Gö 6976 (H). Magnification=60X. The images are representative of 3 independent experiments performed.

Fig. 12. Effect of As(III) on the activation of PKCα

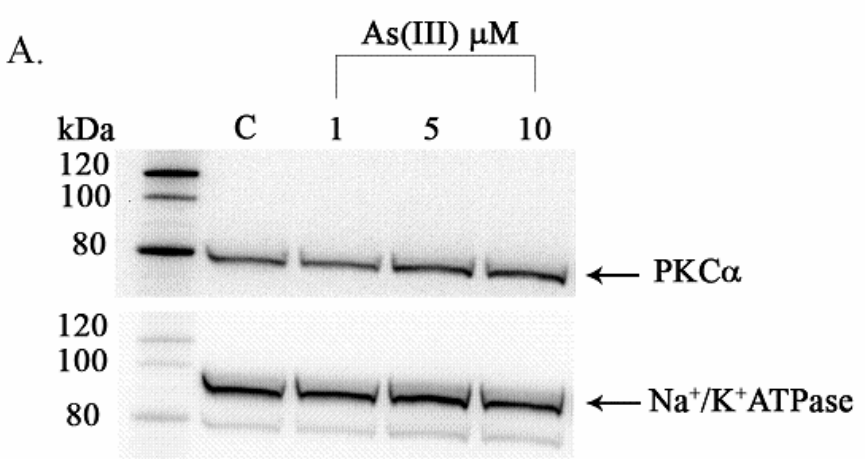

B.

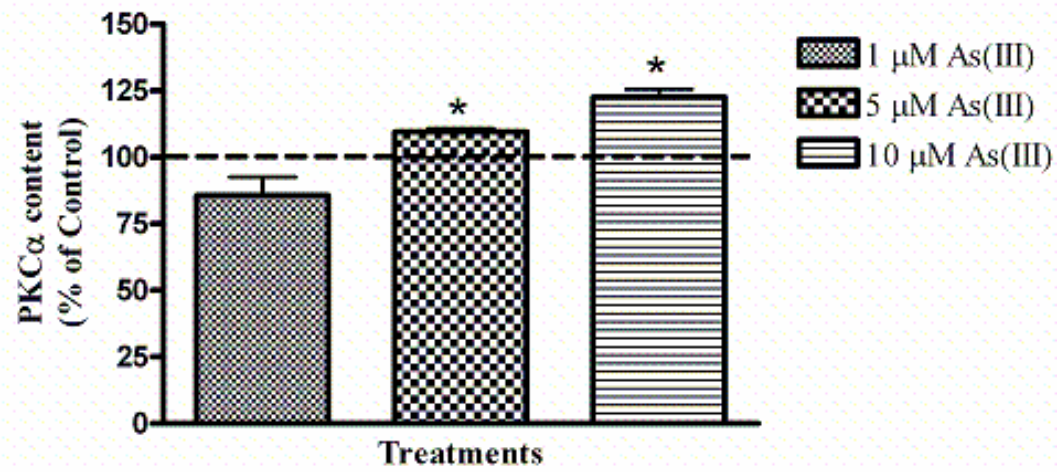

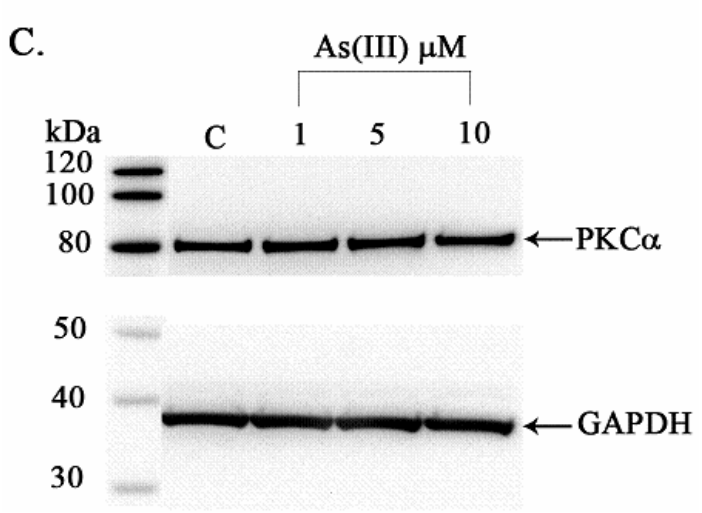
C.
As(III) μM
kDa
C
1
5
10
120
100
80
PKCα
50
40
30
GAPDH

D.

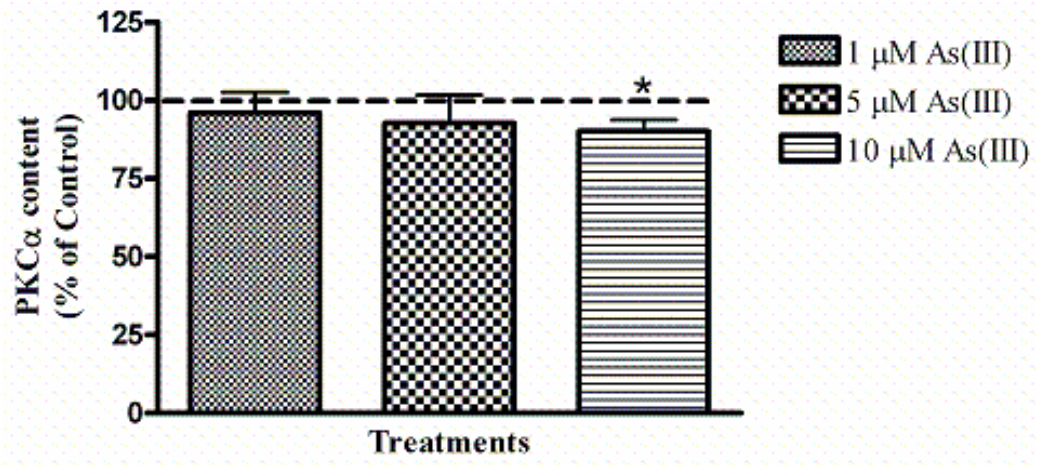
125
100
75
50
25
0
PKCα content
(% of Control)
*
Treatments
1 μM As(III)
5 μM As(III)
10 μM As(III)

E.

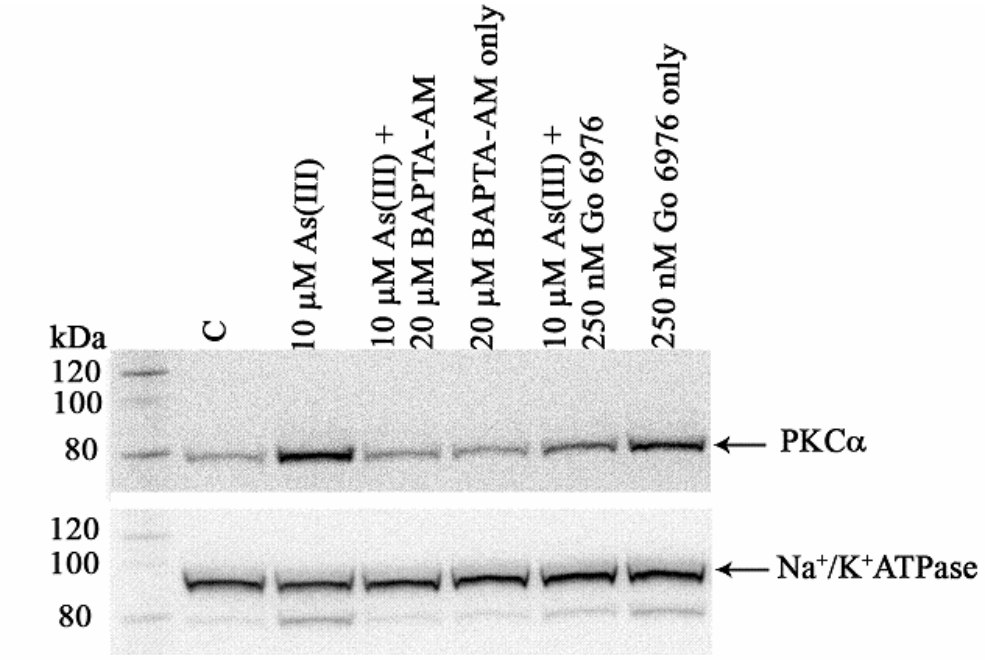
C
10 μM As(III)
10 μM As(III) + 20 μM BAPTA-AM
20 μM BAPTA-AM only
10 μM As(III) + 250 nM Go 6976
250 nM Go 6976 only
kDa
120
100
80
PKCα
120
100
80
Na+/K+ATPase

F.

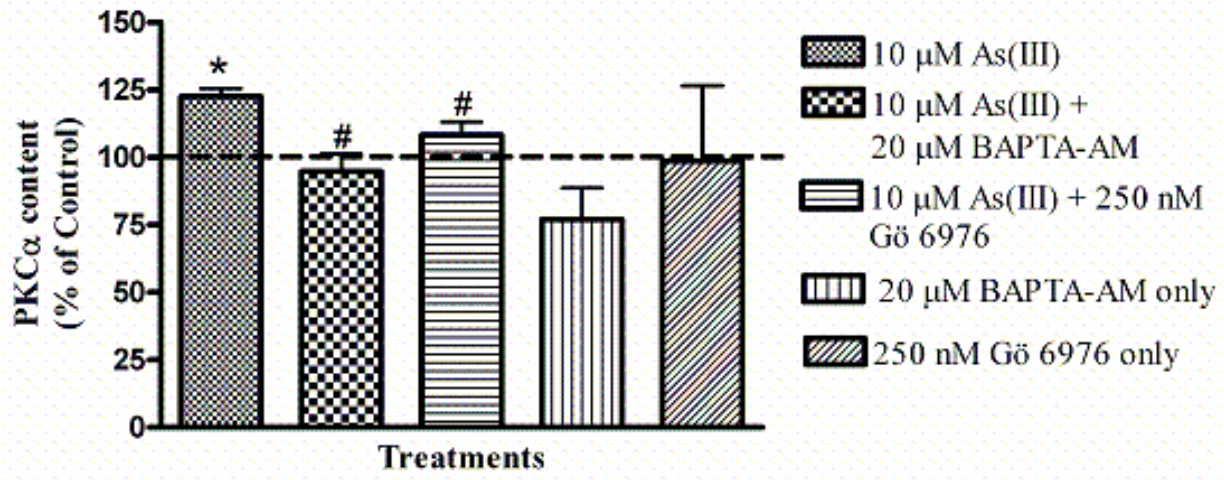
PKCα content (% of Control)
150
125
100
75
50
25
0
*
#
#
Treatments
10 μM As(III)
10 μM As(III) + 20 μM BAPTA-AM
10 μM As(III) + 250 nM Gö 6976
20 μM BAPTA-AM only
250 nM Gö 6976 only

G.

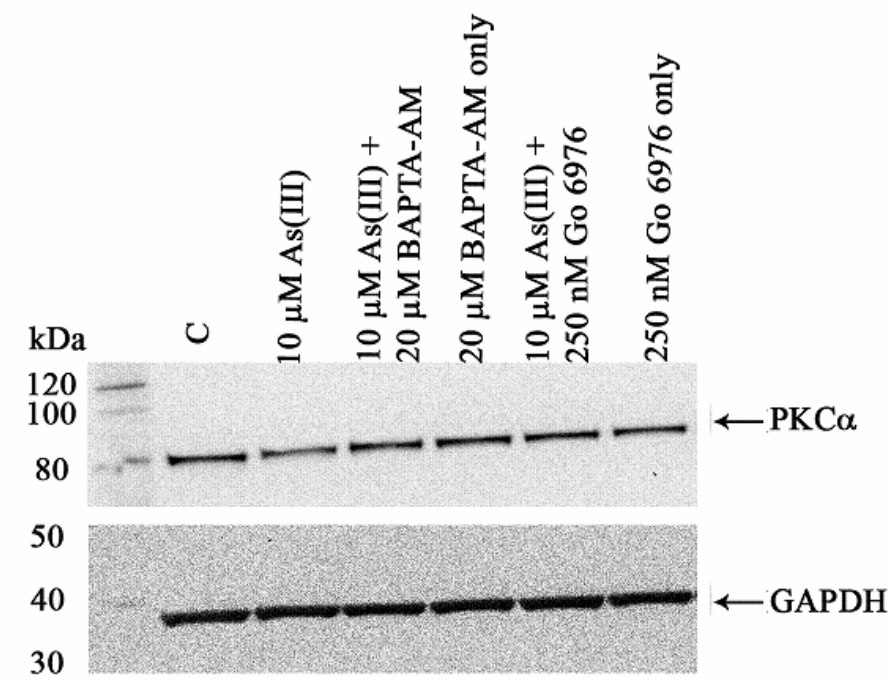
kDa
C
10 μM As(III)
10 μM As(III) + 20 μM BAPTA-AM
20 μM BAPTA-AM only
10 μM As(III) + 250 nM Go 6976
250 nM Go 6976 only
120
100
80
50
40
30
PKCα
GAPDH

H.

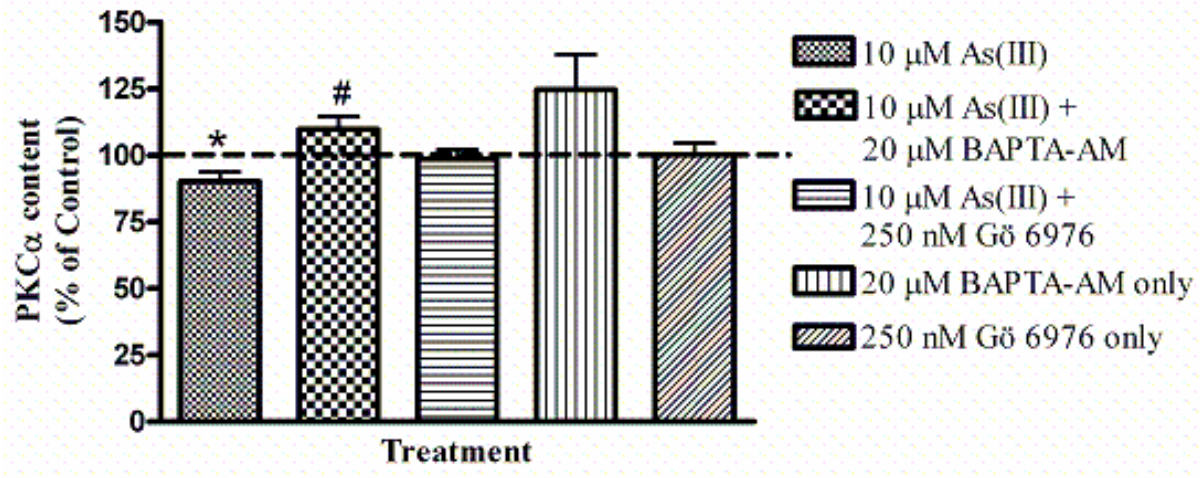
PKCα content (% of Control)
150
125
100
75
50
25
0
*
#
Treatment
10 μM As(III)
10 μM As(III) + 20 μM BAPTA-AM
10 μM As(III) + 250 nM Gö 6976
20 μM BAPTA-AM only
250 nM Gö 6976 only

Fig. 12. Effect of As(III) on the activation of PKCα. Confluent HAECs were treated with 1, 5, and 10 μM As(III) for 1 h or pretreated with 250 nM Gö 6976 and 20 μM BAPTA-AM for 1 h and 30 min, respectively, prior to and during 10 μM As(III) treatment. The lysates were subjected to ultracentrifugation to separate the membrane and cytosolic fractions and the PKCα levels in both fractions were determined by Western blotting. The PKCα content in the membrane fraction is shown in (A and E) upper panel and the lower panel represents the Na^+/K^+ ATPase loading control for the membrane fraction. The percent change in PKCα content in the membrane fraction relative to the control (untreated) is represented in (B and F). The PKCα content in the cytosolic fraction is shown in (C and G) upper panel and the lower panel represents the GAPDH loading control for the cytosolic fraction. The percent change in PKCα content in the cytosolic fraction relative to the control is represented in (D and H). The images in (A, C, E and G) are representative of 3-6 independent experiments performed. The control (100%) is indicated by the dotted line in (B, D, F and H). Error bars represent mean ± SEM for n=3-6. * and # indicates significantly different from control and 10 μM As(III), respectively, with $p<0.05$.

Fig. 13. Effect of As(III) and PMA on the activation of PKCα

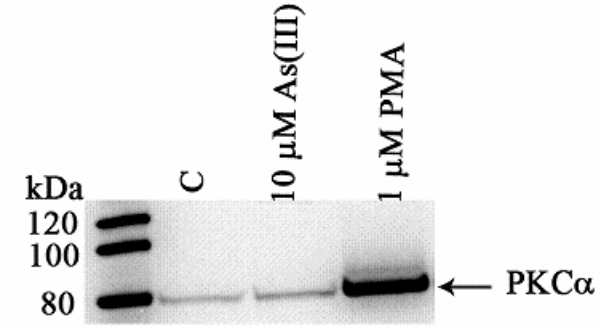

Fig. 13. Effect of As(III) and PMA on the activation of PKCα. Confluent HAECs were treated with 10 μM As(III) or the positive control 1 μM PMA for 1 h. The lysates were subjected to ultracentrifugation to separate the membrane and cytosolic fractions and the PKCα levels were determined by Western blotting. The PKCα content in the membrane fraction is shown. The image is from one experiment performed.

Fig. 14. Effect of A23187 on the activation of PKCα

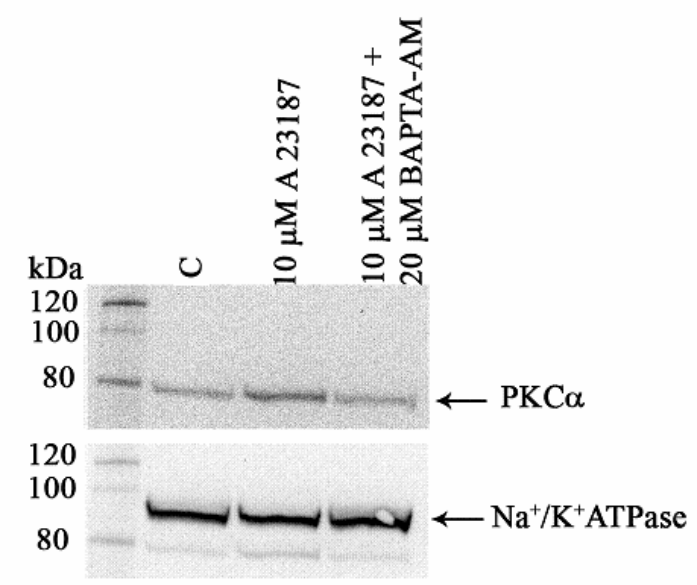

Fig. 14. Effect of A23187 on activation of PKCα. Confluent HAECs were treated with 10 μM A23187 for 10 min or pretreated with 20 μM BAPTA-AM for 30 min prior to and during 10 μM A23187 treatment. The lysates were subjected to ultracentrifugation to separate the membrane and cytosolic fractions and the PKCα levels were determined by Western blotting. The PKCα content in the membrane fraction is shown in the upper panel and the lower panel represents the Na^+/K^+ ATPase loading control for the membrane fraction. The image is from one experiment performed.

Fig. 15. Effect of L-NAME on As(III)-induced activation of PKCα

A.

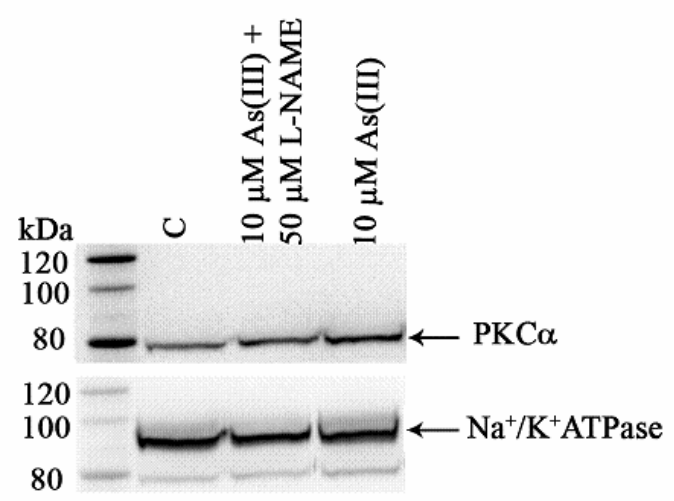

B.

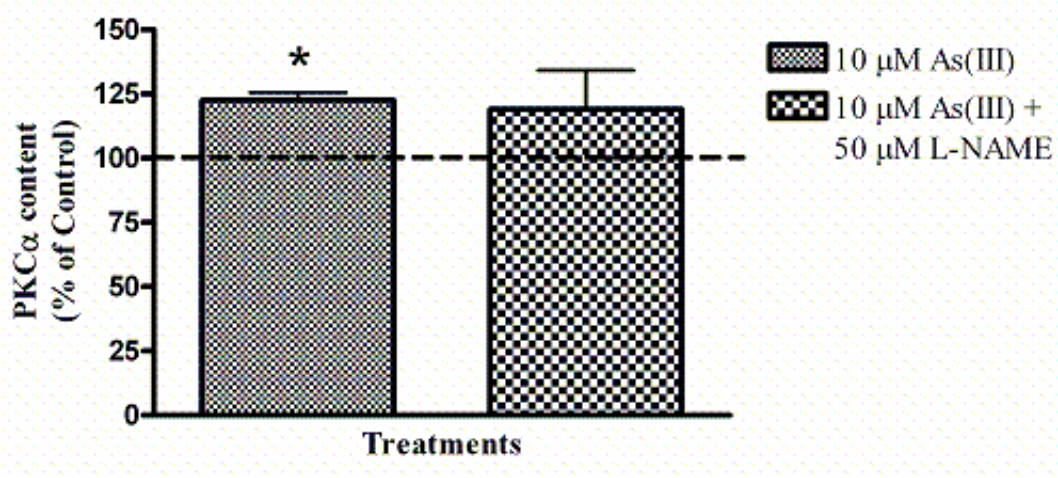

Fig. 15. Effect of L-NAME on As(III)-induced activation of PKCα. Confluent HAECs were treated with 10 μM As(III) for 1 h or pretreated with 50 μM L-NAME for 1 h prior to and during As(III) treatment. The lysates were subjected to ultracentrifugation to separate the membrane and cytosolic fractions and the PKCα levels in both fractions were determined by Western blotting. The PKCα content in the membrane fraction is shown in (A) upper panel and the lower panel represents the Na^+/K^+ ATPase loading control for the membrane fraction. The percent change in PKCα content in the membrane fraction relative to the control (untreated) is represented in (B). The control (100%) is indicated by the dotted line in (B). The image (A) is representative of 5-6 independent experiments performed. Error bars represent mean ± SEM for n=5-6. * indicates significantly different from control with $p<0.001$.

Fig. 16. Effect of FeTPPS on As(III)-induced activation of PKCα

A.

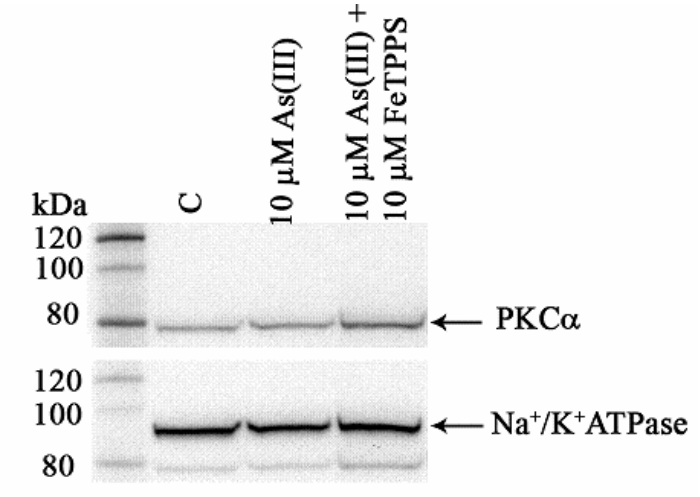

B.

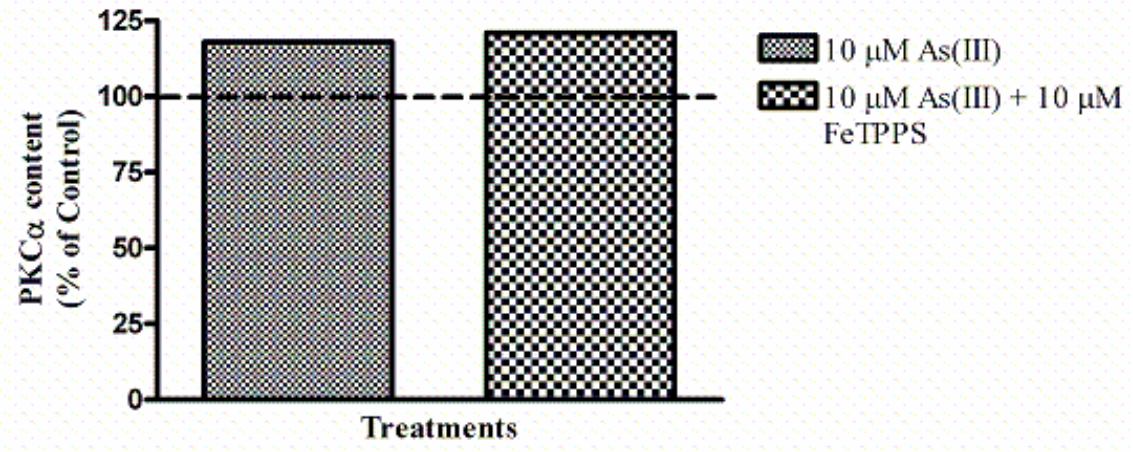

Fig. 16. Effect of FeTPPS on As(III)-induced activation of PKCα. Confluent HAECs were treated with 10 μM As(III) or 10 μM FeTPPS in the presence of 10 μM As(III) for 1 h. The lysates were subjected to ultracentrifugation to separate the membrane and cytosolic fractions and the PKCα levels were determined by Western blotting. The PKCα content in the membrane fraction is shown in (A) upper panel and the lower panel represents the Na^+/K^+ ATPase loading control for the membrane fraction. The percent change in PKCα content in the membrane fraction relative to the control (untreated) is represented in (B). The control (100%) is indicated by the dotted line in (B). The image (A) is representative of 2 independent experiments performed.

Fig. 17. Effect of As(III) on the activation of PKCβ$_1$

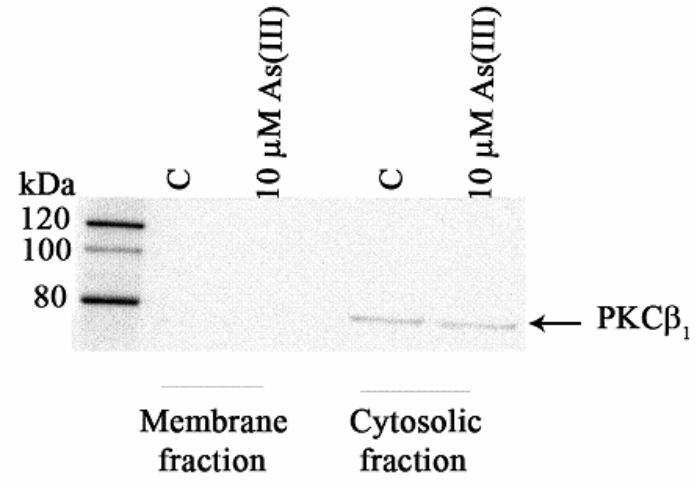

Fig. 17. Effect of As(III) on the activation of PKCβ$_1$. Confluent HAECs were treated with 10 μM As(III) for 1 h. The lysates were subjected to ultracentrifugation to separate the membrane and cytosolic fractions and the PKCβ$_1$ levels in both fractions were determined by Western blotting. The image is representative of 2 independent experiments performed.

Fig. 18. Effect of As(III) on tyrosine phosphorylation of β-catenin and VE-cadherin

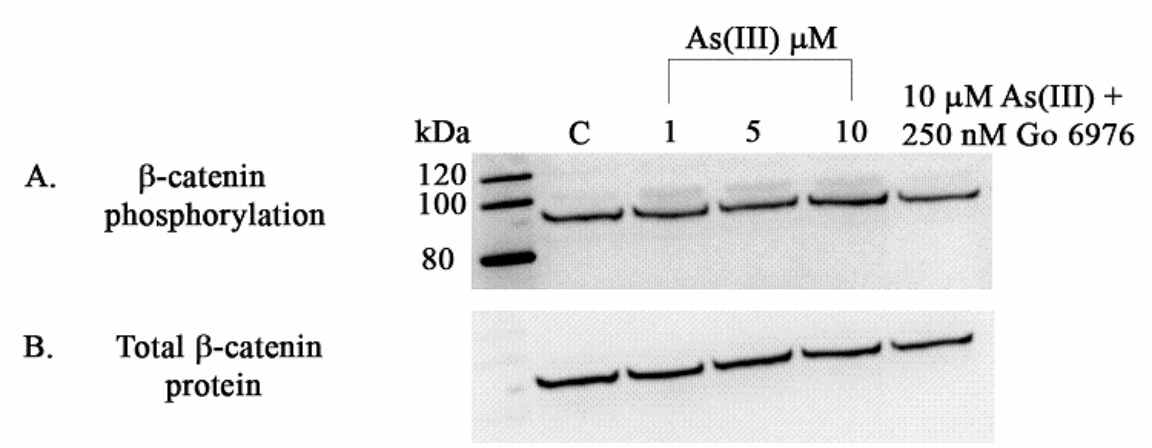

C.

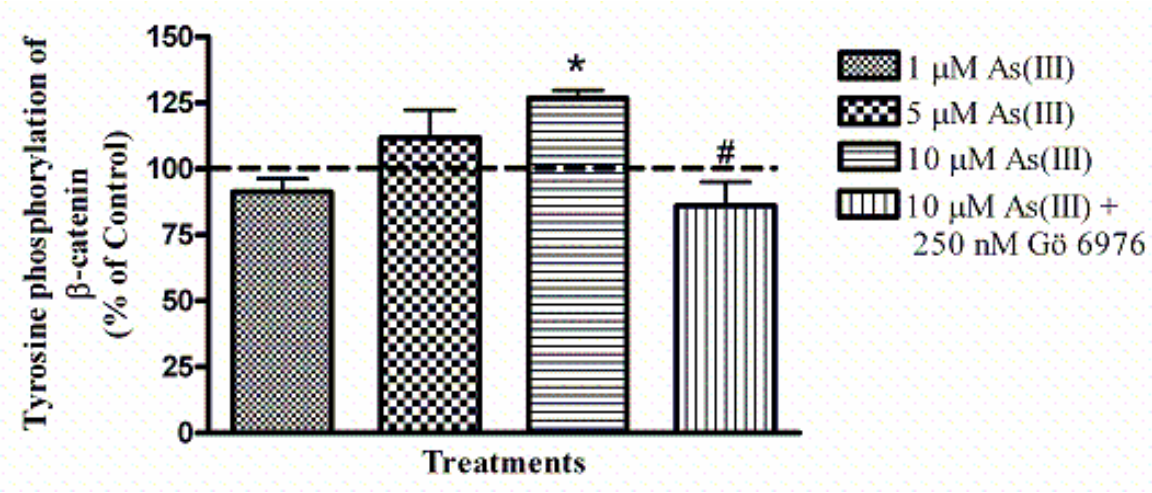

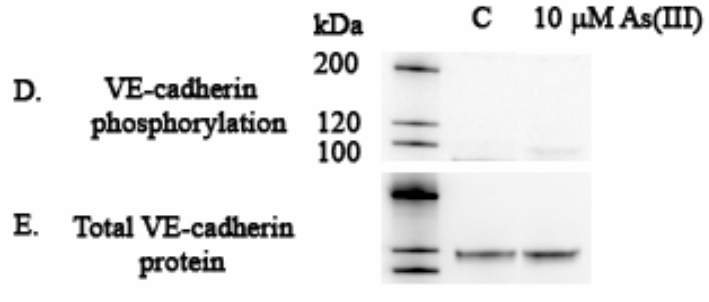

Fig. 18. Effect of As(III) on tyrosine phosphorylation of β-catenin and VE-cadherin. Confluent HAECs were treated with 1, 5, and 10 μM As(III) for 1 h or pretreated with 250 nM Gö 6976 for 1 h prior to and during 10 μM As(III) treatment. The β-catenin was immunoprecipitated, and Western blotting technique was used to analyze the phosphorylation of tyrosine residues (A). The membrane was stripped and reprobed to determine the total β-catenin protein content (B). The images A and B are representative of 4-6 independent experiments performed. The percent change in tyrosine phosphorylation with the various treatments relative to the control (untreated) is represented in (C). The control (100%) is indicated by the dotted line. Error bars represent mean ± SEM for n=4-6. * and # indicates significantly different from control and 10 μM As(III), respectively, with $p<0.05$. Similarly, the VE-cadherin protein was immunoprecipitated, and Western blotting technique was used to analyze the phosphorylation of tyrosine residues (D). The membrane was stripped and reprobed to determine the total VE-cadherin protein content (E). The images D and E are representative of 2 independent experiments performed.

Fig. 19. Effect of As(III) on tyrosine nitration of VE-cadherin and β-catenin

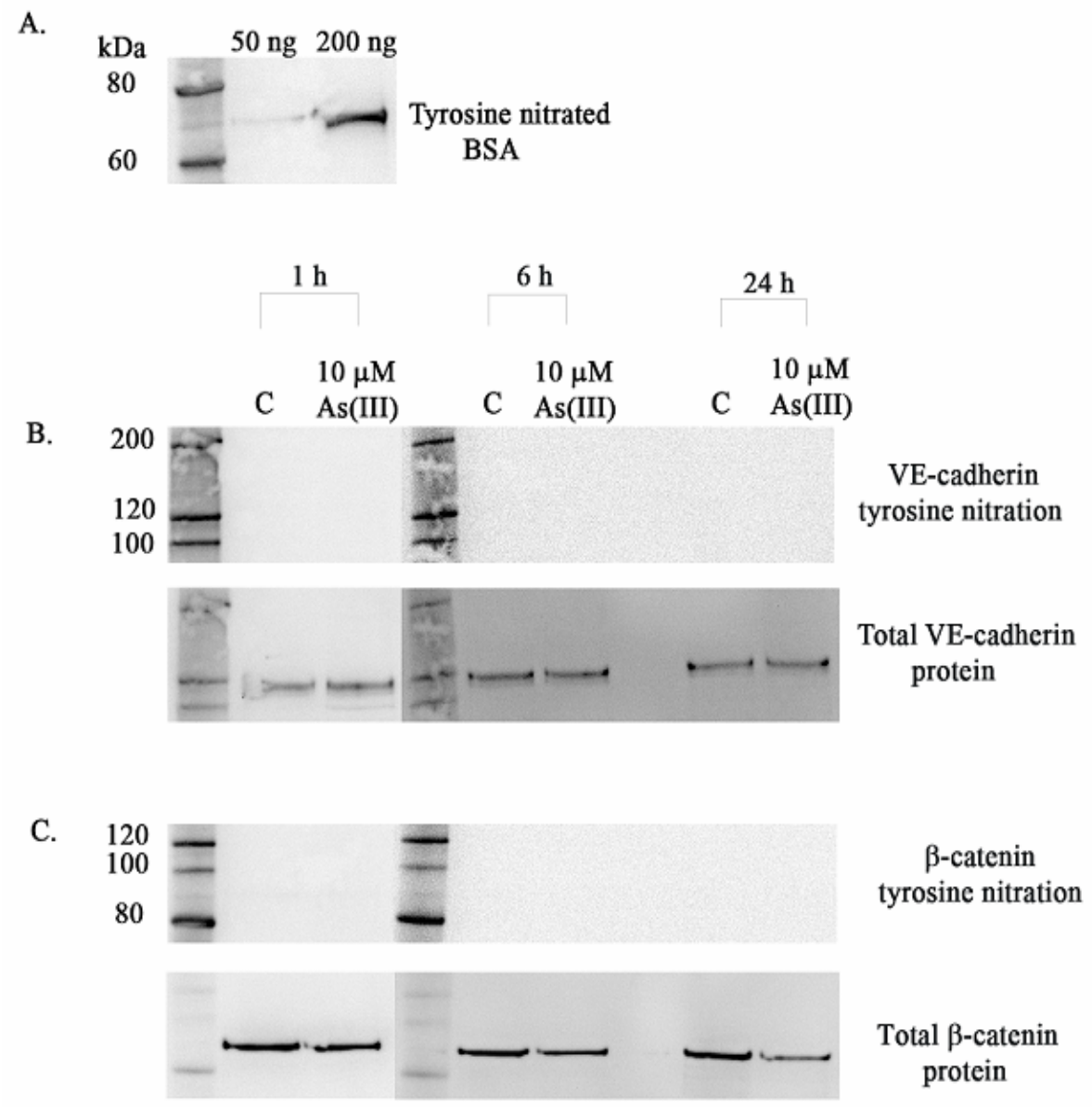

Fig. 19. Effect of As(III) on tyrosine nitration of VE-cadherin and β-catenin. Confluent HAECs were treated with 10 μM As(III) for 1, 6 and 24 h. The VE-cadherin and β-catenin proteins were immunoprecipitated, and Western blotting technique was used to analyze the nitration of tyrosine residues (B and C upper panel). The membranes were stripped and reprobed to determine the total VE-cadherin and β-catenin protein content (B and C lower panel). The images in A, B and C are from one experiment performed. Nitrated BSA was used as a positive control (A).

Fig. 20. Effect of As(III) on VE-cadherin localization and intercellular gap formation at the 1-h time point

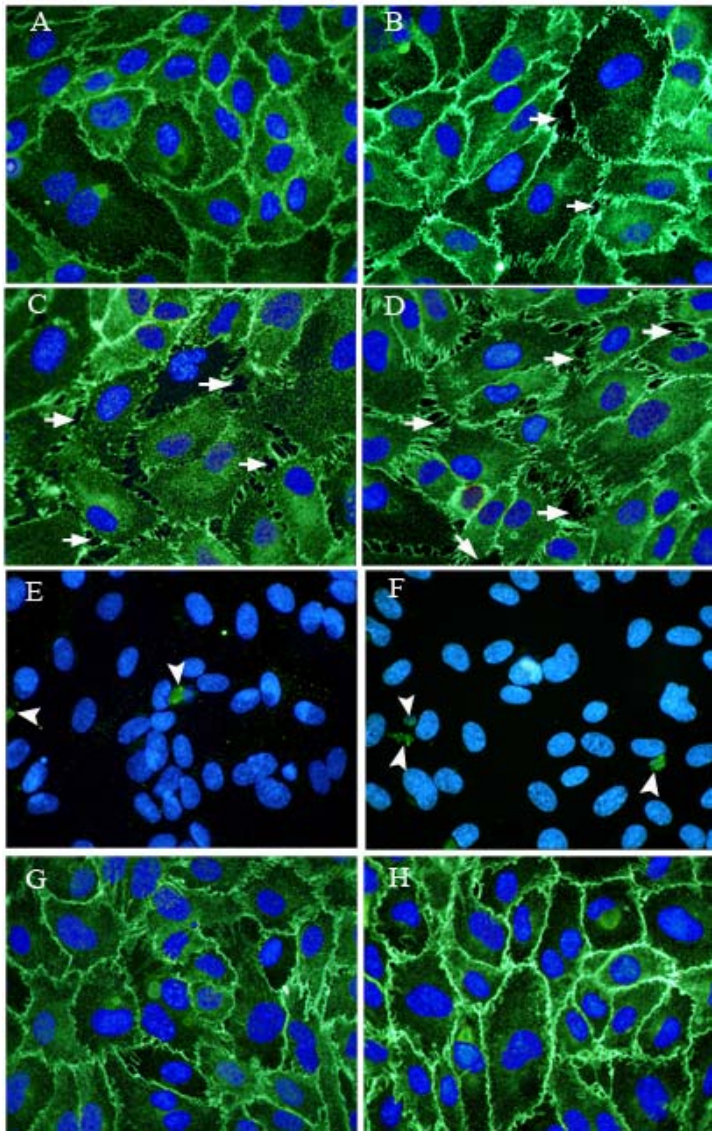

Fig. 20. Effect of As(III) on VE-cadherin localization and intercellular gap formation at the 1-h time point. Confluent HAEC monolayers were either untreated (A) or treated with 1 μM As(III) (B), 5 μM As(III) (C) and 10 μM As(III) (D) for 1 h and the intercellular gaps (indicated with arrows) induced with As(III) treatment were visualized by immunofluorescence staining of VE-cadherin (green). The nuclei were stained with Hoechst (blue). Cleaved caspase-3 staining (green) for untreated (E) and 10 μM As(III) (F) treated cells is indicated by arrowheads. Pretreatment with 250 nM Gö 6976 for 1 h prior to and during 10 μM As(III) treatment (H) inhibited the As(III) induced gaps whereas 250 nM Gö 6976 treatment alone (G) did not have any effect on the endothelial monolayer. Magnification=60X. The images are representative of 4 independent experiments performed.

Fig. 21. Effect of As(III) on VE-cadherin localization and intercellular gap formation at the 6-h time point.

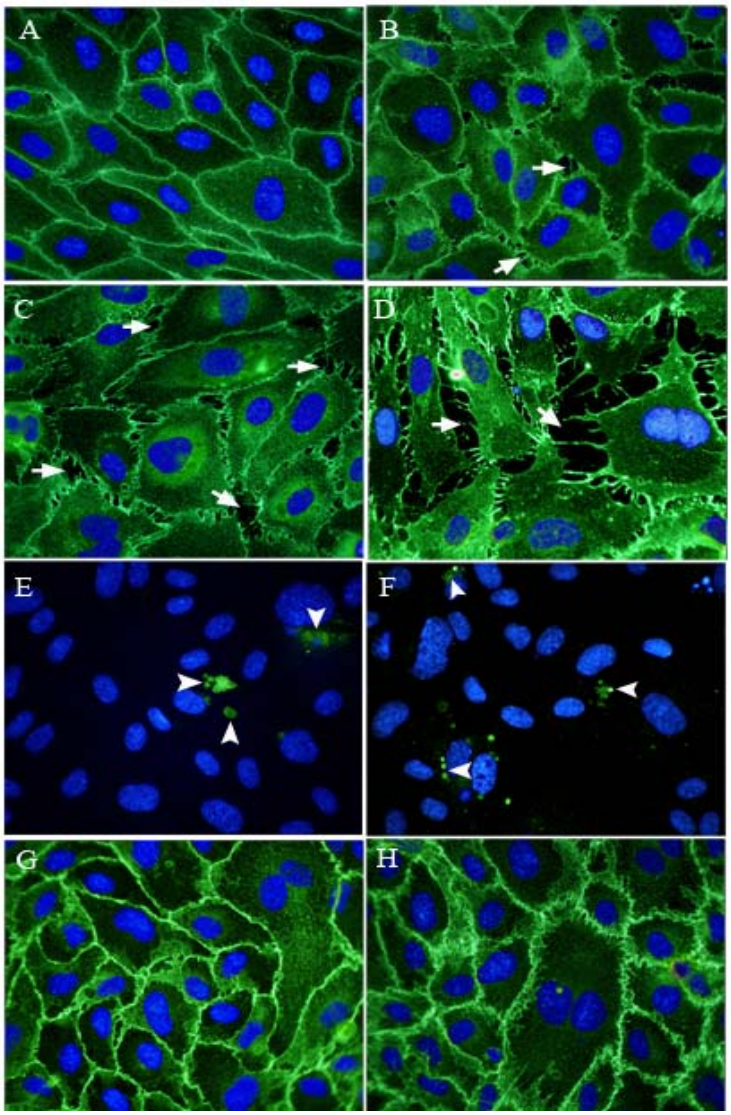

Fig. 21. Effect of As(III) on VE-cadherin localization and intercellular gap formation at the 6-h time point. Confluent HAEC monolayers were either untreated (A) or treated with 1 μM As(III) (B), 5 μM As(III) (C) and 10 μM As(III) (D) for 6 h and the intercellular gaps (indicated with arrows) induced with As(III) treatment were visualized by immunofluorescence staining of VE-cadherin (green). The nuclei were stained with Hoechst (blue). Cleaved caspase-3 staining (green) for untreated (E) and 10 μM As(III) (F) treated cells is indicated by arrowheads. Pretreatment with 250 nM Gö 6976 for 1 h prior to and during 10 μM As(III) treatment (H) inhibited the As(III) induced gaps whereas 250 nM Gö 6976 treatment alone (G) did not have any effect on the endothelial monolayer. Magnification=60X. The images are representative of 4 independent experiments performed.

Fig. 22. Effect of As(III) on VE-cadherin localization and intercellular gap formation at the 12-h time point.

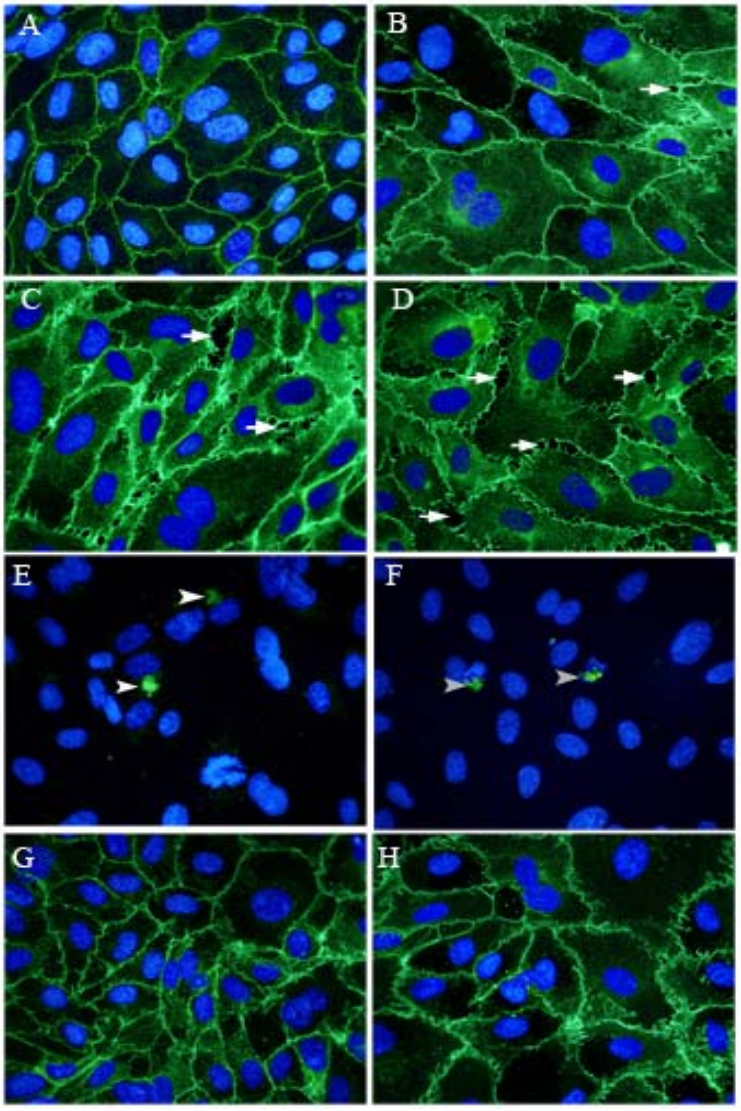

Fig. 22. Effect of As(III) on VE-cadherin localization and intercellular gap formation at the 12-h time point. Confluent HAEC monolayers were either untreated (A) or treated with 1 μM As(III) (B), 5 μM As(III) (C) and 10 μM As(III) (D) for 12 h and the intercellular gaps (indicated with arrows) induced with As(III) treatment were visualized by immunofluorescence staining of VE-cadherin (green). The nuclei were stained with Hoechst (blue). Cleaved caspase-3 staining (green) for untreated (E) and 10 μM As(III) (F) treated cells is indicated by arrowheads. Pretreatment with 250 nM Gö 6976 for 1 h prior to and during 10 μM As(III) treatment (H) inhibited the As(III) induced gaps whereas 250 nM Gö 6976 treatment alone (G) did not have any effect on the endothelial monolayer. Magnification=60X. The images are representative of 4 independent experiments performed.

Fig. 23. Effect of As(III) on VE-cadherin localization and intercellular gap formation at the 24-h time point

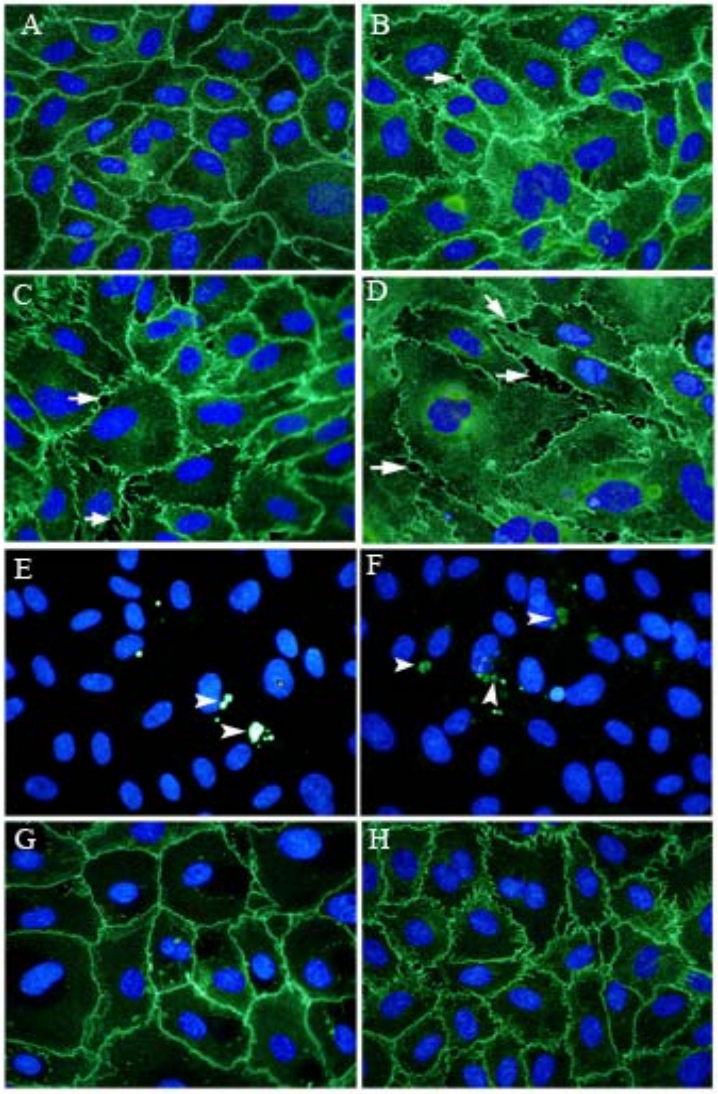

Fig. 23. Effect of As(III) on VE-cadherin localization and intercellular gap formation at the 24-h time point. Confluent HAEC monolayers were either untreated (A) or treated with 1 μM As(III) (B), 5 μM As(III) (C) and 10 μM As(III) (D) for 24 h and the intercellular gaps (indicated with arrows) induced with As(III) treatment were visualized by immunofluorescence staining of VE-cadherin (green). The nuclei were stained with Hoechst (blue). Cleaved caspase-3 staining (green) for untreated (E) and 10 μM As(III) (F) treated cells is indicated by arrowheads. Pretreatment with 250 nM Gö 6976 for 1 h prior to and during 10 μM As(III) treatment (H) inhibited the As(III) induced gaps whereas 250 nM Gö 6976 treatment alone (G) did not have any effect on the endothelial monolayer. Magnification=60X. The images are representative of 4 independent experiments performed.

Fig. 24. Effect of As(III) treatment on VE-cadherin protein content

A.

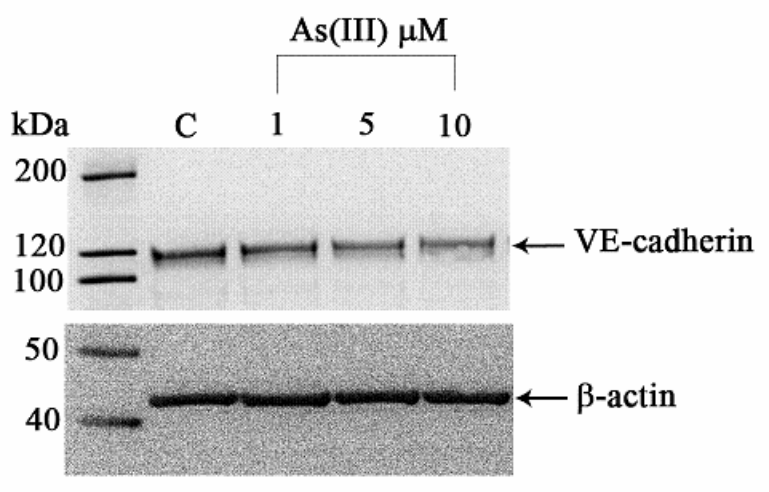

B.

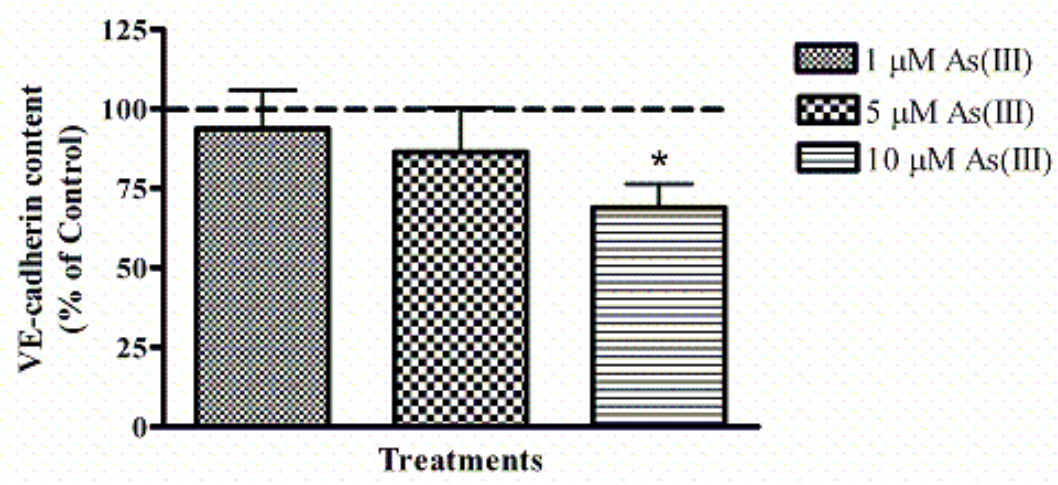

Fig. 24. Effect of As(III) treatment on VE-cadherin protein content. Confluent HAECs were treated with 1, 5 and 10 μM As(III) for 24 h and VE-cadherin protein content was analyzed by Western blotting technique. The VE-cadherin protein content is shown in the (A) upper panel and the lower panel represents the β-actin loading control. The images in (A) are representative of 7 experiments performed. The percent change in VE-cadherin protein relative to the control (untreated) is represented in (B). The control (100%) is indicated by the dotted line in (B). Error bars represent mean ± SEM for n=7. * indicates significantly different from control with $p<0.05$.

Fig. 25. Effect of As(III) exposure on β-catenin localization

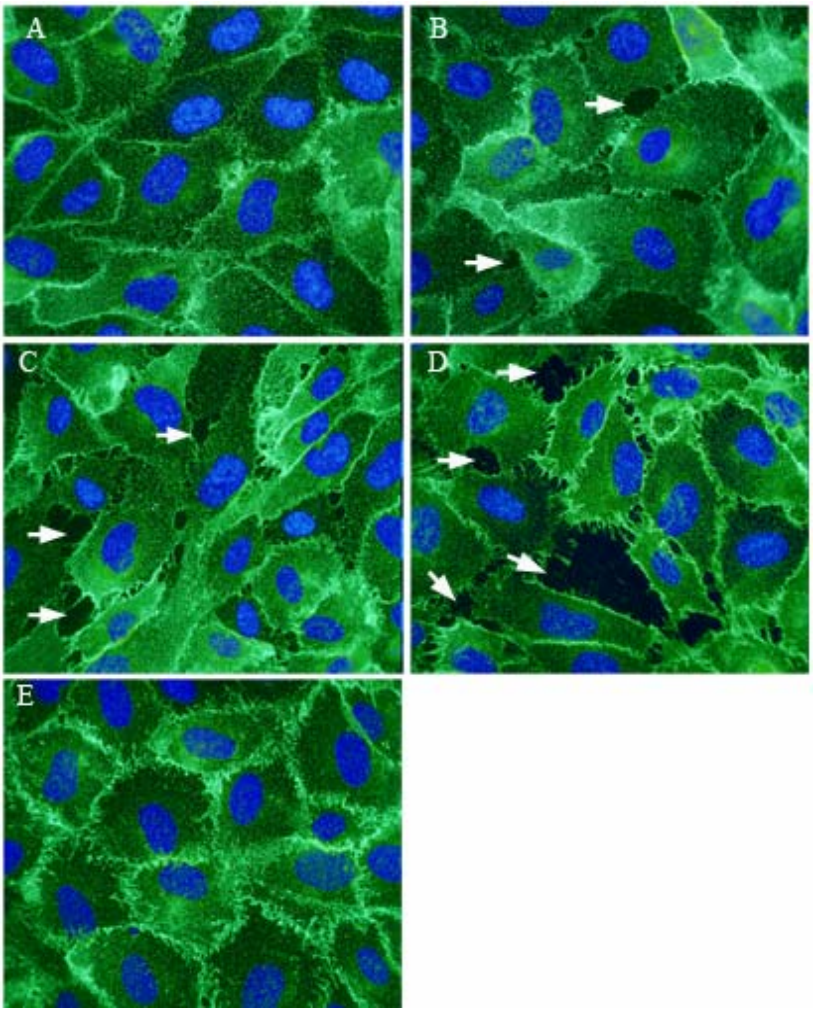

Fig. 25. Effect of As(III) exposure on β-catenin localization. Confluent HAECs were either untreated (A) or treated with 1 μM As(III) (B), 5 μM As(III) (C) and 10 μM As(III) (D) for 6 h and β-catenin localization was visualized by immunofluorescence staining (green). Non-uniform staining or loss of β-catenin was observed wherever gaps occurred (indicated by arrows). Pretreatment with 250 nM Gö 6976 for 1 h prior to and during 10 μM As(III) treatment (E) restored the β-catenin localization at cell-cell junctions. The nuclei were stained with Hoechst (blue). Magnification=60X. The images are representative of 3 independent experiments performed.

Fig. 26. Effect of As(III) exposure on formation of stress fibers at the 1-h time point

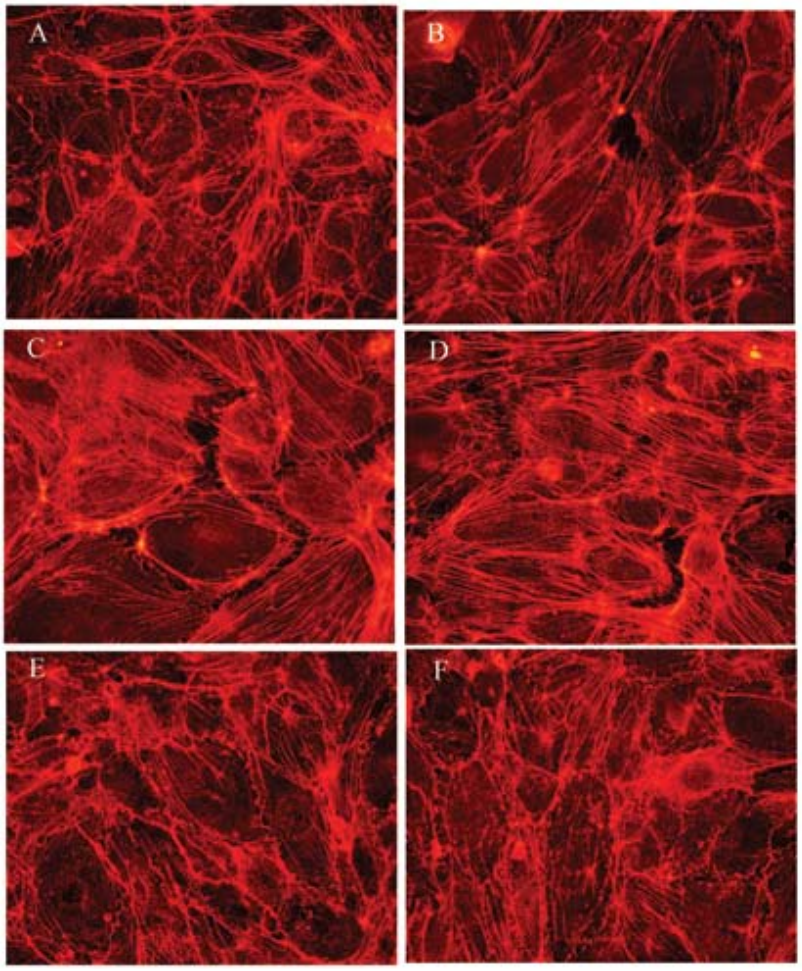

Fig. 26. Effect of As(III) exposure on formation of stress fibers at the 1-h time point. Confluent HAEC monolayers were either untreated (A) or treated with As(III); 1 μM (B), 5 μM (C) and 10 μM (D) for 1 h and the stress fibers induced with As(III) treatment were visualized by immunofluorescence staining with Alexa Fluor 568-conjugated phalloidin (red). Pretreatment with 250 nM Gö 6976 for 1 h prior to and during 10 μM As(III) treatment (F) inhibited the As(III) induced stress fibers whereas 250 nM Gö 6976 treatment alone (E) did not have an effect on stress fiber formation. Magnification=60X. The images are representative of 4 independent experiments performed.

Fig. 27. Effect of As(III) exposure on formation of stress fibers at the 6-h time point

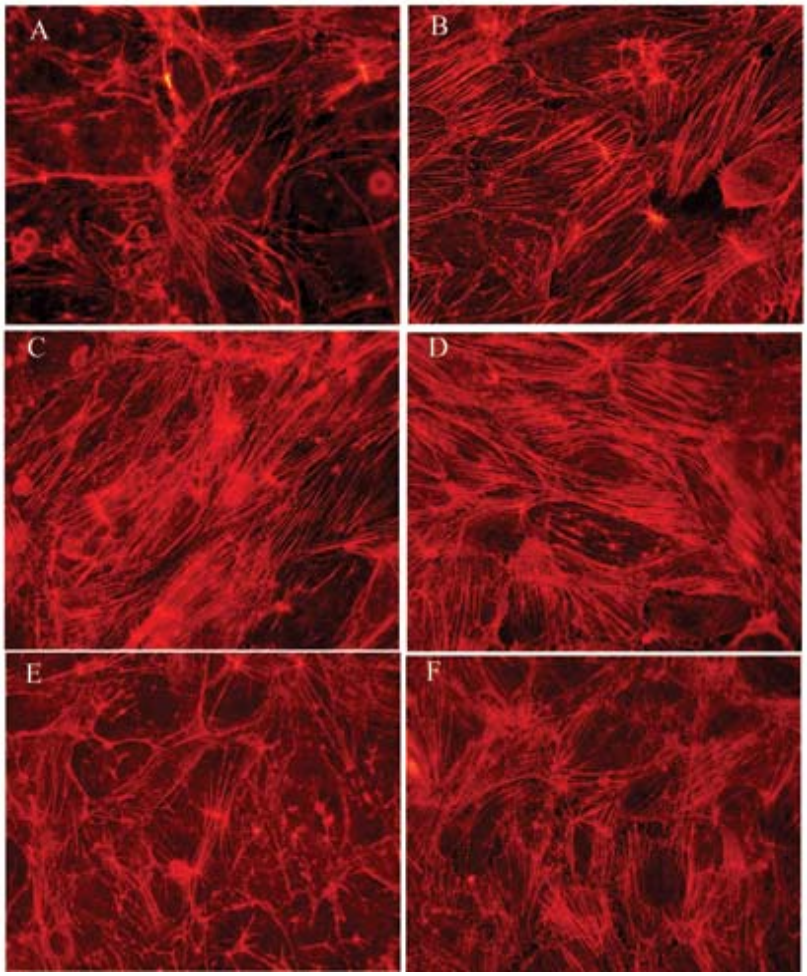

Fig. 27. Effect of As(III) exposure on formation of stress fibers at the 6-h time point. Confluent HAEC monolayers were either untreated (A) or treated with As(III); 1 μM (B), 5 μM (C) and 10 μM (D) for 6 h and the stress fibers induced with As(III) treatment were visualized by immunofluorescence staining with Alexa Fluor 568-conjugated phalloidin (red). Pretreatment with 250 nM Gö 6976 for 1 h prior to and during 10 μM As(III) treatment (F) reduced the As(III) induced stress fibers whereas 250 nM Gö 6976 treatment alone (E) did not have an effect on stress fiber formation. Magnification=60X. The images are representative of 4 independent experiments performed.

Fig. 28. Effect of As(III) exposure on formation of stress fibers at the 12-h time point.

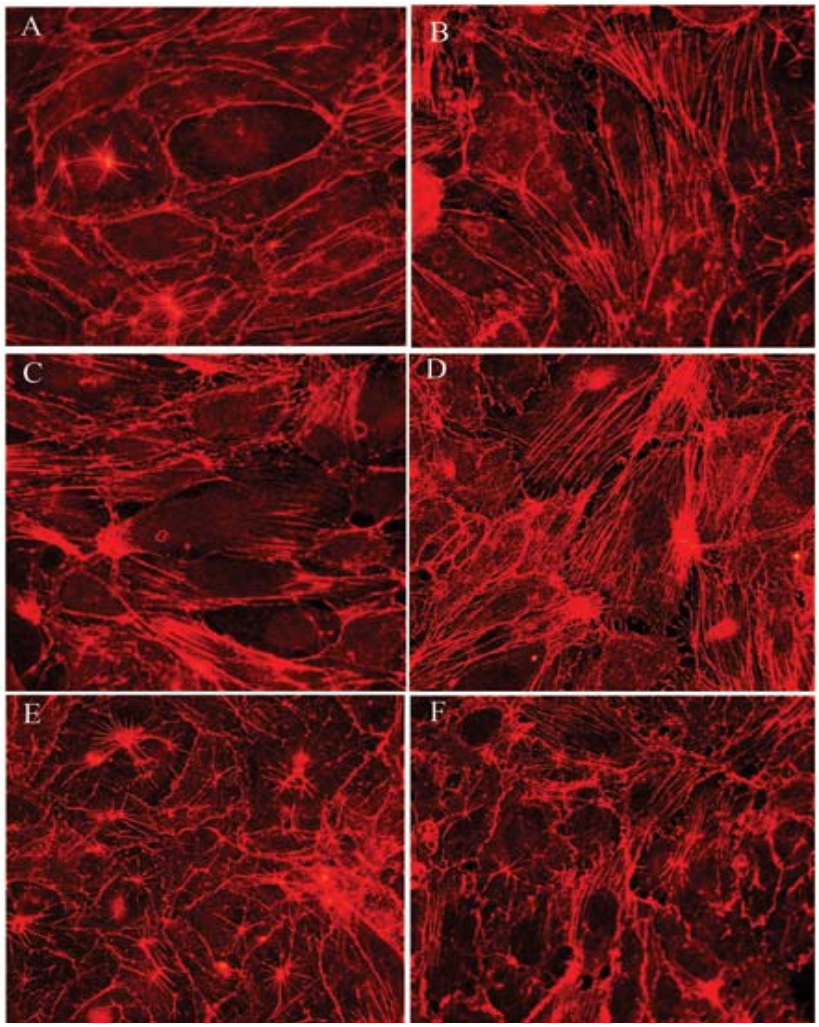

Fig. 28. Effect of As(III) exposure on formation of stress fibers at the 12-h time point. Confluent HAEC monolayers were either untreated (A) or treated with As(III); 1 μM (B), 5 μM (C) and 10 μM (D) for 12 h and the stress fibers induced with As(III) treatment were visualized by immunofluorescence staining with Alexa Fluor 568-conjugated phalloidin (red). Pretreatment with 250 nM Gö 6976 for 1 h prior to and during 10 μM As(III) treatment (F) inhibited the As(III) induced stress fibers whereas 250 nM Gö 6976 treatment alone (E) did not have an effect on stress fiber formation. Magnification=60X. The images are representative of 4 independent experiments performed.

Fig. 29. Effect of As(III) exposure on formation of stress fibers at the 24-h time point

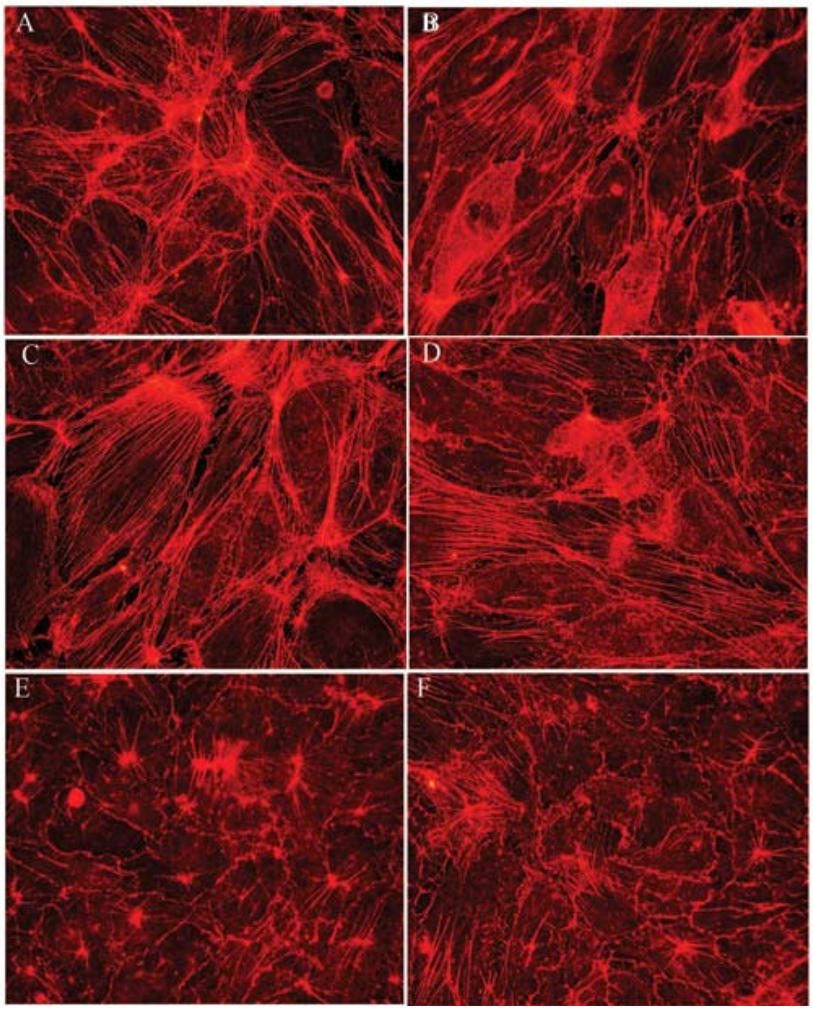

Fig. 29. Effect of As(III) exposure on formation of stress fibers at the 24-h time point. Confluent HAEC monolayers were either untreated (A) or treated with As(III); 1 μM (B), 5 μM (C) and 10 μM (D) for 24 h and the stress fibers induced with As(III) treatment were visualized by immunofluorescence staining with Alexa Fluor 568-conjugated phalloidin (red). Pretreatment with 250 nM Gö 6976 for 1 h prior to and during 10 μM As(III) treatment (F) inhibited the As(III) induced stress fibers whereas 250 nM Gö 6976 treatment alone (E) did not have an effect on stress fiber formation. Magnification=60X. The images are representative of 4 independent experiments performed.

Fig. 30. Effect of As(III) on endothelial permeability

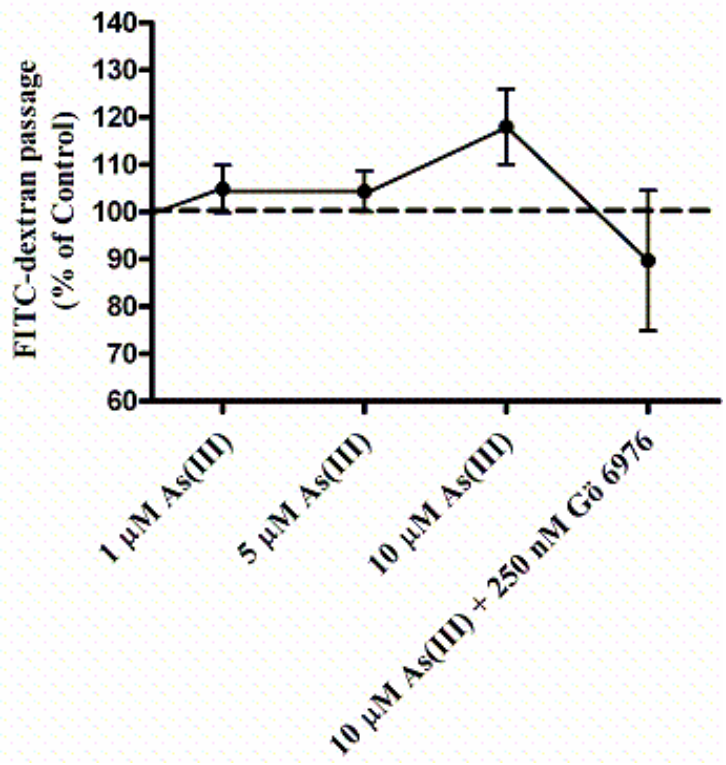

Fig. 30. Effect of As(III) on endothelial permeability. Confluent HAECs were treated with 1, 5, and 10 μM As(III) for 6 h or pretreated with 250 nM Gö 6976 for 1 h prior to and during 10 μM As(III) treatment. Monolayer permeability was measured using FITC-dextran. The control (100%) is indicated by the dotted line. Error bars represent mean ± SEM for n=4-5.

3.6 Discussion

The results from this study show that PKCα is a key mediator in the proposed mechanism for As(III)-induced atherosclerosis. The data shows that PKCα plays a crucial role in localization of the adherens junction proteins, VE-cadherin and β-catenin, and in regulating endothelial gap formation, stress fiber formation and vascular permeability. As(III) treatment induced intercellular gaps thereby disrupting the endothelial monolayer as evidenced by loss or non-uniform staining of VE-cadherin and β-catenin where the gaps appeared. Reduced VE-cadherin protein content was also detected; a finding that may in part be responsible for the observed intercellular gaps. An increased plasma concentration of VE-cadherin has been associated with coronary atherosclerosis (Soeki et al., 2004), and *in vitro* studies have shown that hydrogen peroxide induces internalization of VE-cadherin and gap formation (Kevil et al., 1998). Hence, the decreased VE-cadherin may be due to internalization and degradation or release into the cell culture medium.

β-catenin was found to be phosphorylated with 5 and 10 μM As(III) treatments, but no tyrosine phosphorylation of VE-cadherin was detected. There are several non-receptor tyrosine kinases such as Fyn, Fer, cMet, Abl and Src that have been shown to associate with and modulate the phosphorylation state of β-catenin and its association with cadherin (Lilien and Balsamo, 2005) during various developmental and physiological processes. In particular, phosphorylation of β-catenin at tyrosine 654 by Src has been shown to cause a fivefold reduction in its affinity for E-cadherin (Roura et al., 1999), which belongs to the same class of type I classical cadherins as VE-cadherin (Ivanov et al., 2001). The phosphorylation and dephosphorylation state of adherens junction proteins plays a critical role in the formation and/or maintenance of stable cell-

cell adhesions (Lilien and Balsamo, 2005, Schnittler, 1998). Therefore, tyrosine phosphorylation of β-catenin could potentially reduce its affinity for association with VE-cadherin and cause dissociation or loosening of the adherens junctions. As(III) has been shown to stimulate Src kinase activity in intact endothelial cells, but not recombinant Src activity (Barchowsky et al., 1999b). This suggests that As(III) does not affect Src activity directly, but one or more intermediates likely exist between As(III) and Src activation, one of which potentially could be PKC. Consistent with this, Chang et al. (2001) have demonstrated that association of activated PKC with the anchoring protein, receptor for activated C kinase, promotes its binding to Src tyrosine kinase. Therefore, a cooperative interaction between PKC and Src is feasible. This may explain the tyrosine phosphorylation of β-catenin as a consequence of PKC activation, which is a serine/threonine kinase.

Arsenic has been shown to increase Ca^{2+}-dependent PKC activity in Chinese hamster ovary cells at high doses after 4-h treatment (Liu and Huang, 1997). Similarly, transient activation of PKCα was observed with 20 μM arsenic treatment in a mouse epidermal cell line (Chen et al., 2000). Our results showed that 5 and 10 μM As(III) treatment induced significant activation of PKCα at the 1-h time point in a Ca^{2+}-dependent manner. The downstream effects of As(III)-induced PKCα activation were confirmed by using the cPKC inhibitor, Gö 6976. Inhibition of PKCα prevented gap formation and restored VE-cadherin and β-catenin at the cell-cell junctions. Tyrosine phosphorylation of β-catenin induced by As(III) was also reduced to basal levels. The effects of activation of PKCα and β on endothelial integrity in different pathophysiological circumstances have been well documented (Yuan, 2003). Activation

of PKCα by thrombin has been shown to modulate endothelial integrity by induction of stress fibers and increased endothelial permeability (Sandoval et al., 2001). Also, tyrosine phosphorylation of β-catenin has been observed that is cPKC-dependent (Cohen et al., 1999). Activation of PKCβ_1 was not detected with As(III) treatment. The PKCβ_1 and β_2 isoforms have been shown to follow similar activation/membrane translocation kinetics in several cell lines using similar activators (Blobe et al., 1996, Goodnight et al., 1995, Wang et al., 2004). Therefore, it appears that PKCα and not PKCβ plays a significant role in As(III)-induced endothelial disruption.

Formation of stress fibers induced by As(III) was also abolished or reduced with Gö 6976 treatment. Studies have demonstrated the relation between PKCα activation, stress fiber formation and cell contraction. It has been found that PKCα induces the activation of myosin by serine/threonine phosphorylation of myosin light chain, which results in actin-myosin interaction and subsequent stress fiber formation and cell contraction (Tiruppathi et al., 2003). Therefore, PKC inhibition plausibly inhibited the contractile force exerted by the stress fibers. Confluent endothelial cells consist of a band of actin filaments concentrated along the cell borders known as a dense peripheral band (DPB) that is also present *in vivo* (Gabbiani et al., 1983, Schnittler, 1998). The cadherin-catenin complex associates with the actin filaments of DPB, which is important for junctional stability. Our results showed that actin filaments were present in untreated cells along the cell borders and were mostly absent in central regions of the cell. Treatment with As(III) resulted in loss of DPB and an increase in stress fibers traversing the cells. The effect of As(III) was observed to be concentration- and time-dependent with the maximum stress fibers being formed with 10 μM As(III) at the 6-h time point.

Actin reorganization associated with disruption of the endothelial barrier is characterized by increased stress fiber density and reduction or loss of DPB (Lum and Roebuck, 2001). Stress fibers have the molecular machinery to generate contractile force and have been associated with gap formation and increased endothelial permeability (Pellegrino et al., 2004, Yuan, 2003).

Vascular permeability changes are associated with loss of endothelial integrity. Chen et al. (2004) and Tsai et al. (2005) showed that As(III) alters endothelial permeability in rodents. Using FITC-dextran, we found a 5% increase in endothelial permeability with 1 and 5 μM As(III) and approximately a 19% increase with 10 μM As(III) treatment that was inhibited by Gö 6976 treatment. These changes were not as great as expected based on the gap formation observed and actin stress fiber formation. However, Chen et al. (2004) and Tsai et al. (2005) have clearly demonstrated that even a small increase in permeability could be pathologically important. Taken together, these results suggest that As(III) induces tyrosine phosphorylation of β-catenin, which modulates adherens junction assembly resulting in non-uniform distribution or loss of VE-cadherin as well as β-catenin at the cell-cell junctions and promotes the formation of stress fibers which culminates in intercellular gap formation and increased permeability.

As(III) has been shown to modulate several signaling pathways by generation of oxidative and nitrosative stress in different cell systems such as BAECs and porcine aortic endothelial cells (Barchowsky et al., 1996, Barchowsky et al., 1999a, Bunderson et al., 2002). In particular, peroxynitrite and its donor, SIN-1, have been shown to induce nitration of PKCα, actin as well as β-catenin and alter their function (Knepler et al., 2001, Chakraborti et al., 2005, Knapp et al., 2001). We hypothesized, therefore, that As(III)-

induced peroxynitrite may play a role in endothelial barrier modulation. However, no peroxynitrite generation was observed with As(III) treatment in HAECs, although an increase was observed in BAECs. This was confirmed by the absence of nitration of VE-cadherin and β-catenin as well as an inability by a nitric oxide synthase inhibitor and a peroxynitrite decomposition catalyst, L-NAME and FeTPPS, to inhibit PKCα activation. The generation of reactive species with As(III) has been observed to be species specific. For example, no nitric oxide formation was observed with As(III) (≤5 μM) in porcine aortic endothelial cells (Barchowsky et al., 1999a) whereas Kao et al. (2003), demonstrated that As(III) (<5 μM) induces the production of nitric oxide in HUVECs. The observed differences could also be attributed to different experimental conditions. The differential effects of As(III) in the production of reactive species have been reviewed in detail by Gurr et al. (2003) and Kumagai and Pi, (2004).

While the results presented here show PKCα dependency for the effects of As(III) on endothelial cell-cell adhesion, monolayer integrity and vascular permeability, they do not suggest that As(III) effects on endothelium are restricted to the PKCα pathway. Other signal transduction pathways intersect with PKCα signaling. The PKC enzymes are serine/threonine kinases, and it has been suggested that crosstalk exists between the tyrosine and serine/threonine kinase signaling cascades (Bauman and Scott, 2002, Chang et al., 2001). Involvement of tyrosine kinases introduces the possibility that vascular endothelial growth factor (VEGF), a key modulator of adherens junction stability that signals through a tyrosine kinase pathway, may be involved. VEGF has been implicated in arsenic-related toxicity through activation of PKCδ in smooth muscle cells (Soucy et al., 2004). In addition, the VEGF receptor tyrosine kinases have been shown to signal

with PKCα activation and downstream AKT signaling (Gliki et al., 2002). Moreover, VEGF signals through a Ras-MEK-ERK pathway independent of PKCα suggesting that not all As(III)-related effects may be PKCα dependent. Stress kinases such as p38 and c-Jun amino-terminal kinase (JNK) could also potentially be involved in the observed effects of As(III). Barchowsky et al. (1999b) showed that high levels of As(III) can induce cellular stress and activate stress kinases including p38. On the other hand, lower concentrations have been shown to induce DNA synthesis and reactive oxygen species (Barchowsky et al., 1996) without activating stress kinases (Barchowsky et al., 1999b). The role of these alternative pathways in endothelial arsenic toxicity is the subject for future investigations.

In summary, we have determined a potential mechanism for arsenic-induced atherosclerosis. This study demonstrates that As(III)-induced activation of PKCα leads to tyrosine phosphorylation of β-catenin and formation of stress fibers. Tyrosine phosphorylation of β-catenin may cause weakening of the adherens junctions, and this effect, in association with the contractile force generated by stress fibers, results in gap formation and increased endothelial permeability. Proteins at the adherens junctions are largely responsible for maintaining the barrier and normally allow passage of selected molecules. Injury to the endothelium can promote accumulation of oxLDLs and monocytes/macrophages in the intima of blood vessels (Lusis, 2000), ultimately leading to formation of foam cells. The intercellular gaps and increased permeability caused by arsenic could potentially accelerate/enhance influx of oxLDLs and monocytes/macrophages across the endothelium and contribute significantly to the progression of atherosclerosis.

3.7 References

1. Andriopoulou, P., Navarro, P., Zanetti, A., Lampugnani, M.G., Dejana, E., 1999. Histamine induces tyrosine phosphorylation of endothelial cell-to-cell adherens junctions. Arterioscler. Thromb. Vasc. Biol. 19, 2286-2297.
2. Barchowsky, A., Dudek, E.J., Treadwell, M.D., Wetterhahn, K.E., 1996. Arsenic induces oxidant stress and NF-κB activation in cultured aortic endothelial cells. Free Radic. Biol. Med. 21(6), 783-790.
3. Barchowsky, A., Klei, L.R., Dudek, E.J., Swartz, H.M., James, P.E., 1999a. Stimulation of reactive oxygen, but not reactive nitrogen species, in vascular endothelial cells exposed to low levels of arsenite. Free Radic. Biol. Med. 27(11/12), 1405-1412.
4. Barchowsky, A., Roussel, R.R., Klei, L.R., James, P.E., Ganju, N., Smith, K.R., Dudek, E.J., 1999b. Low levels of arsenic trioxide stimulate proliferative signals in primary vascular cells without activating stress effector pathways. Tox. Appl. Pharmacol. 159, 65-75.
5. Bauman, A.L., Scott, J.D., 2002. Kinase- and phosphatase-anchoring proteins: harnessing the dynamic duo. Nat. Cell Biol. 4, E203-E206.
6. Beckman, J.S., 1996. Oxidative damage and tyrosine nitration from peroxynitrite. Chem. Res. Toxicol. 9, 836-844.
7. Beckman, J.S., Koppenol, W.H., 1996. Nitric oxide, superoxide and peroxynitrite: the good, the bad, and the ugly. Am. J. Physiol. 271, C1424-C1437.
8. Beckman, J.S., Ye, Y.Z., Anderson, P.G., Chen, J., Accavitti, M.A., Tarpey, M.M., White, R., 1994. Extensive Nitration of protein tyrosines in human

atherosclerosis detected by immunohistochemistry. Biol. Chem. Hoppe Seyler. 375, 81-88.

9. Blobe, G.C., Stribling, S., Fabbro, D., Stabel, S., Hannun, Y.A., 1996. Protein kinase C βII specifically binds to and is activated by F-actin. J. Biol. Chem. 271(26), 15823-15830.
10. Bunderson, M., Brooks, D.M., Walker, D.L., Rosenfeld, M.E., Coffin, D.J., Beall, H.D., 2004. Arsenic exposure exacerbates atherosclerotic plaque formation and increases nitrotyrosine and leukotriene biosynthesis. Toxicol. Appl. Pharmacol. 201, 32-39.
11. Bunderson, M., Coffin, J.D., Beall, H.D., 2002. Arsenic induces peroxynitrite generation and cyclooxygenase-2 protein expression in aortic endothelial cells: possible role in atherosclerosis. Toxicol. Appl. Pharmacol. 184, 11-18.
12. Byers, H.R., White, G.E., Fujiwara, K., 1984. Organization and function of stress fibers in cells in vitro and in situ. Cell Muscle Motil. 5, 83-137.
13. Chakraborti, T., Das, S., Chakraborti, S., 2005. Proteolytic activation of protein kinase Cα by peroxynitrite in stimulating cytosolic phospholipase A_2 in pulmonary endothelium: Involvement of a pertussis toxin sensitive protein. Biochemistry. 44, 5246-5257.
14. Chang, B.Y., Chiang, M., Cartwright, C.A., 2001. The interaction of Src and RACK1 is enhanced by activation of protein kinase C and tyrosine phosphorylation of RACK1. J. Biol. Chem. 276(23), 20346-20356.

15. Chen, N., Ma, W., Huang, C., Ding, M., Dong, Z., 2000. Activation of PKC is required for arsenite-induced signal transduction. J. Environ. Pathol. Toxicol. Oncol. 19(3), 297-305.
16. Chen, S-C., Tsai, M-H., Wang, H-J., Yu, H-S., Chang, L.W., 2004. Vascular permeability alterations induced by arsenic. Hum Exp Toxicol. 23, 1-7.
17. Cohen, A.W., Carbajal, J.M., Schaeffer JR, R.C., 1999. VEGF stimulates tyrosine phosphorylation of β-catenin and small-pore endothelial barrier dysfunction. Am. J. Physiol. 277, H2038-H2049.
18. Colangelo, S., langille, B.L., Steiner, G., Gotlieb, A.L., 1998. Alterations in endothelial F-actin microfilaments in rabbit aorta in hypercholesterolemia. Arterioscler. Thromb. Vasc. Biol. 18, 52-56.
19. Esser, S., Lampugnani, M.G., Corada, M., Dejana, E., Risau, W., 1998. Vascular endothelial growth factor induces VE-cadherin tyrosine phosphorylation in endothelial cells. J.Cell Sci. 111, 1853-1865.
20. Gabbiani, G., Gabbiani, F., Lombardi, D., Schwartz, S.M., 1983. Organization of actin cytoskeleton in normal and regenerating arterial endothelial cells. Proc Natl. Acad. Sci. USA. 80, 2361-2364
21. Gliki, G., Wheeler-Jones, C., Zachary, I., 2002. Vascular endothelial growth factor induces protein kinase C (PKC)-dependent Akt/PKB activation and phosphatidylinositol 3'-kinase-mediated PKCδ phosphorylation: Role of PKC in angiogenesis. Cell Biol. Int. 26(9), 751-759.

22. Goodnight, J., Mischak, H., Kolch, W., Mushincki, J.F., 1995. Immunocytochemical localization of eight protein kinase C isozymes overexpressed in NIH 3T3 fibroblast. J. Biol. Chem. 270(17), 9991-10001.
23. Gurr, J-R., Yih, L-H., Samikkannu, T., Bau, D-T., Lin, S-Y., Jan, K-Y., 2003. Nitric oxide production by arsenite. Mutat. Res. 533, 173-182.
24. Guyton, J.R., Shaffer, D.R., Henry, P.D., 1989. Stress fibers in endothelial cells overlaying atherosclerotic lesions in rabbit aorta. Am. J. Med. Sci. 298(2), 79-82.
25. Ischiropoulos, H., 1998. Biological tyrosine nitration: a pathophysiological function of nitric oxide and reactive oxygen species. Arch. Biochem. Biophys. 356, 1-11.
26. Ivanov, D.B., Philippova, M.P., Tkachuk, V.A., 2001. Structure and functions of classical cadherins. Biochemistry 66(10), 1174-1186.
27. Kao, Y-H., Yu, C-L., Chang, L-W., Yu, H-S., 2003. Low concentrations of arsenic induce vascular endothelial growth factor and nitric oxide release and stimulate angiogenesis in vitro. Chem. Res. Toxicol. 16, 460-468.
28. Kawakami, T., Kawakami, Y., Kitaura, J., 2002. Protein kinase Cβ (PKCβ): normal finctions and diseases. J. Biochem. 132, 677-682.
29. Kevil, C.G, Ohno, N., Gute, D.C., Okayama, N., Robinson, S.A., Chaney, E., Alexander, J.S., 1998. Role of cadherin internalization in hydrogen peroxide-mediated endothelial permeability. Free Radic. Biol. Med. 24(6), 1015-1022.
30. Klotz, L.O., Schroeder, P., Sies, H., 2002. Peroxynitrite signaling: receptor tyrosine kinases and activation of stress-responsive pathways. Free Radic. Biol. Med. 33(6), 737–743.

31. Knapp, L.T., Kanterewicz, B.I., Hayes, E.L., Klann, E., 2001. Peroxynitrite-induced tyrosine nitration and inhibition of protein kinase C. Biochem. Biophys. Res. Commun. 286, 764-770.
32. Knepler, J.L., Taher, L.N., Gupta, M.P., Patterson, C., Pavalko, F., Ober, M.D., Hart, C.M., 2001. Peroxynitrite causes endothelial cell monolayer barrier dysfunction. Am. J. Physiol. Cell Physiol. 281(3), C1064-C1075.
33. Kumagai, Y., Pi, J., 2004. Molecular basis for arsenic-induced alteration in nitric oxide production and oxidative stress: implication of endothelial dysfunction. Toxicol. Appl. Pharmacol. 198, 450-457.
34. Lilien, J., Balsamo, J., 2005. The regulation of cadherin-mediated adhesion by tyrosine phosphorylation/dephosphorylation of β-catenin. Curr. Opin. Cell Biol. 17, 459-465.
35. Liu, F., Jan, K.Y., 2000. DNA damage in arsenite and cadmium treated bovine aortic endothelial cells. Free Radic. Biol. Med. 28, 55-63.
36. Liu, Y., Huang, H., 1997. Involvement of calcium-dependent protein kinase C in arsenite-induced genotoxicity in Chinese hamster ovary cells. J. Cell. Biochem. 64, 423-433.
37. Lum, H., Roebuck, K.A., 2001. Oxidant stress and endothelial cell dysfunction. Am. J. Physiol. Cell Physiol. 280, C719-C741.
38. Lusis, A.J., 2000. Atherosclerosis. Nature 407, 233-241.
39. Lynn, S., Shiung, J.N., Gurr, J.R., Jan, K.Y., 1998. Arsenite stimulates poly (ADP-ribosylation) by generation of nitric oxide. Free Radic. Biol. Med. 24, 442-449.

40. Martiny-Baron, G., Kazanietz, M.G., Mischak, H., Blumberg, P.M., Kochs, G., Hug, H., Marmé, D., Schächtele, C., 1993. Selective inhibition of protein kinase C isozymes by the indolocarbazole Gö 6976. J. Biol. Chem. 268(13), 9194-9197.

41. Mattila, P., Majuri, M-L., Tiisala, S., Renkonen, R., 1994. Expression of six protein kinase C isotypes in endothelial cells. Life Sci. 55(16), 1253-1260.

42. Nagpala, P.G., Malik, A.B., Vuong, P.T., Lum, H., 1996. Protein kinase C β_1 overexpression augments phorbol ester-induced increase in endothelial permeability. J. Cell. Physiol. 166, 249-255.

43. Newton, A.C., 2001. Protein Kinase C: Structural and Spatial Regulation by Phosphorylation, Cofactors, and Macromolecular interactions. Chem. Rev. 101, 2353-2364.

44. Pellegrino, M., Kazmierczak, E.F., LeBlanc, J.C., Cho, T., Cao, K., Marcovina, S.M., Boffa, M.B., Cote, G.P., Koschinsky, M.L., 2004. The apolipoprotein(a) component of lipoprotein(a) stimulates actin stress fiber formation and loss of cell-cell contact in cultured endothelial cells. J. Biol. Chem. 279(8), 6526-6533.

45. Pryor, W.A., Squadrito, G.L., 1995. The chemistry of peroxynitrite: a product from the reaction of nitric oxide with superoxide. Am. J. Physiol. Lung Cell Mol. Physiol. 268, L699-L722.

46. Radi, R., Peluffo, G., Alvarez, M.N., Naviliat, M., Cayota, A., 2001. Unraveling peroxynitrite formation in biological systems. Free Radic. Biol. Med. 30(5), 463-488.

47. Rahman, M., Tondel, M., Ahmad, S.A., Chowdhury, I.A., Faruquee, M.H., Axelson, O., 1999. Hypertension and arsenic exposure in Bangladesh. Hypertension 33(1), 74-78.

48. Roura, S., Miravet, S., Piedra, J., Herreros, A.G., Dunach, M., 1999. Regulation of E-cadherin/catenin association by tyrosine phosphorylation. J. Biol. Chem. 274(51), 36734-36740.

49. Sandoval, R., Malik, A.B., Minshall, R.D., Kouklis, P., Ellis, C.A., Tiruppathi, C., 2001. Ca^{2+} signaling and PKCα activate increased endothelial permeability by disassembly of VE-cadherin junctions. J. Physiol. 533(2), 433-445.

50. Schnittler, H.J., 1998. Structural and functional aspects of intercellular junctions in vascular endothelium. Basic Res. Cardiol. 93(3), 30-39.

51. Simeonova, P.P., Hulderman, T., Harki, D., Luster, M.I., 2003. Arsenic exposure accelerates atherogenesis in apolipoprotein $E^{-/-}$ mice. Environ. Health Perspect. 111, 1744-1748.

52. Simeonova, P.P., Luster, M.I., 2004. Arsenic and atherosclerosis. Toxicol. Appl. Pharmacol. 198, 444-449.

53. Soeki, T., Tamura, Y., Shinohara, H., Sakabe, K., Onose, Y., Fukuda, N., 2004. Elevated concentration of soluble vascular endothelial cadherin is associated with coronary atherosclerosis. Circ J. 68, 1-5.

54. Soucy, N.V., Klei, L.R., Mayka, D.D., Barchowsky, A., 2004. Signaling pathways for arsenic-stimulated vascular endothelial growth factor-A expression in primary vascular smooth muscle cells. Chem. Res. Toxicol. 17, 555-563.

55. Tiruppathi, A., Minshall, R.D., Paria, B.C., Vogel, S.M., Malik, A.B., 2003. Role of Ca^{2+} signaling in the regulation of endothelial permeability. Vascul Pharmacol. 39, 173-185.

56. Tsai, M-H., Chen, S-C., Wang, H-J., Yu, H-S., Chang, L.W., 2005. A mouse model for study of vascular permeability changes induced by arsenic. Toxicol. Mech. Methods 15, 433-437.

57. Tseng, C.H., Chong, C.K., Tseng, C.P., Hsueh, Y.M., Chiou, H.Y., Tseng, C.C., Chen, C.J., 2003. Long-term arsenic exposure and ischemic heart disease in arseniasis-hyperendemic villages in Taiwan. Toxicol. Lett. 137(1-2), 15-21.

58. Wang, C.H., Jeng, J.S., Yip, P.K., Chen, C.L., Hsu, L.I., Hsueh, Y.M., Chiou, H.Y., Wu, M.M., Chen, C.J., 2002. Biological gradient between long-term arsenic exposure and carotid atherosclerosis. Circulation 105, 1804-1809.

59. Wang, Y., Pampou, S., Fujikawa, K., Varticovski, L., 2004. Opposing effect of angiopoietin-1 on VEGF-mediated disruption of endothelial cell-cell interactions requires activation of PKCβ. J. Cell. Physiol. 198, 53-61.

60. White, G.E., Gimbrone, M.A Jr., Fujiwara, K., 1983. Factors influencing the expression of stress fibers in vascular endothelial cells in situ. J. Cell Biol. 97, 416-424.

61. Wong, A.J., Pollard, J.D., Herman, I.M., 1983. Actin filament stress fibers in vascular endothelial cells in vivo. Science 219, 867-869.

62. Yuan, S.Y., 2003. Protein kinase signaling in the modulation of microvascular permeability. Vascul. Pharmacol. 39, 213-223.

63. Zhao, H., Joseph J., Fales, H.M., Sokoloski, E.A., Levine, R.L., Vasquez-Vivar, J., Kalyanaraman, B., 2005. Detection and characterization of the product of hydroethidine and intracellular superoxide by HPLC and limitations of fluorescence. Proc. Natl. Acad. Sci. USA. 102(16), 5727-5732.

64. Zhao, H., Kalivendi, S., Zhang, H., Joseph J., Nithipatikom, K., Vasquez-Vivar, J., Kalyanaraman, B., 2003. Superoxide reacts with hydrothidine but forms a fluorescent product that is distinctly different from ethidium: potential implications in intracellular fluorescence detection of superoxide. Free Radic. Biol. Med. 34(11), 1359-1368.

Chapter 4

Conclusions

4.1 Conclusions

Arsenic contamination of ground water is a global problem and millions of people worldwide are exposed to arsenic through drinking water. Arsenic exposure has been associated with the development of cardiovascular diseases such as carotid atherosclerosis (Wang et al., 2002), ischemic heart disease (Tseng et al., 2003) and hypertension (Rahman et al., 1999). Atherosclerosis is the fundamental cause of major cardiovascular diseases including ischemic heart disease, myocardial infarction and stroke. Arsenic levels exceeding 20 ppb in drinking water have been associated with increased mortality from various cardiovascular diseases (Engel and Smith, 1994). In addition to the United States, other countries including Taiwan, Bangladesh, India, China, Vietnam and Argentina have high levels of arsenic in ground water ranging from 50-14,000 ppb (Wang and Wai, 2004).

Our laboratory has focused on elucidating the mechanisms of arsenic-induced atherosclerosis. In this study, the role of arsenic in atherogenesis was determined by (1) characterizing the time- and concentration-dependent effects of sodium arsenite [As(III)] on the initiation and progression of atherosclerosis in ApoE-/- /LDLr-/- atherosclerotic mouse model, (2) determining the effects of As(III)-induced peroxynitrite on the activation of calcium dependent cPKC isotypes, α and β, in human aortic endothelial cells and (3) determining whether activation of cPKC isotypes, α and β, by As(III) are involved in endothelial barrier disruption.

The time- and concentration-dependent effects of environmentally relevant concentrations of arsenic in the development of atherosclerosis were investigated using the ApoE-/- /LDLr-/- mouse model that is a well-established animal model of human atherosclerosis (Ishibashi et al., 1994, Jawein et al., 2004). Atherosclerotic plaque development was determined by measuring the percent occlusion of the innominate artery, which is a small vessel that connects the aortic arch to the right subclavian and right carotid arteries. Development of atherosclerotic lesions in this artery has been shown to progress at a highly consistent rate and closely resemble that of the human condition (Rosenfeld et al., 2000).

The temporal effects of arsenic were determined by exposing the mice to 10 ppm As(III) in drinking water for 5 or 10 weeks. Histology revealed that mice treated with As(III) showed an increasing trend in atherosclerotic plaque formation within the innominate arteries compared to the controls at both 5 and 10 weeks. Analysis of IL-6 levels in the serum obtained from mice treated with As(III) for 10 weeks showed an increasing trend compared to the control mice. These results suggest that As(III) contributes to atherogenesis at an early stage of the disease.

The concentration-dependent effects of arsenic were analyzed by exposing the ApoE-/- /LDLr-/- mice to 1, 5 and 10 ppm As(III) in drinking water for 20 weeks. A significant increase in occlusion of the innominate arteries was observed with 1 and 5 ppm As(III). Our laboratory has previously shown that exposure to 10 ppm As(III) for 18 weeks significantly increases atherosclerotic plaque formation in ApoE-/- /LDLr-/- mice (Bunderson et al., 2004). However, in this study an increasing trend in occlusion was observed with 10 ppm As(III), and serum IL-6 levels were significantly elevated in this

group. These results demonstrate the significance of low levels of arsenic in the onset and progression of atherosclerosis in this animal model. Surprisingly, sVCAM-1 levels were lower at both the 10 and 20 week time points in 10 ppm As(III) treated mice compared to the control mice. However, this does not suggest that there is reduced expression of endothelial VCAM-1.

The endothelium is the most important barrier between the blood and vessel wall and it that allows passage of only selected molecules. Damage to the endothelium can result in increased permeability and promote the accumulation of oxidized LDLs and monocytes into the blood vessel intima. Chen et al. (2004) and Tsai et al. (2005) have documented that As(III) increases endothelial permeability in rodents. Also, As(III) exacerbates the development of atherosclerosis (Bunderson et al., 2004, Simeonova et al., 2003). Therefore, a rational approach was to determine whether As(III) affects the integrity of the endothelial monolayer.

We determined the role of PKCα and β in As(III)-mediated disruption of endothelial monolayer integrity. The translocation of PKC from cytosol to the membrane is an important step in its activation process (Newton, 2001). Therefore, HAECs were exposed to 1, 5 and 10 μM As(III), and cPKC activation was analyzed at the 1-h time point by determining the protein content in the membrane and cytosolic fractions by Western blotting technique. Treatment with 5 and 10 μM As(III) induced a significant increase in PKCα activation as determined by quantifying the protein content in the membrane fraction. No change was observed with 1 μM As(III) treatment. In the cytosolic fraction, a decrease in the PKCα content was observed with increasing As(III) concentration indicative of PKCα translocation from the cytosol to the membrane.

Treatment of the cells with the cPKC inhibitor, 250 nM Gö 6976, for 1 h or with the intracellular Ca^{2+} chelator, 20 μM BAPTA-AM, for 30 min, prior to and during 10 μM As(III) treatment inhibited the PKCα activation. The phorbol ester, PMA, and Ca^{2+} ionophore, A23187, were used as positive controls. $PKC\beta_1$ was only detected in the cytosolic fraction and no protein was detected in the membrane fraction at the 1-h time point. Since, no activation of $PKC\beta_1$ was detected, the effect of As(III) on $PKC\beta_2$ was not analyzed.

As(III) treatment failed to induce generation of peroxynitrite in HAECs as analyzed by immunofluorescence staining for 3-nitrotyrosine as well as with the hydroethidine assay that measures the conversion of hydroethidine to its oxidized fluorescent product ethidium. Also, pretreatment of HAECs with the peroxynitrite decomposition catalyst, FeTPPS, or the nitric oxide synthase inhibitor, L-NAME, did not inhibit/affect the activation of PKCα. However, a significant increase in 3-nitrotyrosine was observed in BAECs treated with 10 μM As(III).

The integrity of the vascular endothelium is largely maintained by proteins of the adherens junctions; VE-cadherin and β-catenin. The association of VE-cadherin with β-catenin is critical for the stability of adherens junctions, and tyrosine phosphorylation of either one or both the proteins can alter endothelial integrity. The effect of As(III) exposure on tyrosine phosphorylation of VE-cadherin and β-catenin was analyzed at 1 h in HAECs by immunoprecipitation followed by Western blotting. Treatment of cells with 1 μM As(III) showed no change in tyrosine phosphorylation as compared to the control (untreated), whereas an increasing trend in tyrosine phosphorylation was observed with 5 μM As(III), and 10 μM As(III) treatment resulted in a significant increase in tyrosine

phosphorylation of β-catenin. The increase in tyrosine phosphorylation induced by 10 μM As(III) was completely inhibited by 250 nM Gö 6976. No tyrosine phosphorylation of VE-cadherin was detected. Also, no tyrosine nitration of VE-cadherin or β-catenin was detected, which further confirmed the absence of peroxynitrite generation with As(III) treatment.

The effect of As(III) on cell-cell adhesion was analyzed with immunofluorescence staining for VE-cadherin. HAECs were treated with 1, 5 and 10 μM As(III) for 1, 6, 12 and 24 h. A concentration-dependent increase in gap formation and loss or non-uniform staining of VE-cadherin was observed with As(III) treatment at all time points, and the frequency and size of gaps observed were maximal at the 6-h time point. The cPKC inhibitor, Gö 6976, inhibited gap formation at all concentrations of As(III) treatment, and uniform distribution of VE-cadherin could be observed at cell-cell junctions. A similar concentration-dependent effect of As(III) was also observed on β-catenin distribution as analyzed at the 6-h time point. The frequency of gap formation was greater with 10 μM As(III) than with 1 and 5 μM As(III), and non-uniform distribution or loss of β-catenin staining was evident wherever gaps could be observed. Also, 250 nM Gö 6976 treatment inhibited the gap formation induced by 10 μM As(III) and restored the β-catenin staining at cell-cell junctions.

Analysis of the effect of As(III) treatment on VE-cadherin protein content at the 24-h time point revealed approximately 8, 15 and 30% reductions in VE-cadherin protein with 1, 5 and 10 μM As(III) treatment, respectively. Protein content was analyzed by Western blotting.

The cadherin/catenin complex associates with the actin cytoskeleton, which is crucial for maintaining junctional stability and structural integrity of the endothelial cell monolayer. Reorganization of actin microfilaments into stress fibers can adversely affect monolayer integrity, since it can lead to dissociation of the cadherin/catenin complex from the actin cytoskeleton. The effects of 1, 5 and 10 μM As(III) on reorganization of actin microfilaments were analyzed at 1, 6, 12 and 24 h by immunofluorescence staining using fluorophore-conjugated phalloidin. A concentration-dependent increase in stress fiber formation was observed with As(III) treatment at all time points, and the density of stress fibers observed was maximal at the 6-h time point. The cPKC inhibitor, Gö 6976, inhibited/reduced stress fiber formation at all concentrations of As(III) treatment.

As(III) treatment resulted in gap formation and stress fiber formation that was maximal at the 6-h time point. Hence, the effect of 1, 5 and 10 μM As(III) treatment on endothelial permeability was analyzed at the 6-h time point. A 5% increase in permeability was observed with 1 and 5 μM As(III) treatment, whereas 10 μM As(III) induced approximately a 19% increase. Treatment with 250 nM Gö 6976 inhibited the increase in permeability induced by 10 μM As(III).

Taken together, this study demonstrates that As(III) induces activation of PKCα without peroxynitrite formation in HAECs. No activation of PKCβ was observed at the time point analyzed. As(III)-induced activation of PKCα leads to tyrosine phosphorylation of β-catenin and formation of stress fibers. Tyrosine phosphorylation of β-catenin may cause weakening of the adherens junctions, and this effect, in association with the contractile force generated by stress fibers, results in gap formation and increased endothelial permeability. The intercellular gaps and increased permeability

caused by As(III) could potentially accelerate/enhance influx of oxLDLs and monocytes/macrophages across the endothelium and contribute significantly to the progression of atherosclerosis. Accordingly, environmentally relevant concentrations of arsenic induce significant increases in atherosclerotic plaque formation in the ApoE-/-/LDLr-/- mouse. The process of atherosclerosis is plausibly initiated or accelerated by arsenic at an early stage. The arsenic-induced, cPKC-dependent, signaling pathway mediating endothelial barrier disruption is outlined in Fig. 31.

Fig. 31. Schematic of arsenic mediated endothelial disruption and development of atherosclerosis

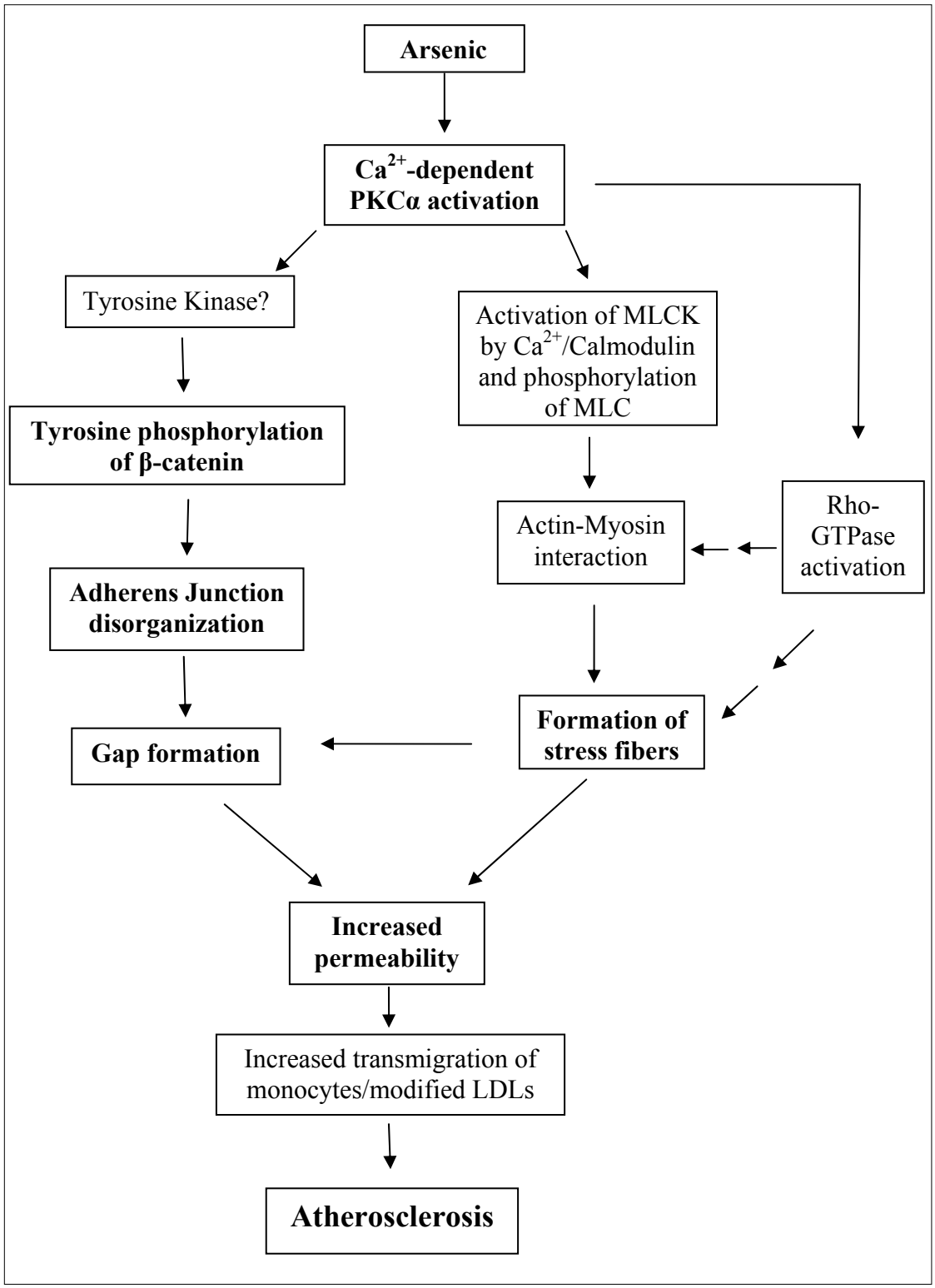

4.2 Future Directions

The increase in vascular permeability with arsenic treatment has been demonstrated *in vivo* in rodents (Chen et al., 2004, Tsai et al., 2005). Visualization of stress fiber formation as well as cell retraction or gap formation after arsenic treatment *in vivo* will provide affirmation to the *in vitro* effects observed. Our study demonstrated PKCα mediated disruption of the endothelial monolayer. Arsenic is a versatile molecule and affects signaling pathways in multiple ways. The mechanism(s) of arsenic-induced activation of PKCα needs to be elucidated. PKC is a very important signaling molecule that has a host of cellular substrates and plays an important role in several physiological and pathological processes. Determining the specific substrate(s) of PKCα that mediates downstream tyrosine phosphorylation of adherens junction proteins and endothelial disruption will be crucial. This will help in designing specific pharmacological intervention strategies without affecting other physiological processes.

4.3 References

1. Bunderson, M., Brooks, D.M., Walker, D.L., Rosenfeld, M.E., Coffin, D.J., Beall, H.D., 2004. Arsenic exposure exacerbates atherosclerotic plaque formation and increases nitrotyrosine and leukotriene biosynthesis. Toxicol. Appl. Pharmacol. 201, 32-39.
2. Chen, S-C., Tsai, M-H., Wang, H-J., Yu, H-S., Chang, L.W., 2004. Vascular permeability alterations induced by arsenic. Hum Exp Toxicol. 23, 1-7.
3. Engel, R.R., Smith, A.H., 1994. Arsenic in drinking water and mortality from vascular disease: an ecologic analysis in 30 counties in the United States. Arch. Environ. Health. 49, 418-427.
4. Ishibashi, S., Herz, J., Maeda, N., Goldstein, J.L., Brown, M.S., 1994. The two-receptor model of lipoprotein clearance: Test of the hypothesis in "knockout" mice lacking the low density lipoprotein receptor, apolipoprotein E, or both proteins. Proc. Natl. Acad. Sci. USA. 91, 4431-4435.
5. Jawein, J., Nastalek, P., Korbut, R., 2004. Mouse models of experimental atherosclerosis. J. Physiol. Pharmacol. 55(3), 503-517.
6. Newton, A.C., 2001. Protein Kinase C: Structural and Spatial Regulation by Phosphorylation, Cofactors, and Macromolecular interactions. Chem. Rev. 101, 2353-2364.
7. Rahman, M., Tondel, M., Ahmad, S. A., Chowdhury, I. A., Faruquee, M. H., and Axelson, O., 1999. Hypertension and arsenic exposure in Bangladesh. Hypertension. 33(1), 74-78.

8. Rosenfeld, M.E., Polinsky, P., Virmani, R., Kauser, K., Rubanyi, G., Schwartz, S.M., 2000. Advanced atherosclerotic lesions in the innominate artery of the ApoE knockout mouse. Arterioscler Thromb Vasc Biol. 20, 2587-2592.

9. Simeonova, P.P., Hulderman, T., Harki, D., Luster, M.I., 2003. Arsenic exposure accelerates atherogenesis in apolipoprotein $E^{-/-}$ mice. Environ. Health Perspect. 111, 1744-1748.

10. Tsai, M-H., Chen, S-C., Wang, H-J., Yu, H-S., Chang, L.W., 2005. A mouse model for study of vascular permeability changes induced by arsenic. Toxicol. Mech. Methods. 15, 433-437.

11. Tseng, C.H., Chong, C.K., Tseng, C.P., Hsueh, Y.M., Chiou, H.Y., Tseng, C.C., Chen, C.J., 2003. Long-term arsenic exposure and ischemic heart disease in arseniasis-hyperendemic villages in Taiwan. Toxicol. Lett. 137(1-2), 15-21.

12. Wang, C.H., Jeng, J.S., Yip, P.K., Chen, C.L., Hsu, L.I., Hsueh, Y.M., Chiou, H.Y., Wu, M.M., Chen, C.J., 2002. Biological gradient between long-term arsenic exposure and carotid atherosclerosis. Circulation 105(15), 1804-1809.

13. Wang, J.S., Wai, C.M., 2004. Arsenic in drinking water-A global environmental problem. J. Chem. Educ. 81(2), 207-13.

Chapter 5

Role of Arsenic in Endothelial Cell Activation and Uptake of Modified Lipids by Macrophages

5.1 Objective

Atherosclerosis is an inflammatory disease, initiated by activation of the endothelium and characterized by expression of cell adhesion molecules and secretion of proinflammatory cytokines and chemokines. These events promote the transmigration of leukocytes into the subendothelial matrix, resulting in the growth of atheroma. The objective of this study was to determine whether arsenic induces endothelial cell activation and promotes uptake of modified lipids by macrophages, thereby mimicking the events of the initiation and progression of the atherosclerotic disease processes.

5.2 Introduction

Atherogenesis begins with the endothelial cells lining the vessel wall. Activated endothelial cells express cell adhesion molecules such as E-selectin, intercellular cell adhesion molecule-1 (ICAM-1) and vascular cell adhesion molecule-1 (VCAM-1). E-selectin is involved with the rolling and tethering of leukocytes to the activated endothelium, whereas ICAM-1 and VCAM-1 promote firm adhesion of leukocytes via interaction with the integrin molecules expressed on leukocytes (Blankenberg et al., 2003). In particular, VCAM-1 and not ICAM-1 has been demonstrated to function primarily in monocyte recruitment to the blood vessel intima (Cybulsky et al., 2001). In addition to the cell adhesion molecules, proinflammatory cytokines such as interleukin-1

(IL-1), IL-6, macrophage colony-stimulating factor (M-CSF), granulocyte macrophage colony-stimulating factor (GM-CSF) and tumor necrosis factor α (TNFα) produced by various cell types such as endothelial cells, macrophages and smooth muscle cells play an important role in the atherosclerotic process (Tedgui and Mallat, 2006) by instigating a self-perpetuating inflammatory process.

The cytokine, M-CSF, stimulates the differentiation of monocytes into macrophages in the subendothelium as well as expression of macrophage scavenger receptors (Lusis, 2000). The uptake of modified low density lipoproteins (LDL) by resident macrophages is mediated by scavenger receptors. Class A scavenger receptor, SR-A, and class B scavenger receptor, CD36, are the two scavenger receptors of primary importance. It has been demonstrated that SR-A and CD36, together, are responsible for uptake of the majority of modified LDLs by macrophages (Kunjathoor et al., 2002). The uptake of these modified LDLs by resident macrophages leads to formation of lipid-laden macrophages known as foam cells. *In vivo* studies have demonstrated that mice lacking either of these scavenger receptors show a reduction in atherosclerotic lesions (Suzuki et al., 1997, Febbraio et al., 2000).

Conflicting results have been documented regarding the effects of arsenic on IL-6 production. *In vitro* experiments suggest that high concentration of arsenic inhibits IL-6 production (Hershko et al., 2002), whereas *in vivo* studies have demonstrated increased IL-6 production with arsenic treatment (Liu et al., 2000). Evidence showing a clear and direct relationship between arsenic exposure and expression of cell adhesion molecules, an indicator of endothelial activation, was lacking when our study was proposed. However, Tsou et al. (2005) have since shown that arsenic enhances TNFα-induced

expression of VCAM-1. The effect of arsenic on the uptake of modified lipids by macrophages also remains unknown. Therefore, the objective of this study was to determine whether arsenic modulates the process of atherosclerosis at an early stage using an *in vitro* cell system.

5.3 Materials and Methods

5.3.1 Cell culture. Human aortic endothelial cells (HAECs) were purchased from Cambrex Bio Science (Walkersville, MD) and were grown in the supplier's formulated medium: EBM-2 medium supplemented with EGM-2 SingleQuots (0.04% hydrocortisone, 0.4% hFGF-B, 2% FBS and 0.1% each of VEGF, R^3-IGF-1, ascorbic acid, heparin, hEGF and GA-1000). Bovine aortic endothelial cells (BAECs) were provided by Dr. J. Douglas Coffin of The University of Montana, Missoula and were originally a gift from Dr. Steve Schwartz of The University of Washington. Cells were grown in Dulbecco's Modified Eagle Medium (DMEM) with penicillin/streptomycin and L-glutamine, and supplemented with 15% FBS (Mediatech, Inc., Herndon, VA). Endothelial cells were used between passages 2 and 10. The human monocytes, THP-1 cells, were a gift from Dr. Elizabeth Putnam of The University of Montana, Missoula and were grown in suspension in RPMI 1640 medium (Mediatech, Inc., Herndon, VA) containing 2 mM L-glutamine, 10 mM HEPES and 1.5 g/l sodium bicarbonate, and adjusted to contain 4.5 g/l glucose, 1.0 mM sodium pyruvate, 0.05 mM 2-mercaptoethanol and 10% FBS (Mediatech, Inc., Herndon, VA). The mouse macrophages, RAW 264.7 cells, were a gift from Dr. Andrij Holian of The University of Montana, Missoula and were grown in DMEM with penicillin/streptomycin and L-

glutamine, and supplemented with 10% FBS. Cells were incubated at 37 ^{0}C under a humidified atmosphere containing 5% CO_2.

5.3.2 Enzyme-linked immunosorbent assay. HAECs were seeded at a density of $5x10^4$ or $1x10^5$ cells/well in 24-well plates for 24-48 h. Confluent cells were treated with 1, 5 and 10 μM As(III) (GFS Chemicals, Columbus, OH) for 1, 6, 12, 24 and 48 h. After respective time points, medium containing As(III) was removed and cells were exposed to fresh medium without As(III) for 24 h. IL-6 released in the medium without As(III) was assayed by ELISA (BD biosciences, San Diego, CA) according to manufacturer's instructions.

5.3.3 Flow cytometric analysis of VCAM-1 expression. HAECs were seeded at a density of $1x10^6$ cells/flask in 25 cm^2 cell culture flasks for 48 h. Confluent cells were treated in serum free medium with 1, 5 and 10 μM As(III) for 24 h. Cells were trypsinized using trypsin (0.025%)/EDTA (0.01%) solution (Cambrex Bio Science, Walkersville, MD). This concentration of trypsin/EDTA has been shown not to affect the VCAM-1 protein during trypsinization (Zhang and Frei, 2002, van der Zijpp et al., 2003). Cells were collected by centrifugation and resuspended in phosphate buffered saline (PBS)/5% FBS solution. Cells were incubated with allophycocyanin (APC)-conjugated mouse anti-human VCAM-1 monoclonal antibody (concentration = 20 μl/10^6 cells) (BD Biosciences, San Diego, CA) for 45 min at 4 ^{o}C. Cells were then rinsed twice with PBS and fluorescence was analyzed using Becton Dickinson (BD) Facs Aria flow cytometer (San Jose, CA). A total of 10,000-30,000 viable cells were analyzed per experimental

sample. Data were analyzed using BD Facsdiva software. Background binding was detected using an APC-conjugated mouse IgG isotype control (BD Biosciences, San Diego, CA).

5.3.4 Flow cytometric analysis of lipid uptake by macrophages. The effect of serum obtained from ApoE-/- /LDLr-/- mice on the uptake of acetylated LDL by RAW 264.7 macrophage cells was analyzed by flow cytometry. Mice were obtained from Jackson Laboratories (Bar Harbor, ME). All the animals were housed under specific pathogen-free conditions according to IACUC protocols with 12 h light/dark cycle and controlled temperature. ApoE-/- /LDLr-/- mice receiving arsenic treatment were given 1 or 10 ppm As(III) for 18 weeks ad libitum via drinking water. The control group received ddH_2O. The mice were fed a commercial mouse chow diet. Blood was collected from these mice at the end of treatment periods and serum was obtained by centrifugation of the blood at 1,600 rpm for 5 min at 4 ^{0}C and was stored at -80 ^{0}C. The treatment of mice with As(III) and blood collection was done by former graduate student in our laboratory for other experiments. A solution of 15% mouse serum was made with DMEM and 1 ml of this serum solution was exposed to $1x10^6$ RAW 264.7 cells for 24 h at 37 ^{o}C. After 22 h of incubation, 1 μg/ml fluorescein isothiocyanate (FITC)-conjugated acetylated LDL (Molecular Probes, Inc. Eugene, OR) was added to each tube and incubated for 2 h at 37 ^{o}C. Cells were rinsed with PBS and fluorescence was analyzed using the flow cytometer as mentioned above using appropriate controls.

To determine the uptake of acetylated LDLs by RAW 264.7 cells exposed to conditioned medium from BAECs and the role of the scavenger receptor, SR-A, in LDL

uptake, BAECs were seeded at a density of $5x10^5$ cells/well in 6-well plates for 24 h. Cells were treated with 10 μM As(III) for 48 h. Medium containing As(III) was removed after 48 h and cells were incubated with serum free medium without As(III) for 24 h. RAW 264.7 cells ($1x10^6$) were exposed to 1 ml of the BAEC conditioned medium without As(III) for 24 h at 37 ^{0}C. After 21 h of incubation, the SR-A blocking antibody, 2F8 (8 μg/ml), was added wherever necessary and after 22 h, 1 μg/ml FITC-conjugated acetylated LDL was added to each tube. Cells were rinsed with PBS and fluorescence was analyzed using the flow cytometer as mentioned above using appropriate controls. To determine the effective concentration of 2F8 antibody in blocking SR-A, RAW 264.7 cells were incubated with varying concentrations of 2F8 antibody for 45 min followed by incubation with 1 μg/ml FITC-conjugated acetylated LDL for 2 h at 37 ^{0}C. Cells were rinsed with PBS and acetylated LDL uptake was analyzed by flow cytometry.

To determine the uptake of acetylated LDLs by THP-1 cells exposed to conditioned medium from HAECs, HAECs were seeded at a density of $1x10^6$ cells/flask in 25 cm^2 cell culture flask for 48 h. Confluent cells were treated with 1, 5 and 10 μM As(III) for 24 and 48 h. After respective time points, medium containing As(III) was removed and cells were exposed to fresh medium without As(III) for 24 h. Differentiated THP-1 cells ($1x10^6$) were exposed to 1 ml of the HAEC conditioned medium without As(III) for 24 h at 37 ^{0}C. THP-1 cells were differentiated using 33 μg/ml Phorbol 12-Myristate 13-Acetate (PMA) (Sigma-Aldrich, Saint Louis, Missouri). After 22 h of incubation, 1 μg/ml FITC-conjugated acetylated LDL was added to each tube and incubated for 2 h. Cells were rinsed with PBS and acetylated LDL uptake was analyzed by flow cytometry.

5.3.5 Statistical analysis. Results are presented as mean ± standard error of the mean (SEM). When required, data was normalized with its respective control in order to exclude differences in background conditions. Statistical analysis was performed using Student's *t* test when comparing two groups or Bonferroni method for comparing three groups or more. When using the Bonferroni method, the alpha level of each individual test was adjusted downwards to ensure that the overall experiment wise-risk remains at 0.05. Statistical analysis was performed using GraphPad Prism, version 4.00. Alpha error was set at $p<0.05$.

5.4 Results

5.4.1 Effect of As(III) on endothelial VCAM-1 expression

VCAM-1 mediates firm adhesion of leukocytes to the endothelium and transmigration into the blood vessel intima (Blankenberg et al., 2003, Cybulsky et al., 2001). Therefore, we analyzed the effect of As(III) on endothelial VCAM-1 expression by flow cytometry. HAECs were exposed to 1, 5 and 10 μM As(III) for 24 h. No change in VCAM-1 expression was observed with As(III) treatment (Fig. 32).

5.4.2 Effect of As(III) on IL-6 secretion

The proinflammatory cytokine, IL-6, plays an important role in the development of atherosclerosis (Tedgui and Mallat, 2006). HAECs were exposed to 1, 5 and 10 μM As(III) for 1, 6, 12, 24 and 48 h. After the respective time points, As(III) containing medium was replaced with regular medium without As(III) for 24 h, and IL-6 levels were analyzed in medium without As(III) by ELISA. A concentration-dependent decrease in

IL-6 levels was observed with As(III) treatments compared to respective controls at most time points (Fig. 33).

5.4.3 Acetylated LDL uptake by RAW 264.7 cells exposed to mouse serum

Following transmigration of monocytes into the blood vessel intima, the monocytes are differentiated into macrophages and take up modified LDLs leading to formation of foam cells (Lusis, 2000). We therefore analyzed whether serum from As(III) treated mice could promote the uptake of acetylated LDLs by mouse macrophages, RAW 264.7 cells, using flow cytometry. Serum was obtained from mice treated with 1 and 10 ppm As(III) in drinking water for 18 weeks. Exposure of RAW 264.7 cells to serum from 1 ppm As(III) treated mice resulted in a significant increase in acetylated LDL uptake (Fig. 34A), whereas serum from 10 ppm As(III) treated mice showed an increasing trend (Fig. 34B).

5.4.4 Acetylated LDL uptake by RAW 264.7 cells exposed to conditioned medium from As(III)-treated BAECs and the role of SR-A in LDL uptake.

The role of the scavenger receptor, SR-A, expressed by RAW 264.7 cells in the uptake acetylated LDL was analyzed by treating cells with increasing concentration (1, 2, 4, 8 and 10 μg/ml) of the SR-A blocking antibody, 2F8. A concentration-dependent decrease in acetylated LDL uptake was observed with increasing concentration of 2F8 antibody (Fig. 35A). In further experiments 8 μg/ml concentration of 2F8 antibody was used.

To analyze the effect of As(III) on the uptake of acetylated LDLs by RAW 264.7 cells, BAECs were exposed to 10 μM As(III) for 48 h, after which the As(III) containing medium was replaced with serum free medium without As(III) for 24 h. RAW 264.7 cells

were exposed to the conditioned medium from BAECs and an increasing trend in acetylated LDL uptake was observed (Fig. 35B). The acetylated LDL uptake was inhibited by pretreatment of RAW 264.7 cells with 2F8 antibody (Fig. 35B).

5.4.5 Acetylated LDL uptake by THP-1 cells exposed to conditioned medium from As(III)-treated HAECs

The effect of As(III) on acetylated LDL uptake was also analyzed using a human cell system. HAECs were exposed to 1, 5 and 10 μM As(III) for 24 and 48 h. After the respective time points, As(III) containing medium was replaced with regular medium without As(III) for 24 h, and uptake of acetylated LDLs by differentiated THP-1 cells was analyzed using the conditioned medium. At the 24-h time point, differentiated THP-1 cells showed an increasing trend in acetylated LDL uptake with 5 μM As(III), whereas a decreasing trend was observed with 10 μM As(III) (Fig. 36A). At the 48-h time point, exposure of differentiated THP-1 cells to the conditioned medium showed an increasing trend in acetylated LDL uptake with 1 μM As(III), whereas a decreasing trend was observed with 10 μM As(III) (Fig. 36B).

5.5 Figures

Fig. 32. Effect of As(III) on endothelial VCAM-1 expression

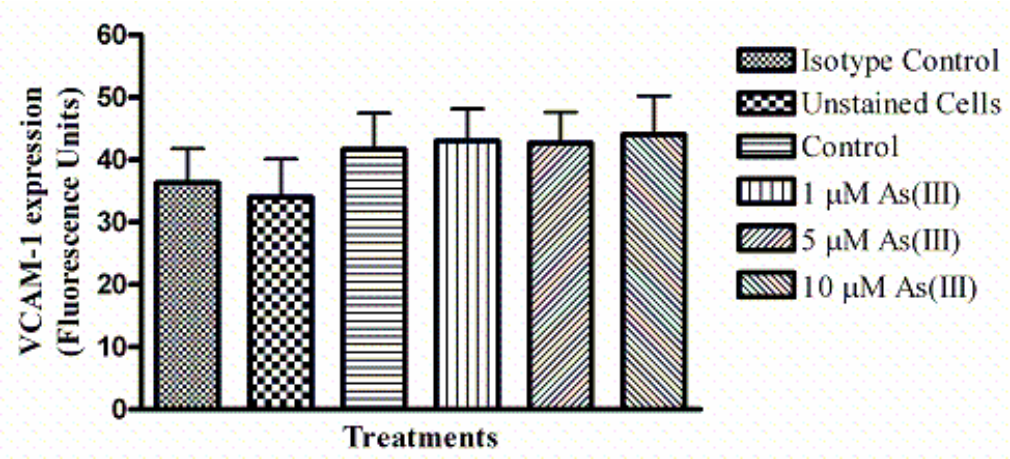

Fig. 32. Effect of As(III) on endothelial VCAM-1 expression. Confluent HAECs were treated with 1, 5 and 10 μM As(III) for 24 h and VCAM-1 expression was analyzed by flow cytometry using an APC-conjugated anti-VCAM-1 antibody.

Fig. 33. Effect of As(III) on IL-6 secretion

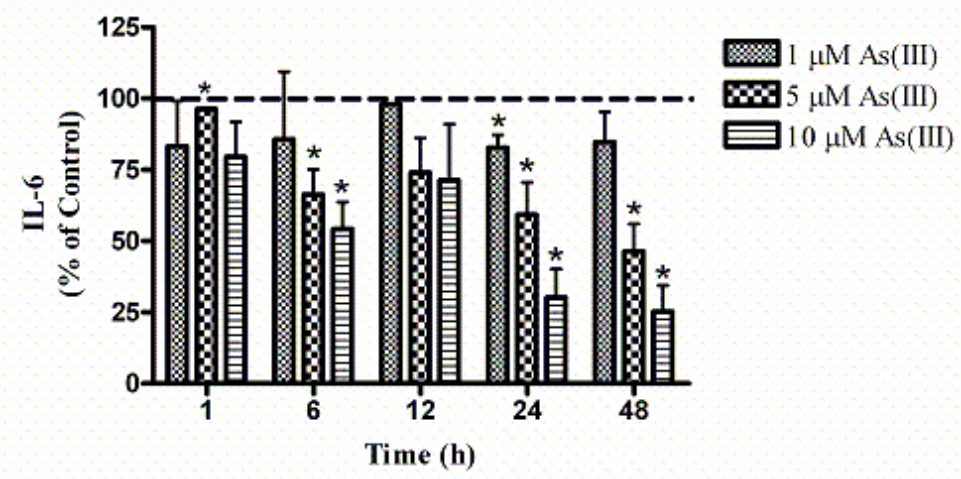

Fig. 33. Effect of As(III) on IL-6 secretion. Confluent HAECs were treated with 1, 5 and 10 μM As(III) for 1, 6, 12, 24 and 48 h. After the respective time points, As(III) containing medium was replaced with medium without As(III) for 24 h. IL-6 levels were measured by ELISA in the medium without As(III). Treatment groups marked with asterisks were significantly different from the respective controls (*, $p<0.05$). The control (100%) is indicated by dotted line. Error bars represent mean ± SEM for n=3-5 experiments.

Fig. 34. Acetylated LDL uptake by RAW 264.7 cells exposed to mouse serum

A.

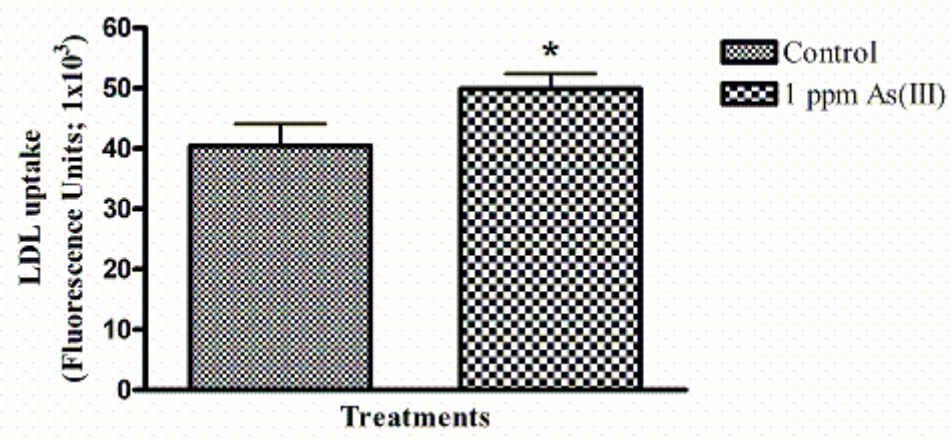

B.

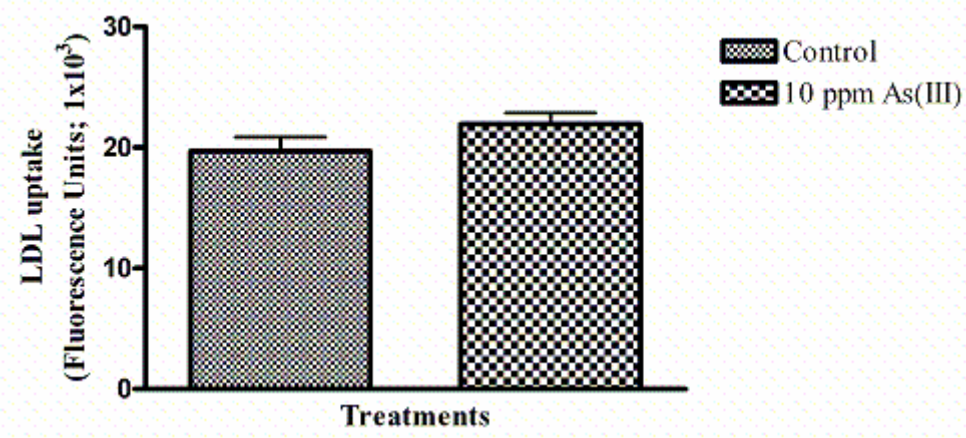

Fig. 34. Acetylated LDL uptake by RAW 264.7 cells exposed to mouse serum. RAW 264.7 cells were exposed to 15% serum from mice treated with 1 ppm (A) and 10 ppm (B) As(III) for 18 weeks. Treatment group marked with asterisk was significantly different from the control (*, $p<0.05$). Error bars represent mean ± SEM for (A) n=8 mice, (B) n=5 mice per group.

Fig. 35. Acetylated LDL uptake by RAW 264.7 cells exposed to conditioned medium from As(III)-treated BAECs and the role of SR-A in LDL uptake

A.

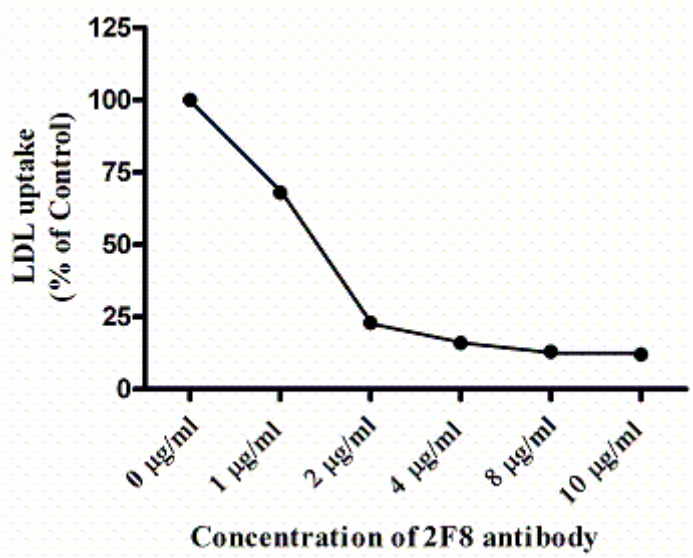

B.

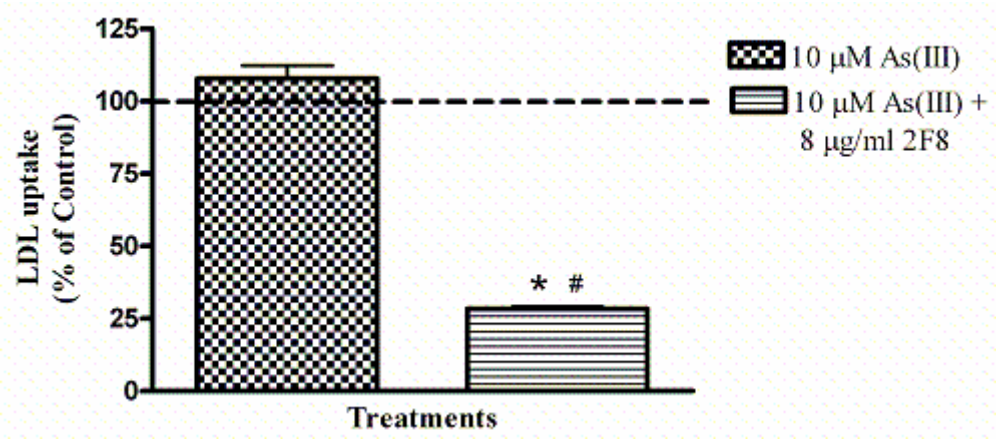

Fig. 35. Acetylated LDL uptake by RAW 264.7 cells exposed to conditioned medium from As(III)-treated BAECs and the role of SR-A in LDL uptake. The concentration-dependent inhibition of acetylated LDL uptake by RAW 264.7 cells was analyzed using the 2F8 antibody, n=1 (A). BAECs were treated with 10 µM As(III) for 48 h and As(III) containing medium was replaced with medium without As(III) for 24 h. Acetylated LDL uptake by RAW 264.7 cells was analyzed using the conditioned medium (B). The control (100%) is indicated by dotted line in (B). Error bars represent mean ± SEM for n=3-4 experiments. Treatment group marked with * and # was significantly different from the control and As(III) treated group, respectively, with $p<0.001$.

Fig. 36. Acetylated LDL uptake by THP-1 cells exposed to conditioned medium from As(III)-treated HAECs

A.

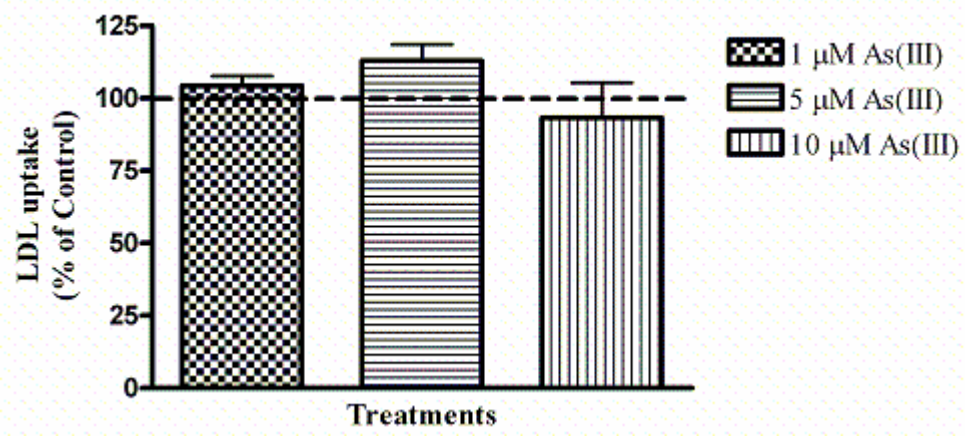

B.

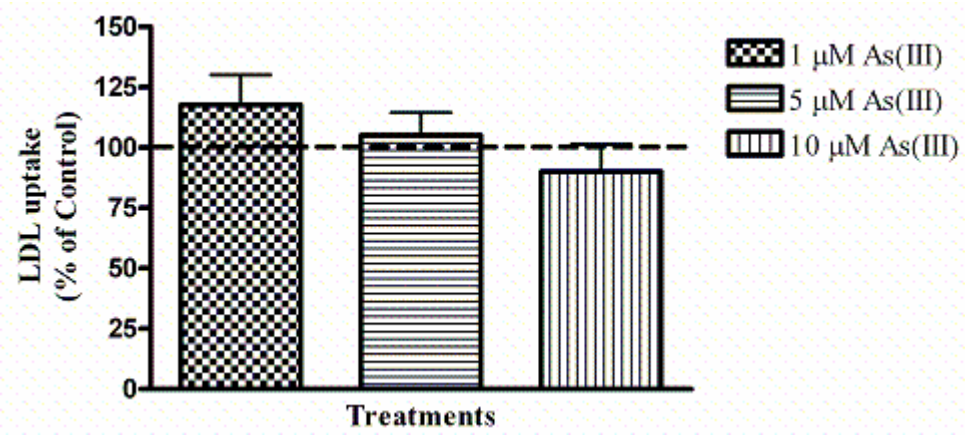

Fig. 36. Acetylated LDL uptake by THP-1 cells exposed to conditioned medium from As(III)-treated HAECs. Confluent HAECs were treated with 1, 5 and 10 μM As(III) for 24 and 48 h. After the respective time points, As(III) containing medium was replaced with medium without As(III) for 24 h. Acetylated LDL uptake by differentiated THP-1 cells was analyzed using the conditioned medium at the 24-h time point (A) and 48-h time point (B). The control (100%) is indicated by dotted line in (A and B). Error bars represent mean ± SEM for n=3 experiments.

5.6 Discussion

Arsenic has been associated with the development of atherosclerosis in epidemiological and animal studies (Bunderson et al., 2004, Simeonova et al., 2003, Wang et al., 2002). *In vitro* studies have suggested several possible mechanisms for the development of cardiovascular diseases such as atherosclerosis (Navas-Acien et al., 2005). We therefore investigated whether arsenic induces endothelial cell activation and promotes uptake of modified lipids by macrophages, thereby mimicking the events in the initiation and progression of the atherosclerotic disease processes. The results of this study suggest that As(III) alone does not induce the expression of the cell adhesion molecule, VCAM-1, or proinflammatiry cytokine, IL-6, in HAECs. Also, no clear evidence was obtained regarding the effects of As(III) on uptake of modified lipids by macrophages.

The VCAM-1 gene is regulated by multiple transcription factors such as nuclear factor-kappa B (NF-κB), activator protein-1 (AP-1), interferon regulatory factor-1 (IRF-1) and Sp-1 (Lechleitner et al., 1998, Neish et al., 1995, Neish et al., 1992, Tsou et al., 2005). Similarly, the IL-6 gene is regulated by multiple transcription factors such as NF-κB, AP-1, C/EBP and CREB (Hershko et al., 2002). NF-κB is considered to be most important in the regulation of VCAM-1 and IL-6 expression. *In vitro* studies suggest that low levels of As(III) (1-5 μM) activate NF-κB (Barchowsky et al., 1996), whereas high As(III) levels (500 μM) inihibit NF-κB activation (Roussel and Barchowsky, 2000, Hershko et al., 2002). Consistent with this, Hershko et al. (2002) demonstrated that 500 μM As(III) treatment inhibits IL-1β-induced IL-6 expression in enterocytes. Although in theory the As(III) concentrations used in the present study should activate NF-κB and

induce IL-6 production, no such outcome was observed. *In vivo* studies using mouse models, however, suggest that arsenic exposure increases serum IL-6 levels (Liu et al., 2000, Chapter 2 of this dissertation). Also, in our study no VCAM-1 expression was observed with As(III) treatment. A similar effect of 10 μM As(III) on VCAM-1 expression was documented by Tsou et al. (2005), where As(III) treatment alone did not induce VCAM-1 expression, but potentiated TNFα-induced VCAM-1 expression. This suggests that As(III) by itself does not induce cell adhesion molecule expression, but in the presence of other inflammatory cues may enhance the process. Simeonova et al. (2003) have demonstrated increased IL-8 mRNA levels with 5 μM As(III) treatment in HAECs. Therefore, it may be possible that arsenic treatment alone may induce only certain inflammatory mediators and exacerbate the effect of others.

Exposure of RAW 264.7 macrophages to conditioned medium from BAECs showed only a modest increasing trend in acetylated LDL uptake with As(III) treatment. The majority of the uptake was mediated by SR-A, which is in sync with other studies (Kunjathoor et al., 2002). Also, no specific effect in acetylated LDL uptake with As(III) treatment was observed using the THP-1/HAEC cell system. However, a significant increase in acetylated LDL uptake was observed with serum from 1 ppm As(III)-treated mice. This suggests that *in vivo* inflammatory conditions may influence the uptake of modified lipids that may not be possible to replicate *in vitro.* Exposure of macrophages to serum from 10 ppm As(III)-treated mice revealed only an increasing trend in acetylated LDL uptake. The reason for this finding is unclear.

The process of atherosclerosis is regulated by different inflammatory mediators secreted by several different cell types such as endothelial cells, leukocytes and smooth

muscle cells. Inflammatory mediators such as cytokines regulate the activity of cells in an autocrine or paracrine fashion and can trigger several different cellular responses depending on the timing and context. For example, the expression of cell adhesion molecules by endothelial cells is regulated by cytokines such as IL-6, IL-1β and TNFα (McDouall et al., 2001, Watson et al., 1996) that are secreted by macrophages, smooth muscle cells and/or endothelial cells, simultaneously or in unique temporal and spatial context. Consistent with this, it has been shown that 5 μM As(III) treatment induces IL-6 and monocyte chemoattractant protein-1 (MCP-1) expression in human smooth muscle cells (Lee et al., 2005). Therefore, stimulatory signals to the endothelial cells from other cell types such as smooth muscle cells could be crucial. This makes it difficult to mimic *in vivo* atherosclerotic conditions in *in vitro* settings. Endothelial and smooth muscle cells in the vasculature along with resident macrophages play significant roles in the process of atherosclerosis. Therefore, co-culture experiments may more adequately reflect *in vivo* conditions during atherogenesis. In summary, arsenic did not increase the expression of VCAM-1 and IL-6 by itself, and the effects of arsenic on the uptake of modified lipids remain unclear in our experimental setting.

5.7 References

1. Barchowsky, A., Dudek, E.J., Treadwell, M.D., Wetterhahn, K.E., 1996. Arsenic induces oxidant stress and NF-κB activation in cultured aortic endothelial cells. Free Radic. Biol. Med. 21(6), 783-790.
2. Blankenberg, S., Barbaux, S., Tiret, L., 2003. Adhesion molecules and atherosclerosis. Atherosclerosis. 170, 191-203.
3. Bunderson, M., Brooks, D.M., Walker, D.L., Rosenfeld, M.E., Coffin, D.J., Beall, H.D., 2004. Arsenic exposure exacerbates atherosclerotic plaque formation and increases nitrotyrosine and leukotriene biosynthesis. Toxicol. Appl. Pharmacol. 201, 32-39.
4. Cybulsky, M.I., Iiyama, K., Li, H., Zhu, S., Chen, M., Iiyama, M., Davis, V., Gutierrez-Ramos, J-C., Connelly, P.W., Milstone, D.S., 2001. A major role for VCAM-1 but not ICAM-1 in early atherosclerosis. J. Clin. Invest. 107, 1255-1262.
5. Febbraio, M., Podrez, E.A., Smith, J.D., Hajjar, D.P., Hazen, S.L., Hoff, H.F., Sharma, K., Silverstein, R.L., 2000. Targeted disruption of the class B scavenger receptor CD36 protects against atherosclerosis lesion development in mice. J.Clin.Invest. 105, 1049-1056.
6. Hershko, D.D., Robb, B.W., Hungness, E.S., Luo, G., Guo, X., Hasselgren, P., 2002. Arsenite inhibits interleukin-6 production in human intestinal epithelial cells by down-regulating nuclear factor-κB activity. Clin. Sci. 103, 381-390.
7. Kunjathoor, V.V., Febbraio, M., podrez, E.A., Moore, K.J., Andersson, L., Koehn, S., Rhee, J.S., Silverstein, R., Hoff, H.F., Freeman, M.W., 2002.

Scavenger receptors class A-I/II and CD36 are the principal receptors responsible for the uptake of midified low density lipoprotein leading to lipid loading in macrophages. J. Biol. Chem. 277(49), 982-88.

8. Lechleitner, S., Gille, J., Johnson, D.R., Petzelbauer., 1998. Interferon enhances tumor necrosis factor-induced vascular adhesion molecule 1 (CD106) expression in human endothelial cells by an interferon-related factor 1-dependent pathway. J. Exp. Med. 187(12), 2023-2030.

9. Lee, P-C., Ho, I-C., Lee, T-C., 2005. Oxidative stress mediates sodium arsenite-induced expression of heme oxygenase-1, monocyte chemoattractant protein-1, and interleukin-6 in vascular smooth muscle cells. Toxicol. Sci. 85, 541-550.

10. Liu, J., Liu, Y., Goyer, R.A., Achanzar, W., Waalkes, M.P., 2000. Metallothionein-I/II null mice are more sensitive than wild-type mice to the hepatotoxic and nephrotoxic effects of chronic oral or injected inorganic arsenicals. Toxicol. Sci. 55(2), 460-467.

11. Lusis, A.J., 2000. Atherosclerosis. Nature. 407, 233-241.

12. McDouall, R.M., Farrar, M.W., Khan, S., Yacoub, M.H., Allen, S.P., 2001. Unique sensitivities to cytokine regulated expression of adhesion molecule in human heart-derived endothelial cells. Endothelium. 8(1), 25-40.

13. Navas-Acien, A., Sharrett, A.R., Silbergeld, E.K., Schwartz, B.S., Nachman, K.E., Burke, T.A., Guallar, E., 2005. Arsenic exposure and cardiovascular disease: A systematic review of epidemiologic evidence. Am. J. Epidemiol. 162(11), 1037-1049.

14. Neish, A.S., Read, M.A., Thanos, D., Pine, R., Maniatis, T., Collins, T., 1995. Endothelial Interferon Regulatory Factor 1 cooperates with NF-κB as a transcriptional activator of vascular cell adhesion molecule 1. Mol. Cell. Biol. 15(5), 2558-2569.

15. Neish, A.S., Williams, A.J., Palmer, H.J., Whitley, M.Z., Collins, T., 1992. Functional analysis of the human vascular cell adhesion molecule 1 promoter. J. Exp. Med. 176, 1583-1593.

16. Roussel, R.R., Barchowsky, A., 2000. Arsenic inhibits NF-κB-mediated gene transcription by blocking IκB kinase activity and IκBα phosphorylation and degradation. Arch. Biochem. Biophys. 377(1), 204-212.

17. Simeonova, P.P., Hulderman, T., Harki, D., Luster, M.I., 2003. Arsenic exposure accelerates atherogenesis in apolipoprotein $E^{-/-}$ mice. Environ. Health Perspect. 111, 1744-1748.

18. Suzuki, H., Kurihara, Y., Takeya, M., Kamada, N., Kataoka, M., Jishage, K., Ueda, O., Sakaguchi, H., Higashi, T., Suzuki, T., Takashima, Y., Kawabe, Y., Cynshi, O., Wada, Y., Honda, M., Kurihara, H., Aburatani, H., Doi, T., Matsumoto, A., Azuma, S., Noda, T., Toyoda, Y., Itakura, H., Yazaki, Y., Horiuchi, S., Takahashi, K., Kruijt, J.K., van Berkel, T.J.C., Steinbrecher, U.P., Ishibashi, S., Maeda, N., Gordon, S., Kodama, T., 1997. A role for macrophage scavenger receptors in atherosclerosis and susceptibility to infection. Nature. 386, 292-296.

19. Tedgui, A., Mallat, Z., 2006. Cytokines in atherosclerosis: Pathogenic and regulatory pathways. Physiol. Rev. 86, 515-581.

20. Tsou, T-C., Yeh, S-C., Tsai, E-M., Tsai, F-Y., Chao, H-R., Chang, L-W., 2005. Arsenite enhances tumor necrosis factor-α-induced expression of vascular cell adhesion molecule-1. Toxicol. Appl. Pharmacol. 209, 10-18.

21. van der Zijpp, Y.J.T., Poot, A.A., Feijen, J., 2003. ICAM-1 and VCAM-1 expression by endothelial cells grown on fibronectin-coated TCPS and PS. J. Biomed. Mater. Res. 65A, 51-59.

22. Wang, C.H., Jeng, J.S., Yip, P.K., Chen, C.L., Hsu, L.I., Hsueh, Y.M., Chiou, H.Y., Wu, M.M., Chen, C.J., 2002. Biological gradient between long-term arsenic exposure and carotid atherosclerosis. Circulation 105(15), 1804-1809.

23. Watson, C., Whittaker, S., Smith, N., Vora, A.J., Dumonde, D.C., Brown, K.A., 1996. IL-6 acts on endothelial cells to preferentially increase their adherence for lymphocytes. Clin. Exp. Immunol. 105, 112-119.

24. Zhang, W-J., Frei, B., 2002. Albumin selectively inhibits TNFα-induced expression of vascular cell adhesion molecule-1 in human aortic endothelial cells. Circ. Res. 55, 820-829.